COLLOIDAL AND ELECTROCHEMICAL ASPECTS OF COPPER-CMP

By

Yuxia Sun

A Dissertation Submitted to the Faculty of the
DEPARTMENT OF MATERIALS SCIENCE AND ENGINEERING

In Partial Fulfillment of the Requirements
For the Degree of
DOCTOR OF PHILOSOPHY
In the Graduate College
THE UNIVERSITY OF ARIZONA
2007

THE UNIVERSITY OF ARIZONA
GRADUATE COLLEGE

As members of the Dissertation Committee, we certify that we have read the dissertation prepared by Yuxia Sun entitled COLLOIDAL AND ELECTROCHEMICAL ASPECTS OF COPPER-CMP and recommend that it be accepted as fulfilling the dissertation requirement for the Degree of Doctor of Philosophy.

_____ Date: 07/30/07
Srini Raghavan

_____ Date: 07/30/07
Supapan Seraphin

_____ Date: 07/30/07
Robert Arnold

_____ Date: 07/30/07
Jim Farrell

Final approval and acceptance of this dissertation is contingent upon the candidate's submission of the final copies of the dissertation to the Graduate College.

I hereby certify that I have read this dissertation prepared under my direction and recommend that it be accepted as fulfilling the dissertation requirement.

_____ Date: 07/30/07
Dissertation Director: Srini Raghavan

STATEMENT BY AUTHOR

This dissertation has been submitted in partial fulfillment of requirements for an advanced degree at The University of Arizona and is deposited in the University Library to be made available to borrowers under rules of the Library.

Brief quotation from this dissertation is allowable without special permission, provided that accurate acknowledgment of source is made. Request for permission for extended quotation or reproduction of this manuscript in whole or in part may be granted by the copyright holder.

SIGNED:_____

Yuxia Sun

ACKNOWLEDGEMENTS

This dissertation would not be completed without the help of many people to whom I am deeply grateful.

First, I would like to thank my advisor, Dr. Srini Raghavan, for his continuous, unconditional support and advice. Dr. Raghavan, beyond being a renowned researcher and well respected, dedicated professor, is a very good mentor to his students, and is always available for valuable advice and discussion.

Second, I would like to thank my master thesis advisor, Dr. Robert Arnold, for introducing me to Surface Chemistry, and accepting me as his student when I came to this country ten years ago and could barely speak English.

I am also very grateful to Dr. Seraphin and Dr. Farrell for educating me through many exciting subjects which have helped me develop a solid and diverse educational background. I would also like to thank them for the time they contributed while on my dissertation committee.

This project could not have been completed without the support and help from Dr. O'Hanlon of the ECE department and Dr. Wendt of the CHE department. I am appreciative for the clean room wet bench provided by Dr. O'Hanlon and the AAS equipment provided by Dr. Wendt.

Last but not least, I would like to thank Dr. Jeon Joong, Dr. Raghavan's former student, for his great support in providing the wafers and performing the TXRF measurements. I also would like to thank Liming Zhang, Wayne Huang, Marcia Workman, Matt Felix, and David Lin for meaningful discussions and assistance I have received, and good memories they have left to me.

Finally, I would like to acknowledge the NSF/SRC Engineering Research Center for Environmentally Benign Semiconductor Manufacturing for providing financial support and a very active platform for discussion and communication between academia and industry.

TABLE OF CONTENTS

TABLE OF CONTENTS - *Continued*

TABLE OF CONTENTS - *Continued*

TABLE OF CONTENTS - *Continued*

LIST OF ILLUSTRATIONS

LIST OF ILLUSTRATIONS - *Continued*

LIST OF TABLES

ABSTRACT

Copper based interconnects with low dielectric constant layers are currently used to increase interconnect densities and reduce interconnect time delays in integrated circuits. The technology used to develop copper interconnects involves Chemical Mechanical Planarization (CMP) of copper films deposited on low-k layers (silica or silica based films), which is carried out using slurries containing abrasive particles. One issue using such a structure is copper contamination over dielectric layers (SiO_2 film), if not reduced, this contamination will cause current leakage. In this study, the conditions conducive to copper contamination onto SiO_2 films during Cu-CMP process were studied, and a post-CMP cleaning technique was discussed based on experimental results. It was found that the adsorption of copper onto a silica surface is kinetically fast (< 0.5 minute). The amount of copper absorbed is pH and concentration dependent and affected by presence of H_2O_2, complexing agents, and copper corrosion inhibitor Benzotrazole. Based on de-sorption results, DI water alone was unable to reduce adsorbed copper to an acceptable level, especially for adsorption that takes place at a higher pH condition. The addition of complex agent, citric acid, proved effective in suppressing copper adsorption onto oxide silica during polishing or post-CMP cleaning by forming stable copper-CA complexes. Surface Complexation Modeling was used to simulate copper adsorption isotherms and predict the copper contamination levels on SiO_2 surfaces.

Another issue with the application of copper CMP is its environmental impact. CMP is a costly process due to its huge consumption of pure water and slurry. Additionally, Cu-CMP processing generates a waste stream containing certain amounts of copper and

abrasive slurry particles. In this study, the separation technique electrocoagulation was investigated to remove both copper and abrasive slurry particles simultaneously. For effluent containing ~40 ppm dissolved copper, it was found that ~90% dissolved copper was removed from the waste streams through electroplating and in-situ chemical precipitation. The amount of copper removed through plating is impacted by membrane surface charge, type/amount of complexing agents, and solid content in the slurry suspension. The slurry particles can be removed ~90% within 2 hours of EC through multiple mechanisms.

CHAPTER 1

INTRODUCTION

1.1 Introduction

As interconnection dimensions continue to shrink and the number of metal layers grows, the need for surface planarity increases. It is well known that global planarization is required to meet the depth of field requirements of lithography tools for the sub-0.5 μm or smaller regime. For example, in sub-0.18 μm integrated devices, a lack of planarity leads to severe problems during lithography, where very short depth of focus is required. As gate size in current semiconductor device approaches to sub-32nm, and metal connection layers increase to 9-11, as described by the International Technology Roadmap for Semiconductor (IRTS) [1.1], Chemical Mechanical Polishing (CMP) becomes an indispensable part of every fab fabrication to achieve the surface planarity required for subsequent processes.

Historically, to achieve a high level of planarization, several methods have been studied. For example, conventional planarization methods include etchback, polishing, laser reflow, and spin-on coating [1.2]. However, these methods do not give sufficient planarity across the entire wafer surface area for advanced processes of Ultra Large Silicon Integrated (ULSI) devices. Currently, although there are researchers working on alternative planarization solutions, chemical mechanical planarization (CMP) is widely accepted as a viable technique for achieving global planarity for ULSI devices with a feature size of 0.25 μm or below.

To make integrated circuits, many complicated processes are integrated together: thin film deposition, lithography, dry/wet etch, diffusion/implantation, electroplating, planarization and so on. Among these processes, metallization, a metal thin film formation process, is one of the key processes in manufacturing ULSI devices, which connects the transistors to the outside environment [1.3]. Metal, as a conductor in integrated circuit (IC) devices, can be deposited through chemical vapor deposition (CVD), physical vapor deposition (PVD)/ sputtering deposition, and electroplating methods. Due to the difficulty in etching high aspect ratio trenches in metal films, a damascene process is used in current technology for creating metal lines and vias. During wafer fabrication, first, a blanket metal film is deposited onto a patterned dielectric film, and then the excess metal film is removed by CMP processes to create a planarized wafer surface. The final planarized surface is composed of metal conductor lines or metal plugs with surrounding dielectric materials such as silicon dioxide (see Figure 2.6).

Improving device performance by continuously reducing interconnect signal delay is a goal that the semiconductor industry strives to achieve. The interconnect signal delay, also called RC delay, is impacted by resistance (R) and capacitance (C) associated with metal line heights and dielectric material capacitances. R is proportional to metal resistivity and C is proportional to the insulator dielectric constant. Using low resistivity metals for interconnects (metals like Au, Ag, Cu) and low dielectric (low-k) insulating materials, reduction of RC delay can be achieved. Copper, due to its excellent conductivity and outstanding electron migration resistance, becomes the dominant

interconnect material in device fabrication along with silica based low dielectric insulation materials [1.4].

With the application of copper as the interconnect material, and CMP employed to remove the excess copper films after copper electroplating, there is a need to explore cost effective solutions and methods to deal with copper contamination, copper waste disposal, and reclaiming the large quantity of water consumed by Cu-CMP processes. It is well known that copper is a fast diffuser in silicon, SiO_2, and other dielectrics. Once it gets on silicon or dielectric SiO_2, it will dramatically reduce the yield due to current leakage [1.5, 1.6]. The requirements for wafer and device surface cleanliness in ULSI manufacturing are very strict. For example, as shown in Table 1.1, the metallic concentration on wafer surfaces needs to be $\leq 10^{10}$ atoms/cm^2 and the particle density on wafer front side needs to be $\leq 0.023/\ cm^2$ to meet the high yield target for year 2007. However, due to the nature of the current CMP process, which is a "dirty" process in an ultra pure device fabrication world, it is very challenging for the CMP process to meet the surface cleanliness requirements.

It is necessary, at this point, to study the mechanisms of copper contamination in dielectric SiO_2 films during Cu-CMP in order to develop an effective Cu-CMP process that has less copper contamination or a post-CMP cleaning step that is able to remove the contaminated copper as well as polishing residue deposited on the wafer surfaces.

During Cu-CMP processing, a large quantity of ultra pure water and slurry that contains abrasive particles is consumed. For a typical Cu-CMP polisher at a 300mm wafer fab, the polisher contains 3 polishing platens (see figure 2.2). The slurry and water

consumption on 3 platens can reach a total of 500-800ml/min. Most polishers have an integrated scrubber cleaner that cleans the wafer after polishing step and will consume ultra pure water up to 600-800 ml/min. As a result, a single polisher can generate 1100-1600 ml of waste every minute. A typical fab can have 20 ~ 30 polishers. It is not surprising to hear that the CMP process alone can consume 30% of the water usage in a clean room fabrication facility [1.7]. Additionally, the effluents of Cu-CMP processing contain a certain amount of copper which is generated by polishing the excess Cu films. As shown in the International Technology Roadmap for Semiconductors [1.8], 85% copper is expected to be reclaimed/recycled by 2010, and that number will increase to 100% after 2011 (Table 1.2). Water recycle/reclaimation is expected for the planarization process for current CMP technology and beyond (see Table 1.3). At this point, it is important to explore efficient separation methods in treating the CMP waste streams to facilitate water and copper reclamation/reuse and meet the local discharge regulations.

Different separation methods have been proposed to treat Cu-CMP effluent such as ultrafiltration, deionization, and Cu electroplating. Those techniques need to be used in sequence to achieve copper and particle removal. Electrocoagulation, which has been explored in a wide range of industrial and laboratory scale water treatment applications, is under investigation for potential treatment of Cu-CMP effluents. A substantial advantage of this approach is the possibility to simultaneously remove suspended matter, organics, bacteria contaminations and metal ions. Therefore, it is important to investigate and understand the copper and abrasive particle (Al_2O_3, SiO_2) removal mechanisms via

Table 1.1. Interconnect Surface Preparation Technology Requirements [1.8]

Year of production	2006	2007	2008	2009	2010	2011	2012	2013
Wafer diameter (mm)	300	300	300	300	300	300	300	300
Wafer edge exclusion (mm)	2	2	2	2	2	2	2	2
Front surface particles								
Killer defect density, D_pR_p (#/cm^2) [A]	0.019	0.023	0.016	0.02	0.025	0.016	0.02	0.025
Critical particle diameter, d_c (nm) [B]	35	32.5	28.5	25	22.5	20	17.5	16
Critical particle density, D_{pw}(#/wafer) [C]	64	80	54	68	86	123.3	155	195
Metallic contamination								
Critical front surface metals (10^9 atoms/cm^2) (D)	10	10	10	10	10	10	10	10
Mobile Ions (10^{10}atoms/cm^2) (E)	5	5	2.5	2.5	2.5	2.5	2.5	2.4
Organic contamination (10^{13} C atoms/cm^2) (F)	1.3	1.2	0.9	0.9	0.9	0.9	0.9	0.9

Solution Exist Solutions Being Pursued No Known Solution

A. Killer defect density is calculated from the formula for 99% yield. Y=0.99=exp(-DpRpAeff). Aeff is the effective chip area. Dp is the effective density and Rp is a defect kill factor indicating the probability that a given defect will kill the device.
B. Critical particle diameter, dc, is defined by yield enhancement as ½ of the metal ½-pitch dimension. This should be considered an "effective" particle diameter as most particulate contamination is irregular in shape.
C. Particles/wafer is calculated using [Rp*3.14159*(wafer radium-edge exclusion)^2]
D. Front surface metallic contamination levels are based on degradation of yield from metallic diffusion into the transistor or leakage of the device from the metal migration.
E. Mobile ions from interconnect are less stringent than the front end line metrics.
F. Organic contamination is usually in the form of a thin layer of hydrocarbon remaining on the wafer after resist strip and clean and after post-CMP clean.

Table 1.2 Chemical and Materials Management Technology Requirements [1.8]

Year of Production	2005	2006	2007	2008	2009	2010	2011	2012	2013
Copper processes	*75% copper reclaimed/recycled*			*85% copper reclaimed/recycled*			*100% copper reclaimed/recycled*		
Planarization (metal CMP)	15% reduction in consumables from baseline			>15% reduction in consumables from baseline			5% reduction in consumables per year		

Table 1. 3 Resource Conservation Technology Requirements (IRTS, 2005)

Year of Production	2005	2006	2007	2008	2009	2010	2011	2012	2013
Copper processes	Copper process optimized to minimize waste to water and land								
Planarization	*Water recycle/reclaim*								
Reduce water use	0.8x (x=1999 baseline)					0.5x (x=1999 baseline)			
Reduce chemical use and consumption	0.8x (x=1999 baseline)					0.5x (x=1999 baseline)			

electrocoagulation in order to evaluate the potential use of this technology in treating Cu-CMP effluents.

1.2 Objectives of Study

In this study, two major aspects that are related to Cu-CMP are addressed. The first aspect addressed is the Cu contamination over SiO_2 dielectric films. The fundamental aspects of Cu contamination on dielectric material (SiO_2) need to be studied in order to fully understand this solid/liquid inter-surface phenomenon under polishing conditions and develop an effective Cu-CMP or post-CMP cleaning process that leads to less copper contamination. Specifically, the objectives of this study for copper contamination over SiO_2 are listed as follows:

- Study copper adsorption on SiO_2 as a function of pH, presence of complex agents (citric acid), oxidizer, and Benzotriazle(BTA).
- Understand copper adsorption kinetics, adsorption and desorption mechanisms on SiO_2.
- Develop strategies to reduce or eliminate copper contamination during Cu-CMP or post-CMP processing.
- Apply Surface Complexation Modeling to simulate and predict the copper adsorption level under certain polishing conditions.

The second part of this study is to explore the application of Electrocoagulation in treating CMP effluents to facilitate the reclamation/recycle of water consumed during CMP process and reclaim/reuse the copper generated by the Cu-CMP process. Specifically, the study focuses on the application of electrocoagulation (EC) as a removal

technique of both slurry particles and copper from Cu-CMP waste streams. Additionally, the factors affecting copper removal under EC and the removal mechanisms of abrasive particles (Al_2O_3 and SiO_2) are investigated. The second objective of this study is as follows:

- Review the environmental regulations that need to be considered in handing Cu-CMP effluents
- Establish a Cu-CMP waste stream model to be used for this study
- Understand simultaneous copper and particle removal mechanisms during electrocoagulation
- Understand the impacts of factors such as membrane type, complexing agents, and solid concentration on copper removal during EC
- Understand the fundamental removal mechanisms of slurry particle alumina and silica under electrocoagulation

CHAPTER 2

Cu-CMP AND CONTAMINATION

In this chapter, the fundamental aspects of CMP, Cu CMP process, and the contamination issues during CMP process as well as current cleaning methods are discussed.

2.1 A Brief Historical Review of CMP

CMP is a technology that has been used for optical finishing of glass and Si surfaces for many decades [2.1, 2.2]. Without polishing, the stacking of an increasing number of interconnect layers generates hills and valleys that create design, yield and reliability problems in complex devices with small features. In order to solve these problems, in the mid-1980s, IBM secretly developed a new process, Chemical Mechanical Planarization (CMP), which is a wafer-wide polishing and planarization process aimed at eliminating the hills and valleys of the dielectric (or oxide) layers [2.3]. This process, made public in 1991, is called oxide CMP. The advantages of this type of polishing process have since prompted the development of new applications of CMP, one of which is metal CMP. Initially, the extra deposited W films were removed by Reactive Ion Etching (RIE) process; this process is replaced by a CMP step, which has proven cost-effective and yield-enhancing [2.4]. The developments led to the advanced aluminum technology shown in Figure 2.1, where a planar surface results after each metallization layer. In this chapter, after a brief description of IC fabrication, traditional

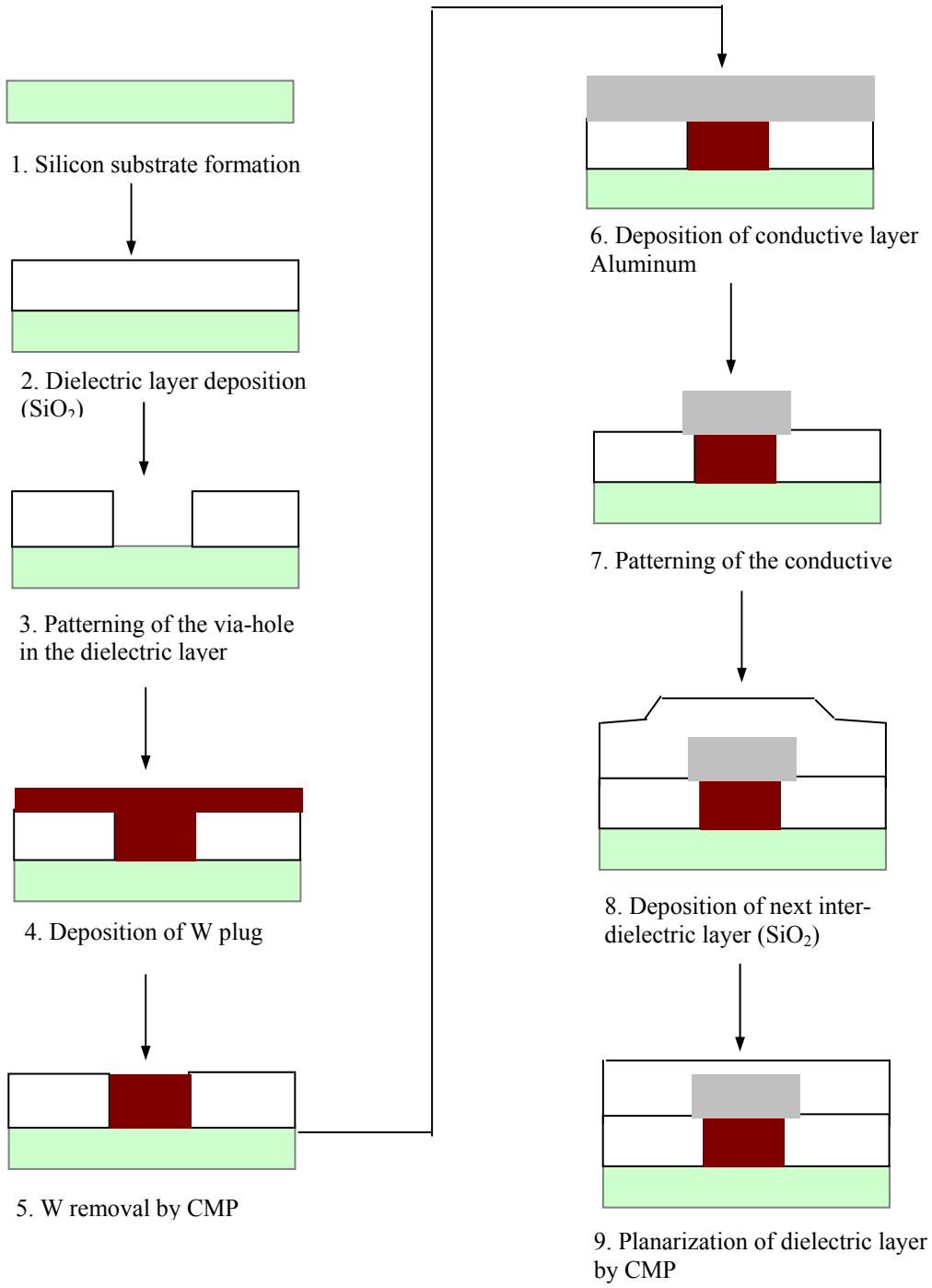

Figure 2.1 Advance aluminum fabrication

and advanced aluminum interconnect technology, the copper interconnect and copper CMP process are described in section 2.3.

The current state of CMP is the result of the semiconductor industry's need to fabricate multilevel interconnections for increasingly complex, dense, and miniaturized devices and circuits [2.4]. At present, CMP is one of the fastest growing segments of the semiconductor equipment and materials market [2.5, 2.6, 2.7].

2.2 CMP Process

As shown in Figure 2.2, a typical CMP process consists of moving the sample surfaces to be polished against a pad that is used to provide support against the sample surface, and to carry particulate slurry between the sample surface and pad to obtain surface planarization. Abrasive particles in the slurry cause mechanical damage on the sample surface, loosening the material for enhanced chemical attack or fracturing off the pieces of surface into slurry where they are dissolved or swept away. Generally, chemistry alone will not achieve planarization because most chemical actions are isotropic. Mechanical grinding alone, theoretically, may achieve the desired material removal but will provoke extensive damage of the material surfaces.

A CMP process includes the following components:

- The surface to be polished
- The pad --- the key media enabling the transfer of mechanical forces to the surface being polished
- The slurry – to provide both chemical and mechanical effects

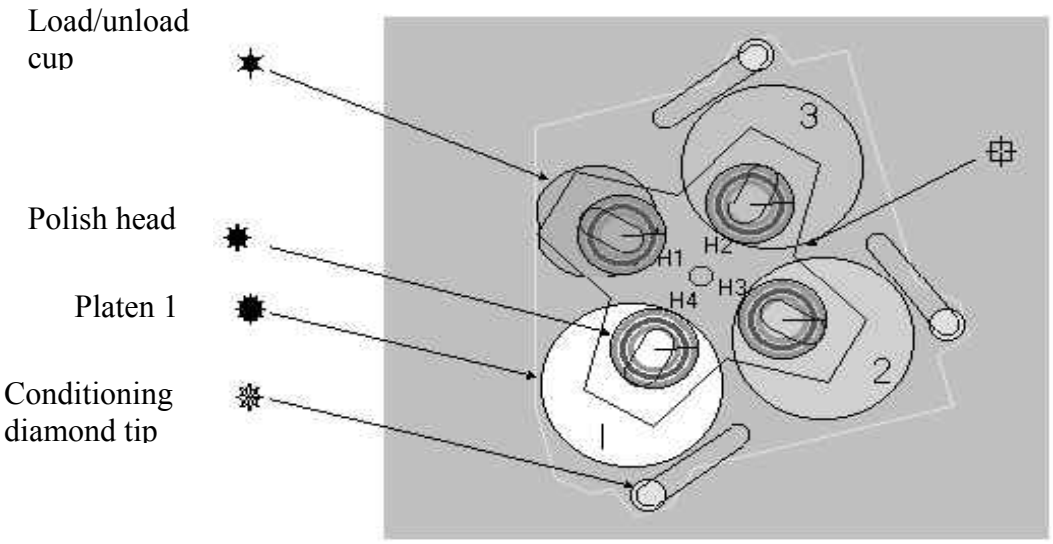

a: Illustration of a polisher contains a load/unload cup and 3 polish platens and 4 polish heads (H1 to H4)

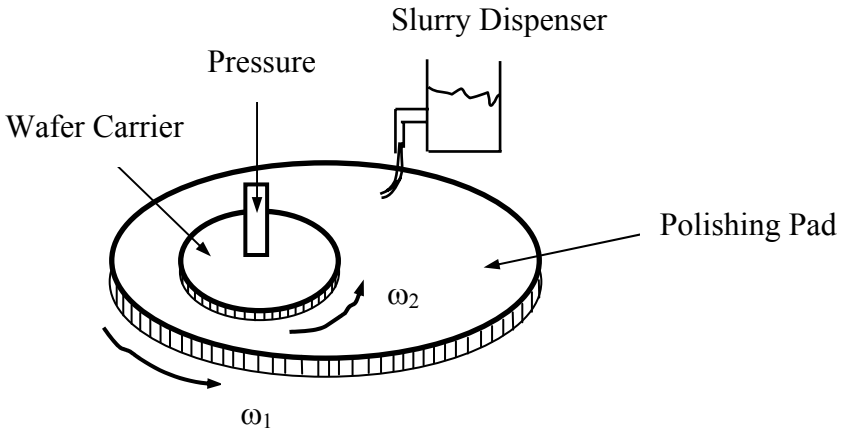

b: Illustration of a single polish head and platen

Figure 2.2 CMP System

Post-CMP cleaning – that may affect the final acceptance criteria for the polished surface.

In general, polishing pads are composed of either a matrix of cast polyurethane foam with filler material to control hardness, or polyurethane impregnated felts. The specific gravity, compressibility, and hardness are important properties to be considered in choosing polishing pads [2.8]. Slurries provide both the chemical action through solution chemistry and the mechanical action through the abrasives. Commonly used abrasives are SiO_2 and Al_2O_3. The abrasive type, size, shape, and concentration determine the physical and chemical interactions between abrasive and liquid, or abrasive and substrate surfaces [2.4]. The last important step of the complete CMP-process sequence is the post-cleaning. Removal of the slurry from the surface without leaving any macroscopic, microscopic, or electrically active defects is very important in making the process useful. CMP slurries and post chemical cleaning should not introduce any chemical or particulate contamination.

2.3 Advantages of CMP Process and Its Application

The unique advantage of CMP is that it achieves global planarization, which is essential in building multilevel interconnections. Measurement of planarity and degrees of planarity are shown in Fig. 2.3 and Table 2.1, respectively. The planarization relaxation distance, R, is defined as the distance traveled over a step, whereupon the original step height (i.e., T) returns [2.9]. The planarization angle (θ) is given by

$$\theta = \arctan (T/R) \qquad (2.1)$$

Table 2.1 Degrees of Planarity [2.9]

Planarity	R (μm)	θ^o
Surface smoothing	0.1 – 0.2	≥ 30
Local planarity	2.0 – 100	30 – 0.5
Global planarity	≥ 100	≤ 0.5

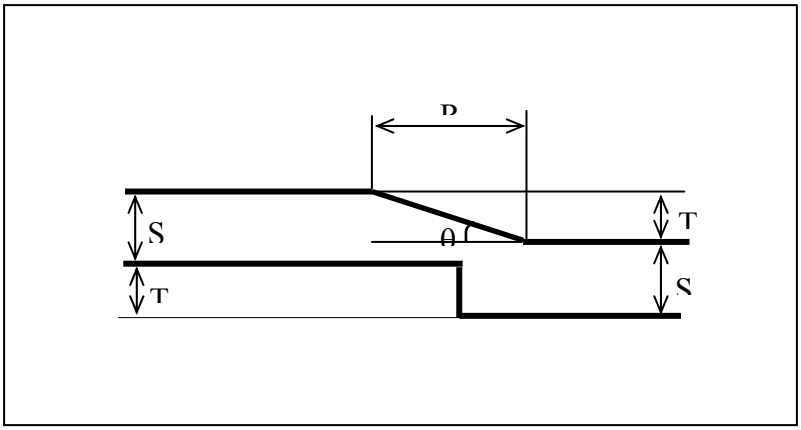

Figure. 2.3 Measurement of Planarity [2.9]

As indicated in Table 2.1, a CMP process should yield the global planarity characterized by $R \geq 100$ and $\theta \leq 0.5^{o}$. The so-called step height reduction (SHR) is defined as

$$SHR = 1 - T_{post}/T_{pre} \qquad (2.2)$$

where T_{post} and T_{pre} are the step height after and before the planarization process, respectively. The rate of planarization can be expressed as the difference between the polish rate of the high and low features [2.4], where the polish rate is obviously defined as the thickness reduction per unit time.

CMP also has the following advantages for improving global surface planarization: (i) CMP allows easier and more accurate alignment of litho images that define the transistor devices to be created; (ii) CMP ensures uniform step coverage for numerous metal layers and dielectric layers. Device yield and reliability are improved via planarization by eliminating the step coverage issues of metal stringers and electromigration.

Another successful application of the CMP process in silicon integrated circuits was building multilevel interconnection structures employing deposited (CVD) tungsten as the via fill metal and sputtered aluminum as the planar interconnection metal. In this application CMP achieved two results: (i) planarization of the SiO_2 surface and (ii) removal of CVD tungsten from horizontal surfaces, thus allowing excellent via fill metal to be then connected to horizontal aluminum interconnections formed by sputter deposition and the subsequent reactive ion etching. Based on this success, the use of CMP has expanded to: (i) a large variety of materials including metals (Al, Cu, Ta, Ti, TiN, W, and their alloys), insulators (SiO_2 and doped SiO_2 glasses, Si_3N_4, and polymers)

(illustrated in Figure 2.4), and polysilicon; (ii) a variety of applications involving even larger area planarization such as those used in multichip modules, IC packaging and flat panel displays; and (iii) planarization of materials at different levels of silicon device and integrated front-end circuit processing, even as early as the polysilicon level [2.4].

During development of the Damacene process for copper technology, it was found that, aside from improving overall device speed, this new technology had other advantages. For example, the number of process steps and related cost could be reduced, possibly by 20-30%, compared to advanced aluminum technology [2.10, 2.11]. As a side benefit, Cu-CMP enables the accurate patterning of very fine lines since etching can be done more precisely in silica than in metal. The manufacturing of copper interconnects is therefore significantly different from the traditional aluminum interconnect process as described in Figure 2.5.

2.4 Cu-CMP Process

2.4.1 Copper-low k Material Structures

The interconnect delay in an integrated circuit is due to the capacitance C and resistance (R) associated with the metal lines. Time delay, RC, is defined as the time it takes for the voltage at one end of a metal line to reach 63% of its final value when a step input is presented at the other end of the line. The resistance R is expressed as:

$$R = \rho \frac{l}{wd}$$

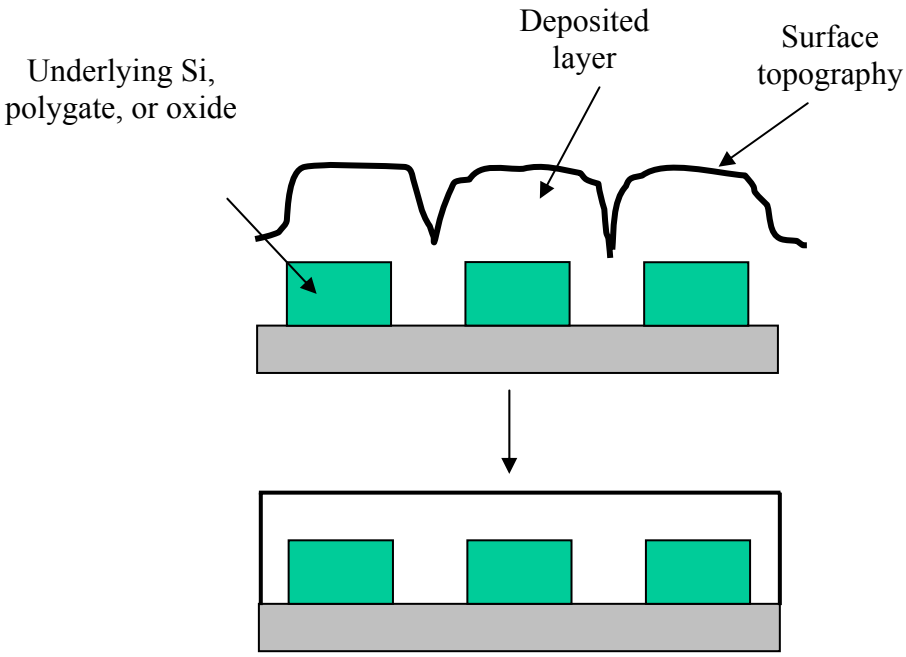

Figure 2.4 Schematic illustration of CMP application

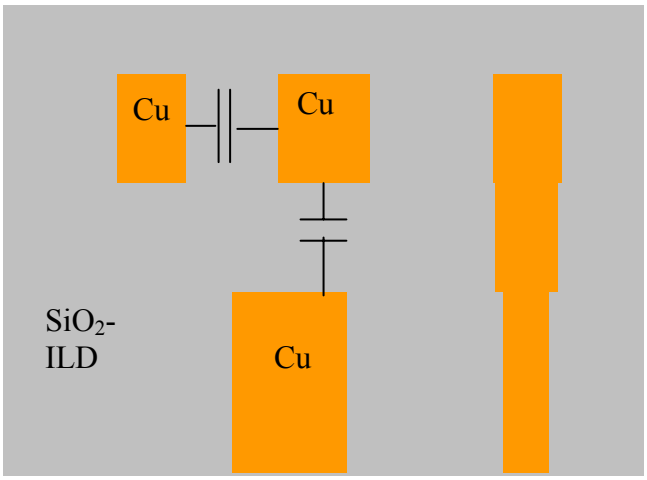

Figure 2.5: Illustration of capacitive coupling between adjacent metal lines

Where ρ is the metal resistivity and l, w, d are the length, width, and thickness of the line respectively. The capacitance C of the line is given by:

$$C = \varepsilon \frac{wl}{t} \qquad (2.3)$$

where t is the thickness between insulators, and $\varepsilon = \varepsilon_0 \times k$ (ε_0 is the permittivity of free space, k is the insulator dielectric constant). Combining the above two equations, the RC Time Delay RC is expressed as:

$$RC = \rho\varepsilon \frac{l^2}{td} \qquad (2.4)$$

To reduce RC delay, the combination of low resistivity metal, low dielectric constant Inter Layer Dielectric (ILD), and multilevel metallization will yield high performance interconnects. Compared with IC metallization schemes that utilize aluminum alloys, in part or in full, as the interconnect metal, copper is the best choice based on its cost and performance out of all metals with lower resistivity than aluminum (resistivity of 2.66 μΩ-cm). Copper has a resistivity only slightly greater than silver and approximately 50% lower than currently used aluminum alloys. It has a higher melting point (933^{o}K) than aluminum (356^{o}K) which leads to greater electromigration resistance. Copper can handle current densities of up to $5 \bullet 10^6$ A/cm^2 before the onset of electromigration failure [2.4, 2.12]. All of those advantages have put copper in the main stream for use as the interconnect metal in the integrated device.

As shown in the equation, RC delay is directly proportional to the dielectric constant of the ILD. Besides switching to copper interconnect, switching from oxide-based ILD to a low k ILD materials significantly decreases the interconnect delay [2.11]. In addition, lowering the dielectric constant lowers cross talk due to capacitive coupling between adjacent metal lines (Figure 2.5) and power dissipation. Currently, the dielectric material remains silica for some interconnect layers and for other layers is still silica based (doped or modified silica material that has a lower dielectric constant).

2.4.2 Cu-CMP Process and Its Contamination Issues

The current technique used in device fabrication for copper based interconnect is called the "dual damacene" process (Figure 2.6). Basically, the technique etches trenches and vias into the dielectric, fills the trenches and vias with copper in one step, and removes excess copper from the field areas using chemical mechanical polishing damascene architecture.

The first step of the dual damascene process (the purpose of which is to fill via holes and interconnect trench lines in one step) is depositing a layer of silicon nitride. This process step deposits approximately 1200-1500 Å of nitride. The nitride layer acts as an etch stop layer to minimize the chance of over-etching of the underlying metal layer during subsequent via etch. Then the inter layer dielectric (ILD), typically silicon oxide or doped silicon oxide, is deposited over the silicon nitride films. The ILD films usually range from 7000 to 21000 Å. Following the lithography process, the ILD is removed

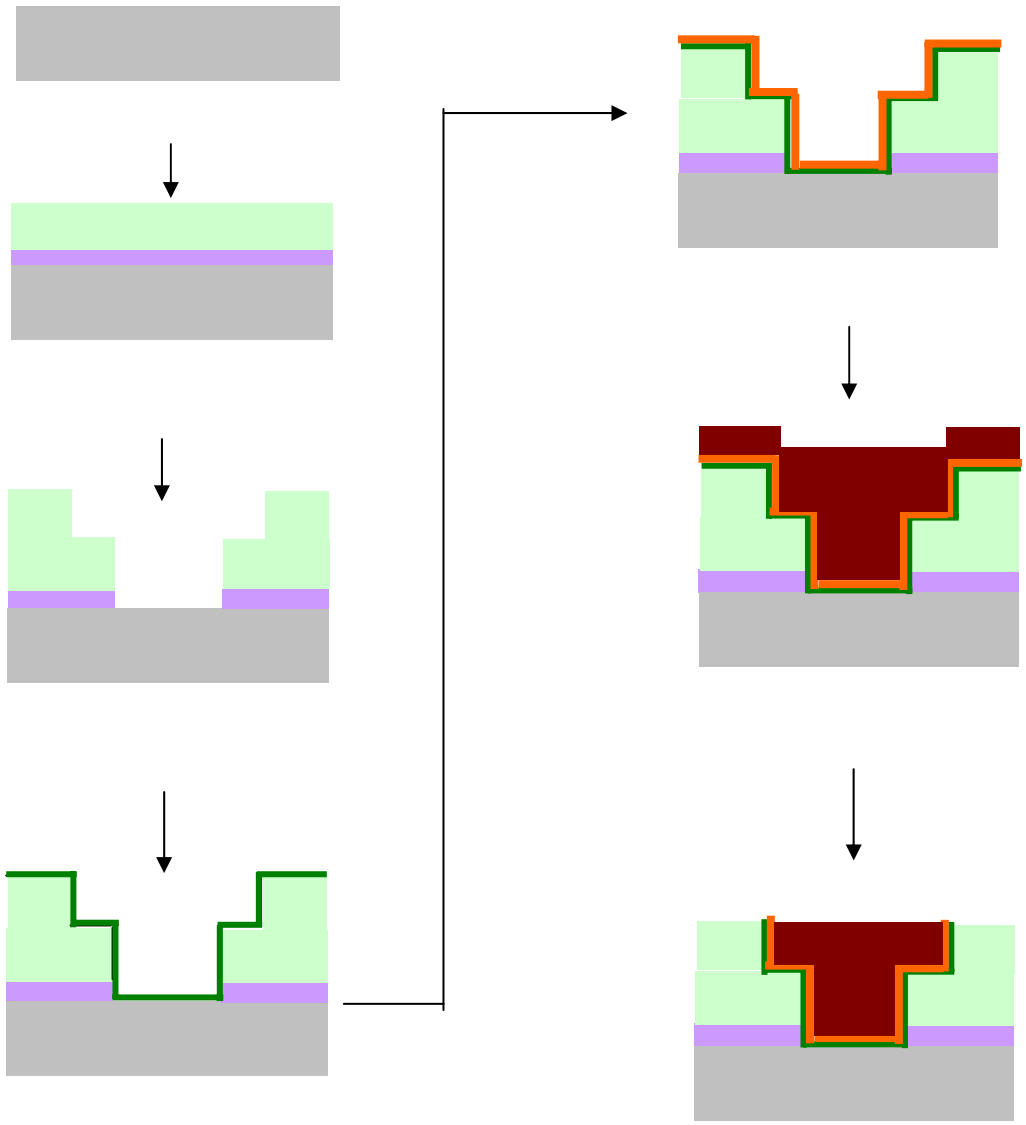

Figure 2.6 Illustration of Cu Damacene Process

where the via will be located. The subsequent process patterns and etches the interconnect trenches, and continues through the silicon nitride layer to form the trench and complete the via holes.

The second step consists of depositing a barrier layer that is conductive but will prevent the copper from migrating to lower levels. This layer is usually a refractory metal or refractory metal compound: tantalum and tantalum nitride are the most common although titanium nitride or tungsten nitride have been proposed [2.13]. This layer is deposited by PVD (Physical Vapor Deposition) and is typically 150-200 Å thick.

Above the barrier layer, a seed layer of copper is deposited by PVD (physical vapor deposition) or by CVD using a Cu(hfac)(TMVS) precursor (TriMethylVinylSilyl hexafluoroacetylacetonate Copper) [2.14, 2.15]. The thickness of this seed layer is ~ 1500 Å. It is critical that the deposited copper seed layer is smooth and continuous. The purpose of this seed layer is to enable the subsequent electrodeposition of copper.

The fourth step is copper deposition by electroplating of the copper in the trenches and the via holes. This step also results in an overcoat of copper on the whole wafer, the thickness of which is of the order of 0.5-1.5 μm [2.16].

The fifth step of the process is a CMP step, the purpose of which is to remove the excess copper and barrier layers, leaving behind the copper interconnect network (see Figure 2.6).

The final step is the deposition of a silicon nitride layer that will encapsulate the copper and isolate it from the above layers.

As the polish approaches the dielectric SiO_2 layers during Cu-CMP, there is great "opportunity" for particles and copper impurities in the slurry to get on SiO_2 surfaces. Control of particulate deposition during CMP as well as the development of post CMP cleaning techniques to remove deposited particles requires an understanding of the surface and solution chemistry of the wafers and particles under polishing conditions [2.17]. Deposition of slurry particles onto the wafer surface can happen by a variety of mechanisms, including mechanical (under the application of applied pressure during CMP), chemical, capillary-pressure and electrostatic interactions [2.18].

Since copper, as a deep-level impurity, can migrate to the semiconductor and adversely affect device performance, copper contamination control is a critical step in fab fabrication. On a smaller scale within each individual die, Cu must be prevented from migrating to the electrically active silicon regions or into dielectric films in order to prevent poisoning of transistors or degradation of the insulating layers. Several materials are effective barriers to copper diffusion, and their use as liner films between copper and silicon or SiO_2 will prevent degradation in the electronic properties of the silicon [2.4] In the case of Cu CMP, however, the post-CMP clean bears the additional challenge of removing Cu completely from the dielectric surface. This task is further complicated by the close proximity to an infinite Cu source (i.e., the embedded Cu damascene features; see Figure 2.6). Any remaining Cu contamination on the dielectric areas would be permanently sealed into the wafer by the subsequent cap layer deposition and remain as a diffusion source and possible leakage path between the encapsulated damascene features [2.19].

2.5 Models and Mechanisms of CMP

The CMP process relies on the inseparable chemical and mechanical interactions among the surface being polished, the pad, and the slurry. This distinguishes it from chemical etching (i.e., solid-liquid interaction) or grinding (pure mechanical action). The following discussion is divided into two sections dealing first with mechanical and then with chemical aspects of CMP.

2.5.1 Mechanical

The first wafer-scale mechanical model for CMP was proposed by Preston in 1927. It relates to the removal rate to the work done by the tangential frictional force exerted by the pad on the wafer. The removal rate in CMP is defined as the average change in the thickness per unit time. Based on the often cited Preston's equation, the removal rate R is given by

$$R = K\nu P \qquad (2.5)$$

where K is the constant proportional to the coefficient of friction, ν is the relative velocity between the pad and the wafer, and P is the pressure arising from the load applied to the wafer. In reality, K is a function of number of parameters, such as the elastic properties of the abrasive oxide and the pad, contact area between the pad and the wafer, viscosity of the slurry, applied load, and the relative speed of the wafer. There have been several new models developed for the CMP process [2.20, 2.21]. They describe specific mechanical aspects of CMP, such as bending of pad, slurry flow, surface morphology, and patterning. A review of these models can be found in articles by Nanz and Camilletti [2.22] and Runnels [2.23]. Tseng and Wang [2.24] re-examined the

Preston equation by considering a combination of the particle indentation and slurry flow. An equation similar to the Preston equation was derived as follows:

$$R = MP^{5/6} V^{1/2} \qquad (2.6)$$

where M is the constant associated with material properties, P is the pressure, and V is the rotational speed.

It should be pointed out that the simple philosophy used for planarization is as follows: the recessed area is relatively protected while the other area is removed. Because abrasive particles, asperities on the pad, and features on the surface to be polished are in micrometers or fractions of micrometers in size, this principle can be extended to microscale in CMP of microelectronic materials. The key to develop a successful CMP model or to understand the mechanism of CMP is to find out how the microscale high spots on the wafer surfaces, which can be grains or clusters of atoms, are produced and removed, and how the low spots on wafer surface are protected while the new recessed areas are created.

2.5.2 Chemical

CMP chemistry contributes to the overall success of both dielectric (oxide) and metal CMP processes by promoting the material removal and maintaining the surface quality of the film to be polished. In CMP of silicon dioxide films, alkaline slurries are employed which can etch the oxide films while polishing. Cook proposed a reaction sequence that accounts for the role of both water and a chemically active abrasive in oxide CMP [2.25], and it was confirmed by other researchers that the importance of water

entry into the oxide during CMP is critical to achieve planarization without scratches [2.26]. They concluded that water entry is the operating mechanism of oxide CMP, which makes the mechanical removal of an oxide by an abrasive easier. It was found that the diffusion of hydrogen ions near the surface is a rate controlling parameter in the polishing behavior of oxide films [2.27].

The chemistry required for metal (Cu and W) CMP is very complex. Ideally, the slurry chemistry should allow fast corrosion or dissolution of higher spots while leaving the recessed area passivated. Kaufman proposed a model for metal CMP that is based on a sequence of steps involving the formation of the passive layer, removal of the passive layer, and reformation of the passive layer at the higher spots [2.28] (Figure. 2.6). Formation of metal oxide on top of metal films during some metal CMP processes has been experimentally detected [2.17]. Similar to the removal mechanism previously mentioned for oxide, mechanical cracking of the metal film under corrosion conditions should be considered as one of the mechanisms for metal CMP [2.4]. Metal CMP in general can be viewed as an erosion-corrosion process [2.18].

2.6 Cu-Contamination over SiO_2 Film during Cu-CMP

2.6.1 Contamination Coming from CMP Processing

During CMP, particle deposition may occur due to electrostatic interactions or due to the polishing pad pressure (mechanical). The electrostatic effects, which depend on electric charging of wafers and particles in an aqueous environment, appear to play a dominant role [2.18, 2.29]. CMP is inherently a “dirty” process in an “ultra pure world” because abrasive particles are used in the polishing slurry, and the slurry chemistry is a

mixture of many components, both organic and inorganic chemicals. In addition, the reaction products of the film during polishing can also contribute to contamination on wafer surfaces after CMP. For example, the dissolved copper species produced during polishing of copper can deposit onto the surrounding dielectric SiO_2 surfaces and cause process-induced metallic ion contamination [2.19].

Typical contaminants that are found on wafer surfaces after CMP and their effects on the device manufacturing are listed in Tables 2.2 and 2.3, respectively. As mentioned earlier, there are stringent requirements for defect levels on the wafer of device surfaces (Table 1.1). Consequently, surface cleaning plays a critical role in semiconductor manufacturing. A general cleaning process can be carried out by wet or dry methods. However, as stated by the International Technology Roadmap for Semiconductor (IRTS) [2.30], "Wet chemical cleaning technologies are favored because of the many inherent properties of aqueous solutions, such as the high solubility of metals, zeta potential control, and efficient sonic energy transfer for megasonic particle removal. Hence, wet chemical surface preparation methods are likely to continue to find wide application in the foreseeable future."

2.6.2 Methods for Post-CMP Cleaning

A complete CMP sequence has to end with an effective post-CMP cleaning process, which leaves the planarized surface defect free (particle and ionic contamination free) and ready for the subsequent steps in the fabrication sequence. Since CMP is a wet process, a wet post-CMP cleaning will be more desirable than other methods. In the

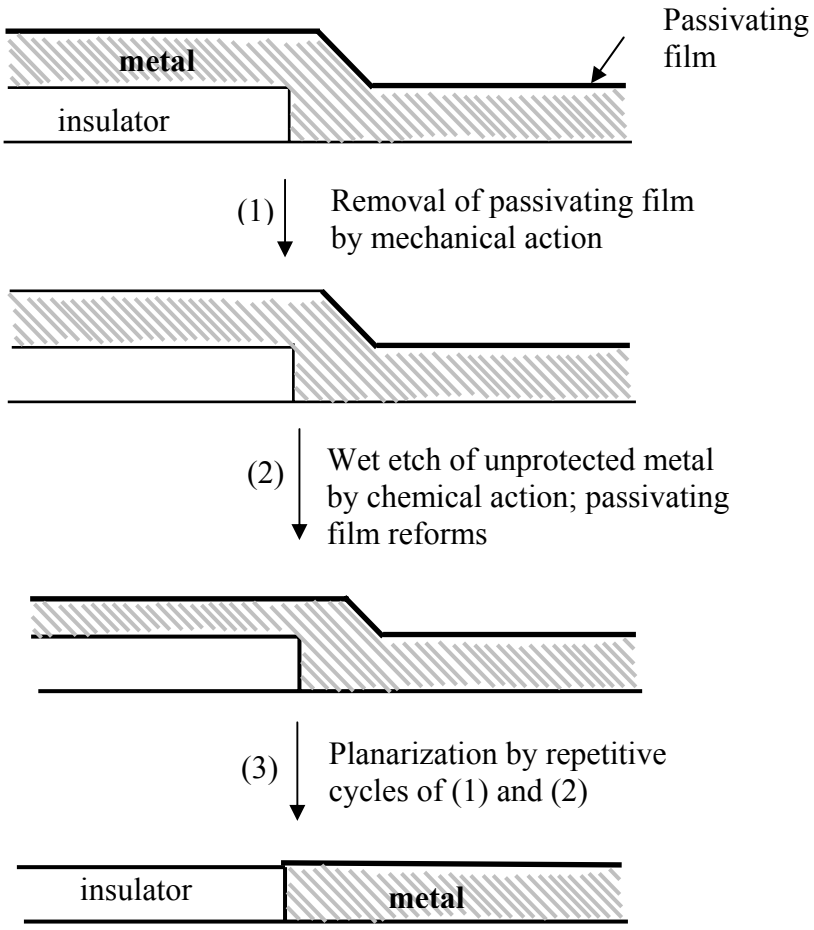

Figure 2.7 A model for metal CMP [2.27]

Table 2.2 Contamination after CMP Process

Contaminants	Oxide CMP	Metal CMP
Paticles	Silica	Alumina or silica, metal fragments
Metallic ions	K^+, Ca^{2+},	$W_xO_y^{(2y-6x)-}$, Cu^{2+}, Al^{3+}, Fe^{3+}, $Fe(CN)_6^{3-}$, $Fe(CN)_6^{4-}$, IO_4^-, I^-/I_2
Organic	Tetramethyl ammonium salts, buffers, surfactants	buffers, surfactants, inhibitors
Mechanical defects	Scratches, stress	Scratches, pudding, plug coring, dishing and erosion, stress

Table 2.3 The Effects of Contamination on Device Performance

Contaminants	Effects
Particles	Causes local roughness and blocks photolithography pinholes in new grown films Shorts by conductive particles
Metallic Contaminants	*Alkali metal ions* (*e.g.* Na^+): high mobility influences electrical characteristics (oxide breakdown field, flatband voltage, leakage current, etc)
	Copper: a fast diffuser in Si Moves in oxide under an electrical field Forms copper Silicide and affects oxidation rate of Si Reduces minority carrier life time Noble metal ions cause electrochemical etching of Si
	Iron and Calcium Remains in oxide after oxidation and degrades gate oxide integrity Ca affects cleaning efficiency of HF
	Aluminum Increases the oxidation rate of Si and the adsorption of water on oxide films.
Organic	Affects wettability and cleanability Promotes other contamination Outgassing during oxidation Poor adhesion of deposited layers

following discussion, only wet cleaning will be covered.

Post-CMP has some unique requirements compared with general non-CMP cleaning. The most obvious distinction may be that there will be much more particulate contamination (as well as metallic contamination after metal CMP than after other processes).

To remove particles from the wafer surface, both chemical and mechanical environments are required to loosen the particle/metal and sweep it away from the surface. Typical cleaning methods include: brush scrubbing, acoustic ultrasonic and megasonic energy for particle removal. Those methods are based on different theoretical considerations, but the result is the same - that is dislodging the particles from the surface. Once particles leave the surface, chemical environments are needed to separate the particle/metal from the surface. At this point, one common method used is the manipulation of surface zeta potentials. Zeta potential is a function of the electrolyte concentration and pH, decreasing with increasing pH and concentration. It is also affected by an addition of surface modifiers such as a surfactant. Thus by varying concentration of electrolytes and pH, or by an addition of a surfactant to brushing materials, one can manipulate the zeta potential at solid surfaces. When the signs of the zeta potential at solid surfaces (wafer and particles) are the same and absolute values are large, a strong repulsion occurs between the particle and the surface leading to particle separation from the surfaces of interest, and eventually to cleaning. To remove metallic, organic contamination after CMP, direct chemical cleaning is another option.

Megasonic Cleaning: Megasonic cleaning is a very effective method for removing particulate contamination [2.31]. Megasonic cleaning uses sonic waves (typically the frequency f = 0.7 MHz) generated by piezoelectric transducers. An oscillating transducer produces sonic waves and the acoustic wavelength, which couples high-frequency pressure waves into a cleaning bath. When the megasonic force exerted on a particle is greater than the van der Waals force between particle and wafer surface, the particle will be dislodged and swept away.

Brush Cleaning (Scrubbing): At present, most CMP cleaning is carried out using brush scrubbing. The most popular model used in the semiconductor industry is the double-sided scrubber from Lam Research. The double-sided scrubbing system is effective for removing both particulate and metallic contaminants in post-CMP applications [2.32]. During brush cleaning, DI water and certain chemicals flow through the brushes and are applied on the surface of spinning wafers. The important part of brush scrubbing is the direct wiping action of the brushes. The brushes, which are soaked with cleaning solutions, can be in direct contact with the wafer surface, providing a wiping motion that is essential to dislodge and wipe away the particles.

Chemical Cleaning: Different chemicals are used to clean different types of contaminants from wafers surfaces. During chemical cleaning, wafers are either immersed in a bath containing cleaning chemicals or the cleaning chemicals are directly sprayed onto wafer surfaces [2.33]. Most of the contaminants during chemical cleaning are either dissolved into bulk chemical solution or migrate away from wafers due to concentration gradients from the wafer surface to the bulk solution. In addition, a

pressure gradient caused by the liquid flow will exert a force at the particles thereby enhancing particle removal. If wafers are spun during cleaning, the centrifugal force will aid the contaminant removal. The purpose of each chemical used in semiconductor fabrication to remove various types of contaminants is summarized in Table 2.4

Chemical Cleaning Using Organic Complexants: Some organic compounds such as citric acid, ethylenediamine (EDA), ethylenediaminetetraacetic acid (EDTA), and phthalic acid have been studied in the cleaning industry [2.33]. These compounds form stable complexes with certain metal ions (Cu^{2+}, Fe^{3+}, Mg^{2+}) to help in removing metal ions adsorbed on wafer surfaces.

A simplified alkali cleaning solution reported by Morinaga et al. [2.34] was actually based on the concept that the addition of a chelating agent to the conventional SC1 [1:1:5 = NH_4OH (29%): H_2O_2(30%) : H_2O] cleaning solution can remove particle and metallic impurity simultaneously (see Table 2.5).

2.6.3 Slurry Considerations to Reduce Contamination after CMP

To eliminate the particulate and metal contaminations that typically occurs during polishing, a consistent high quality slurry is required. High quality slurry maintains its polishing performance while resisting changes to settling and agglomeration tendencies and is free of particle aggregates and agglomerates, as well as ionic contaminants [2.35]. The following factors should be considered when selecting an appropriate slurry for CMP process: pH, buffering agents, oxidizers, complexing agents, viscosity, and abrasive properties. pH affects the dissolution rate of the surface being polished, the formation of

Table 2.4 Summary of Chemicals Used for Silicon Wafers Cleaning

Solution Constituents	Purpose
HF (49%) + H_2O	Etch SiO_2
HF (49%) + NH_4F (40%)	Etch SiO_2
HF(49%) + H_2O_2(30%) + H_2O	Prevent metal deposition on silicon during HF processing.
HF(49%) + HNO_3 (69%)	Etch silicon
HNO_3 (69%)	Remove organics, heavy metals
HF (49%) + HCl (37%)	Prevent metal deposition on silicon during cleaning
HCl (37%) + H_2O_2 (30%) + H2O	Dissolve alkali ions and hydroxides (of Al^{3+}, Fe^{3+}, Mg^{2+}), desorb residual heavy metals by complexing with them
H_3PO_3 (85%)	Etch nitride
H_2SO_4 (98%) + H_2O_2(30%)	Remove heavy organics, oxidize silicon
O_3 (2 ~ 20 ppm) in H_2O	Remove organics, dissolve resists, form a passive oxide layer
H_2SO_4 (98%) + O_3 (2~20 ppm) + H_2O	Remove organics, oxidize silicon
KOH (45%)	Dissolve SiO_2, etch Si
KOH (45%) + IPA	Etch Si
NH_4OH (29%) + H_2O_2 (30%) + H_2O	Remove particles & light organics, desorb trace metals (Au, Ag, Cu, Ni, etc.)
$(CH_3)_4NOH$ (3% TMAH) + H_2O_2 (or surfactant)	Etch silicon, particle removal
$HOCH_2CH_2N(CH_3)_3OH$ (Choline) + H_2O_2 (or surfactant)	Remove particles, metals

Table 2.5 A Simplified Cleaning Recipe [2.34]

<table>
<tr><th colspan="2">Cleaning Solutions</th><th rowspan="2">Contamination</th><th rowspan="2">Removal Mechanism</th></tr>
<tr><th>Simplified</th><th>Conventional</th></tr>
<tr><td rowspan="3">APM(1) + MC1(2)</td><td>HPM(3)
HF/H_2O_2</td><td>Metals</td><td>1. Dissolution (ionization)
2. Prevention of redepositon by oxidizing or complexing agent.
3. Etching for removing metals in oxide film</td></tr>
<tr><td rowspan="2">APM</td><td rowspan="2">Particles</td><td>1. Lift off
(1) etching
(2) dynamic driving force by using high-T or megasonic cleaning tool</td></tr>
<tr><td>2. Prevention of re-deposition
(1) electrostatic repulsion</td></tr>
</table>

(1) APM is a mixture of NH_4OH (29%), H_2O_2 (30%) and H_2O.
(2) MC1 is a complexing agent.
(3) HPM is a mixture of HCl (37%), H_2O_2 (30%) and H_2O.

surface films on materials being polished, the stability of the abrasive suspension, surface charge characterization of abrasives, and the effectiveness of the abrasive. Buffering agents are used to keep the pH constant throughout the polishing process. For metal CMP, most of the chemical reactions are electrochemical in nature. Oxidizers react with metal surfaces to raise the oxidation state of the metal, resulting in either dissolution of the metal or formation of a surface film on the metal. For both tungsten and copper, the polish rate has been shown to be proportional to the rate of these oxidation reactions. Complexing agents increase the solubility of the film being polished, and hence increase the polish rate. Viscosity affects how easily the slurry flows. High slurry viscosity results in poor transport of both reactants and products to and from the wafer surface. Silica (SiO_2) is most often used as an abrasive for oxide polishing, while alumina (Al_2O_3) and silica are used for metal polishing. Abrasive size affects removal rate and surface damage. The distribution of abrasive size has a dramatic effect on surface damage. Monodispersion in abrasive size leads to extremely smooth surfaces, while higher abrasive concentrations leads to higher polish rates [2.4].

Above all, understanding complicated slurry chemistry and choosing an appropriate slurry for copper CMP is the first step towards a successful CMP process.

2.6.4 The Importance of Post-CMP Cleaning

A complete CMP process sequence will end with an effective cleaning process, leaving the planarized surface free of defects and contamination (metallic and particulate) and ready for the next step in the device/circuit fabrication sequence. By microelectronic fabrication standards, CMP is inherently a dirty process. A surface planarized by CMP

may have many undesirable features on or within the surface: particles – from the slurry or from the abraded surface and even from the surroundings; chemical contamination (metallic, inorganic, organic) from the slurry and/or chemical cross-contamination resulting from different materials present on the surface; or surface inclusions formed due to reactions with abrasive particles or pad materials [2.36]. For Cu-CMP, a post-CMP process not only needs to remove the particulate, organic/inorganic contaminations, but also needs to reduce Cu contamination to an acceptable level due to copper innate rapid diffusion in Si and SiO_2 and its impacts on device reliability[2.37].

CHAPTER 3

INTERACTION OF COPPER AND DIELECTRIC SiO_2 DURING Cu-CMP WET PROCESSING

In this chapter, the surface charge development on a dielectric SiO_2 surface in a wet CMP environment will be discussed. The complexation between Cu^{2+} and the functional surface group (SiOH) on SiO_2 surface will be reviewed.

3.1 The Schematic Copper Metallization Structure

Before the investigation of Copper/SiO_2 interaction, it is important to briefly review the Cu-CMP process and to illustrate where the interaction will take place. Figure 3.1 shown below is a schematic copper metallization structure before Cu-CMP, where the dielectric SiO_2 is covered with copper [3.1]. During polishing, copper is gradually removed from the dielectric SiO_2 surfaces by the chemical and mechanical forces coming from the slurry and polish pad/head. The removed copper is mostly in dissolved form (Cu^{2+} or its complex) due to the nature of the slurry (containing strong oxidizing agent, wet processing, complexing agent). Once polish gets on the dielectric layer (see Figure3.2), the copper or dissolved copper in the slurry will interact with SiO_2 leading to copper contamination. The following sections are focused on this interaction and the factors that affect the degree of this interaction.

3.2 The Surface Charge of SiO_2

It is well recognized that oxide surfaces can adsorb a large number of ions and molecules [3.2, 3.3] because molecules located at the surface of the solids experience an

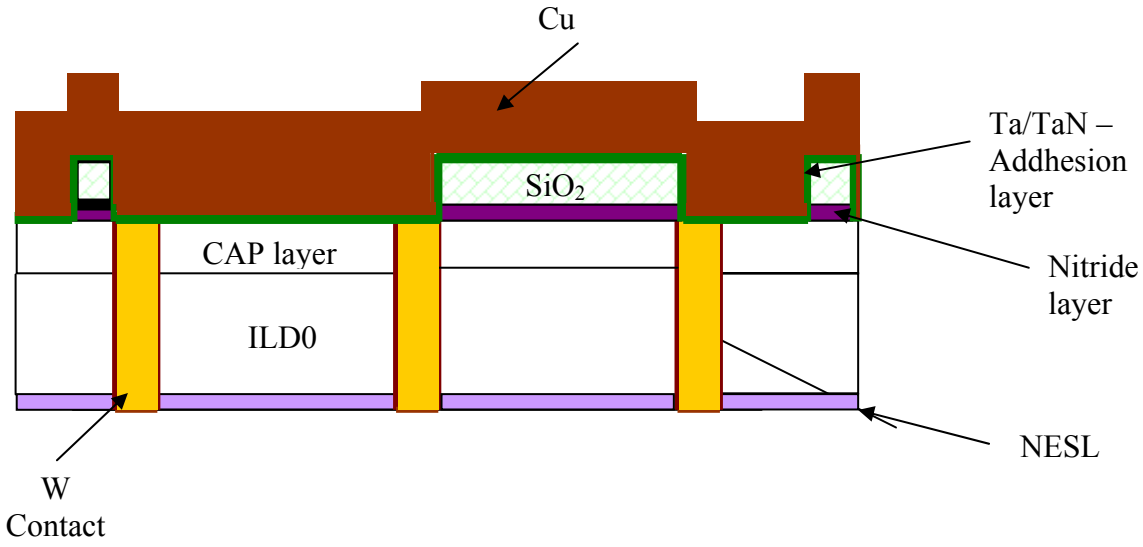

Figure 3.1 Schematic of copper metallization structure (not drawn to scale) --- before Cu-CMP

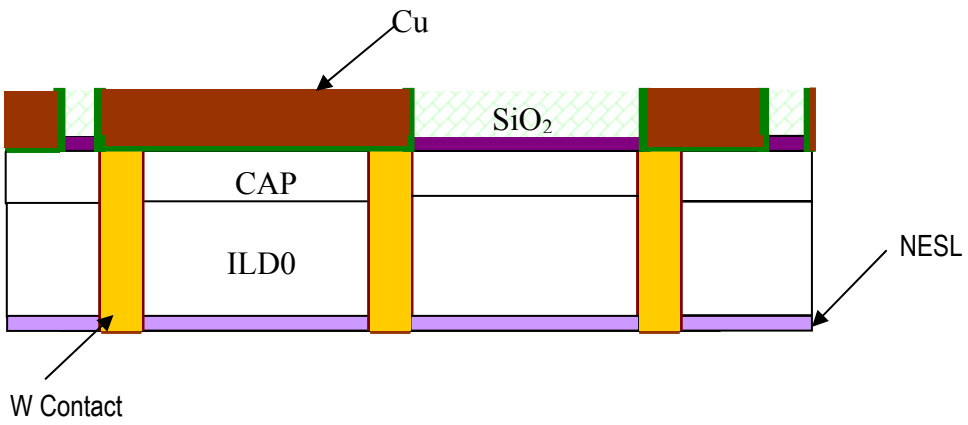

Figure3.2 Schematic structure of post Cu-CMP
(SiO_2 was exposed to the surface)

imbalance of chemical forces [3.4, 3.5]. One way for oxide surfaces to reduce the chemical imbalance is by accumulating cations and anions locally onto the surfaces.

The oxide surface accumulation processes contribute to the presence of hydrolyzed -OH sites at the oxide surfaces [3.5 3.6]. All the oxide surface reactions were related to this site either by forming complexes or ligand exchanges. In a wet CMP process, silica surface, like the surface of iron oxide, aluminum oxide, will have hydrolyzed –OH sites, which are also referred to as surface functional groups (≡SiOH). These functional groups on an oxide surface can behave like an acid by releasing the proton H^+, or like a base by combining with a H^+ depending on the pH of the solution. For SiO_2, in a system without specific adsorption, three species (≡SiOH, $\equiv SiO^-$, $\equiv SiOH_2^+$) exist on a silica surface and the chemical interactions among them are represented by the following reactions:

$$\equiv SiOH \leftrightarrow \equiv SiO^- + H^+ \qquad (3.1)$$

$$\equiv SiOH + H^+ \leftrightarrow \equiv SiOH_2^+ \qquad (3.2)$$

From the reactions shown above, it is obvious that silica surfaces become more negatively charged with an increase in pH because the surface species $\equiv SiO^-$ begin to dominate the surface at high pH. In other words, the net surface charge of SiO_2 is dependent on the pH of the solution in the absence of any specific adsorbed ionic species. Actually, these are the reactions that determine the surface potential of the silica surface.

3.3 Adsorption of Cu-Ions on SiO_2 surface

Cu^+ and Cu^{2+} have a tendency to compete with H^+ for active site ≡SiOH to chemically combine on SiO_2 surfaces. For the adsorption of metals onto a solid surface, e.g., Cu^{2+} onto silica, the surface reactions (which are basically ion exchange reactions) can be represented as follows:

$$\equiv SiOH + Cu^{2+} \leftrightarrow \equiv SiOCu^{+} + H^{+} \qquad (3.3)$$

$$2(\equiv SiOH) + Cu^{2+} \leftrightarrow (\equiv SiO)_2Cu^{0} + 2H^{+} \qquad (3.4)$$

From the reactions shown above, more Cu^{2+} will combine on the surface with the increase of pH because both equilibria (3.3 and 3.4) shift toward product formation. This indicates that more Cu^{2+} contamination will be present on dielectric for a Cu-CMP process that is conducted at higher pH. Also, the level of Cu^{2+} on the surface is clearly determined by the density of ≡SiOH on the surface (concentration of the active sites). More active sites will lead to more Cu^{2+} contaminants on SiO_2 surfaces than SiO_2 surfaces with less active sites at the same pH level. Based on this analysis, copper contamination on SiO_2 is dependent on pH, active site density on SiO_2 surfaces, and the free Cu^+ and Cu^{2+} level in solution. Reducing the pH, the free Cu^+ and Cu^{2+} concentrations in solution lower copper contamination level on SiO_2.

3.4 Chemistry of Citric Acid

Citric acid (below), is a tricarboxylic acid. Citric acid (CA) can dissociate into species H_2Cit^-, $HCit^{2-}$ and Cit^{3-} in a liquid soluiton. Its dominant species in a solution depends on the pH.

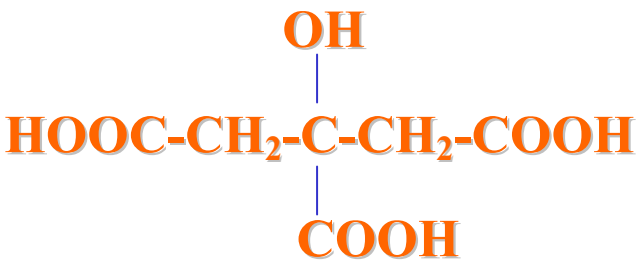

The dissociation reactions in water are shown below:

$$Cit^{3-} + 3H^+ \leftrightarrow H_3Cit \qquad \log K = 14.3 \qquad (3.5)$$

$$Cit^{3-} + 2H^+ \leftrightarrow H_2Cit^- \qquad \log K = 11.2 \qquad (3.6)$$

$$Cit^{3-} + H^+ \leftrightarrow HCit^{2-} \qquad \text{Log } K = 6.4 \qquad (3.7)$$

Citric acid, just like EDTA, EDA, and Phthalic Acid, has a strong tendency to form chelates with metal ions such as Cu^{2+}, Fe^{3+}, Mg^{2+} in a liquid environment and form very stable Metal-Citric complexes. In the presence of Cu^{2+}, the reactions are:

$$Cit^{3-} + Cu^{2+} \leftrightarrow CuCit^- \qquad \log K = 7.2 \qquad (3.8)$$

$$Cit^{3-} + H^+ + Cu^{2+} \leftrightarrow CuHCit \qquad \log K = 17.1 \qquad (3.9)$$

$$Cit^{3-} + 2H^+ + Cu^{2+} \leftrightarrow CuH_2Cit^+ \qquad \log K = 25 \qquad (3.10)$$

From the log K values shown above [3.6], it is not hard to determine that the Cu-CA complexes are stable once formed ($\Delta G^o = -RT\ln K$, so that $\Delta G^o << 0$)

3.5 Cu Contamination and Removal Methods

During Cu CMP processing, if copper is polished in a highly acidic pH regime, it leads to corrosion problems. However, Cu CMP conducted in alkaline conditions produces an unfavorable polish rate (SiO_2 removes faster in alkaline conditions) and will lead to high interlayer dielectric (ILD SiO_2) erosion. Thus, an intermediate pH range of 4 –7 appears to be a desirable choice for Cu CMP.

During Cu CMP, actually a Cu etching process, the reactions that take place at the metal/liquid interface increase the oxidation state of the copper and lead to the production of copper ion species, which, if not well controlled, will have the "opportunity" to combine onto SiO_2 surfaces once polish gets to SiO_2 layers. With the presence of complexing agents such as citric acid, EDTA, or phthalate acid in the slurry mixture, the ionic copper species will form stable complex with those agents, which will leave the solution with less free copper ionic species and therefore lead to less contamination over SiO_2 surfaces [3.7]. The most likely reactions describing this process are:

$$Cu\ (s) \rightarrow Cu^{2+} + 2e^- \qquad (3.11)$$

$$Cu(s) \rightarrow Cu^{+} + 1e^- \qquad (3.12)$$

$$2Cu^{+} + H_2O \rightarrow Cu_2O + 2H^{+} \qquad (3.13)$$

$$Cu^{2+} + 2\ (R\text{-}COO)^- \rightarrow Cu(OOCR)_2 \qquad (3.14)$$

In the reactions listed above, (R-COO-) represents a variety of complexing agents. It should be noted that reaction 3.11 and 3.12 are half-reactions and require corresponding reduction reactions to act as an electron sink. Oxidizing agents such as

hydrogen peroxide or dissolved oxygen are usually present in the slurry mixture and act as electron acceptors.

From a chemistry standpoint, an effective way to employ and prevent copper ion adsorption onto SiO_2 surfaces is by introducing additives, which are capable of forming stable, soluble complexes with copper ions, such that the copper ions remain in solution. The complex agent, citric acid, is one such complexing agent.

3.6 Surface Complexation of Cu^{2+} over SiO_2

It is believed that metallic contamination results from the interaction between the metal ions in solution and the solid wafer surface, which follows the same mechanisms as on colloidal particle surfaces [3.8, 3.9]. It has been noted that different metal ions behave differently. Strictly speaking, metallic contamination on oxide surfaces can be due to both the adsorption of dissolved metal species and the precipitation of insoluble metal compounds on the solid surface. During metal CMP processes, metallic contamination on the oxide surface occurs as a result of the adsorption of metal species because the CMP slurry is chemically designed to dissolve the removed metal films. Therefore, the discussion below is focused on the surface complexation between metal ions and the solid oxide surface.

The chemistry of SiO_2 surface used in IC is very similar to the chemistry of other particle oxides, such as iron oxides, and aluminum oxides [3.9]. Oxides usually possess a large surface area, and those surfaces have the tendence to accumulate cations and anions onto the surfaces of its hydrolyzed -OH sites [3.4]. A surface complexation model

(SCM) [3.11], which will be explained further in the next section, has been frequently used to quantitatively describe the reactions at oxide surfaces.

3.7 Surface Complexation Modeling (SCM)

3.7.1 Double Layer Theory and Zeta Potential

It is well known that solid surfaces can develop surface charges in an aqueous medium by many mechanisms; these include (i) adsorption of H^+ and OH^- ions, (ii) selective adsorption of positive or negative ions, (iii) ionization of surface groups, and (iv) fixed charges in the matrix structure exposed due to counter ion release. Regardless of the actual charging mechanism, the surface charge has to be balanced by the counter ions with an opposite sign, which is the basis of so called Electric Double Layer (EDL) theory (Figure 3.1). Crudely, the distance from the surface when the surface potential drops to 1/e its value (i.e. ψ_0/e) is called the "double layer thickness" (= $1/\kappa$). The double layer thickness is closely related to the ionic strength of the solution [3.12, 3.13].

The surface potential is not experimentally measurable. A more commonly used and experimentally measurable quantity is the zeta potential (ζ). As illustrated in Fig 3.3, zeta potential is the potential in the double layer at a short distance (i.e., typically of the order of a diameter of a hydrated counter ion) from the surface of the solid. Both surface potential and zeta potential are a function of the solution pH. Development of positive or negative charge at a given pH depends on the nature of the cation/anion bonding and the acid/base characteristics of the surface MOH groups (note: M denotes metal atom). The solution pH at which the surface bears no net charge is called the Point of Zero Charge (PZC). The solution pH at which the zeta potential $\zeta = 0$ is called the Iso Electric Point

(IEP). IEP equals PZC if adsorption of ions occurs completely by electrostatic forces. Some of the reported PZC values for materials of interest to the semiconductor industry are tabulated in Table 3.1.

3.7.2 Principles of SCM

Surface complexation modeling has been widely used to quantitatively define cation and anion distribution between an oxide solid surface and a bulk solution. In this study, SCM will be used to describe the interaction between Cu^{2+} and SiO_2 surfaces.

The principal of SCM [3.11] is as follows:

- Sorption of cation/anion on oxide surfaces takes place at specific coordination sites. (≡ Si-OH Site).
- Sorption reactions can be described using mass law equations.
- Surface charge results from the sorption reactions.
- The effect of surface charge on (further) sorption can be corrected by a factor derived from the electrical double layer (EDL) theory to the mass law constants for surface reaction.

Table 3.1 Reported PZC values of Some Materials

Material	PZC
Si	3 – 4
SiO_2	2 – 4
Si_3N_4	3 – 5.5
Al_2O_3	8 – 9
TiO_2	5 – 6
PVA	~ 2
Nylon	~ 6

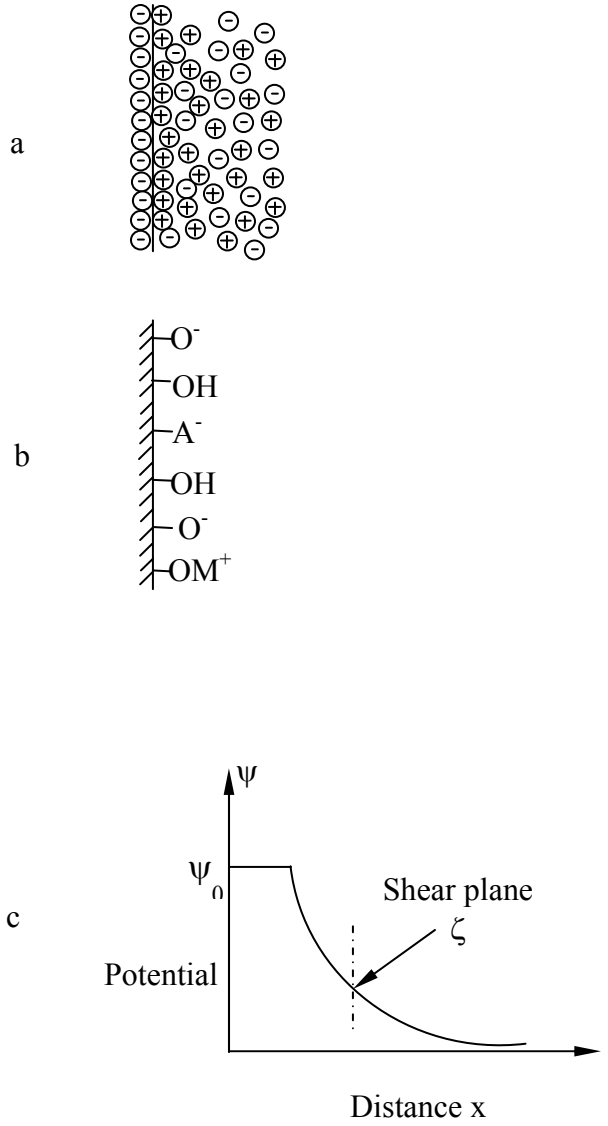

Figure 3.3 The diffuse double layer

a) Diffuseness results from thermal motion in solution.
b) Schematic representation of ion binding on an oxide surface on the basis of the surface complexation model.
c) The electric surface potential, ψ,falls off (simplified model) with distance from the surface. The decrease with distance is exponential. At the plane of shear (moving particle) a zeta potential can be established with the help of electrophoretic mobility measurements.

3.7.3 Solid-Liquid Interface Chemical Action

Based on the surface complexation model, the silica surface can behave as an acid or base depending on the solution pH. In a system without specific adsorption, three species exist on the silica surface and the chemical interactions among them are represented by the following reactions:

$$\equiv SiOH \leftrightarrow \equiv SiO^- + H^+ \qquad (3.15)$$

$$\equiv SiOH + H^+ \leftrightarrow \equiv SiOH_2^+ \qquad (3.16)$$

From eqs. (3.15) and (3.16), it is clear that the silica surface becomes less positive, or more negative, as the solution pH increases. This is because the species of $\equiv SiO^-$ begins to dominate the surface speciation at high pH values. The double layer criterion in the modeling is reflected by the Boltzmann equation, which relates the surface concentrations of species to their concentrations in the bulk solution. The Boltzmann equation can be written as

$$[M^{n+}]_s = [M^{n+}]_b \exp(-n\psi_0 F/kT) \qquad (3.17)$$

$[M^{n+}]_s$ where the surface concentration of ion M^{n+} with n^+ charge (note: the ion can also be an anion with a negative charge) is the concentration of M^{n+} in the bulk solution, ψ_0 is the surface potential (which can be approximated as the zeta potential), F is the Faraday constant, k is the Boltzmann constant, and T is the absolute temperature. In the case of eqs. (3.15) and (3.16), M is H^+ and n is equal to 1.

For the adsorption of metals onto a solid surface, e.g., Cu^{2+} onto silica, the surface complexation reactions can be written as follows:

$$\equiv SiOH + Cu^{2+} \leftrightarrow \equiv SiOCu^+ + H^+ \qquad (3.18)$$

$$2(\equiv SiOH) \leftrightarrow (\equiv SiO)_2Cu^0 + 2H^+ \quad (3.19)$$

Two of the important parameters in such models are the density of active-OH sites on the solid surface that can adsorb cation and anion species and the equilibrium constants of the surface adsorption reactions, both of which can be experimentally determined. Based on the mass law equations and the mass conservation principle, the level of metallic contamination on the solid oxide surface in a solution (containing a known initial amount of metal species and with a known pH and ionic strength) can be calculated using commercially available programs.

The copper species in water [3.6]:

$H^+ + OH^- \leftrightarrow H_2O$ LogK = 14.0

$Cu^{2+} + OH^- \leftrightarrow CuOH^+$ Log K = 7.69

$Cu^{2+} + 2OH^- \leftrightarrow Cu(OH)_2^o$ LogK = 13.68

$2Cu^{2+} + 2OH^- \leftrightarrow Cu_2(OH)_2^{2+}$ LogK = 10.18

$Cu^{2+} + 3OH^- \leftrightarrow Cu(OH)_3^-$ Log K = 26.85

Reactions on the surfaces for the case of Cu^{2+}/SiO_2 system:

$\equiv SiOH + H^+ \leftrightarrow \equiv SiOH_2^+$

$\equiv SiOH \leftrightarrow \equiv SiO^- + H^+$

$\equiv SiOH + Cu_s^{2+} \leftrightarrow \equiv SiOCu^+ + H_s^+$

$2(\equiv SiOH) + Cu_s^{2+} = (\equiv SiO)_2Cu^o + 2H_s^+$

For the reaction on the solid surface for one of the reactions ($\equiv SiOH + Cu_s^{2+} \leftrightarrow \equiv SiOCu^+ + H_s^+$), the K_s value will be:

$$K_s = \frac{[\equiv SiOCu^+]\{H_s^+\}}{[\equiv SiOH]\{Cu_s^{2+}\}} \qquad (3.20)$$

Where:

$$\{X_s^z\} = \{X_b^z\}\{e^{-z\Psi/RT}\}$$

S - surface;
b - bulk;
z - valence of ion,
Ψ - interfacial potential

Just like the reaction in the liquid, we know all the K_s values for the reactions on the surface, and therefore the amount of Cu^{2+} on the surface of SiO_2 can be calculated out.

3.7.4 Software Program

FITEQL and Minteqa2 are geochemical equilibrium speciation modeling computer programs for dilute aqueous systems [3.14, 3.15]. These models can be used to calculate the equilibrium composition of dilute aqueous solutions. It can also be used to extract the surface acidity constant based on Acid-Base titration results and calculate out the surface binding constants based on adsorption data. Considering multiple solid phases under a variety of conditions, the models can calculate the mass distribution between dissolved and adsorbed species.

The data required to predict the equilibrium condition consist of a chemical description of the sample model including total dissolved concentrations for the components of interest and any other relevant invariants including pH and ionic strength.

Prodefa2 is an interactive program designed to ask questions about the chemical system to be modeled and build the appropriate Minteqa2 input file from the answers.

Minteqa2/Prodefa2 software program [3.14] was used in our case to assist in the calculation of copper distribution between bulk solution and SiO_2 surfaces.

The model inputs for the case are:

Site density (OH-Site/nm^2); {2 OH-site/nm^2 for Cabosil (300) SiO_2}
Surface Area of Particle/Wafer (m^2/g); {416 m^2/g for Cabosil(300) SiO_2}
Solid concentration (g/L)
Total Cu concentration;
log K values for the reactions (in solution and surface).
Ionic Strength
pH

Model Outputs:
Equilibrium concentrations of species in solution and surface (adsorbed).
Cu^{2+}, $CuOH^{+}$, $Cu(OH)_2$, $Cu(OH)^{3-}$, $Cu_2(OH)_2^{2+}$ (in solution)
$(\equiv SiO)Cu^{+}$, $(\equiv SiO)_2Cu^{o}$, $(\equiv SiO^{-})$, $(\equiv SiOH_2^{+})$ (on surface)

Based on model output the equilibrium Cu concentration

Copper in aqueous phase = $[Cu^{2+}] + [CuOH^{+}] + [Cu(OH)_2] + [Cu(OH)^{3-}] + 2[Cu_2(OH)_2^{2+}]$

Copper adsorbed = $[(\equiv SiO)Cu^{+}] + [(\equiv SiO)_2Cu^{o}]$

The software program, FITEQL, is used to extract particle SiO_2 surface acidity constants based on Acid-Base titration results. It also is used to extract the copper and particle SiO_2 binding constants based on copper adsorption data with particle SiO_2. See Appendix A for the input and output data fields of the software program.

CHAPTER 4

EXPERIMENTS AND RESULTS OF Cu-SiO_2 INTERACTION

In this chapter, the material and methods that are used to conduct the Cu contamination reaction over SiO_2 will be presented. The results will be then discussed to facilitate the understanding of Cu^{2+}/SiO_2 interactions.

4.1 Materials and Methods

4.1.1 Wafers

6'' TEOS wafers were used for the copper contamination immersion experiments.

4.1.2 Chemicals:

Citric acid solutions used in this study were prepared from citric acid monohydrate purchased from Fisher.

Cupric nitrate (99.3%) from Sigma was used to prepare the copper based solutions.

Semiconductor grade chemicals (i.e., H_2O_2, KNO_3, NH_4OH, HCl, HNO_3, KOH) were used in this study. Unless otherwise notified, all pH adjustments were made with KOH or HNO_3.

4.1.3 Uptake Measurement of Copper by Silica Particle and TEOS wafer

Cu uptake on particle: The uptake of copper onto high purity Cabosol (330) silica surface was determined through the analysis of the copper level in the bulk solution after uptaking by using a Perkin-Elmer Atomic Adsorption Spectrophotometer (AAS) (model 2380) technique. The experiments were conducted by suspending ~ 0.5g SiO_2 in

solutions that contained various concentrations of Cu ions (1 ~ 120 ppm). The pH 4.0 and 6.0 were maintained by adding dilute 0.01 M KOH and 0.01 M HNO_3. Prior to Atomic Adsorption (AA) analyses, the supernatants were achieved by centrifuging (Beckman J2-21).

Contamination experiments on wafer surface: Copper contamination on TEOS wafer surfaces was carried out on a Bold Technologies wet bench with 625CP temperature controller, 870R resistivity monitor, and 870D Auto-Kleen. Six inch wafer samples were immersed in a quartz bath containing copper ion spiked solutions. After contamination, wafer samples were rinsed in overflow DI water for a certain period of time. All wafers were dried using a Laurell Technologies WS-200-8NPP\HFP single wafer spin dryer at ~ 4000 rpm for 1.5 min.

4.1.4 Cu Contamination Analysis on Wafer Surface

The technique of total X-ray fluorescence (TXRF) was used to measure copper contamination on flat wafer surfaces. A Rigaku 3700 system with a minimum detection limit of 2×10^9 atoms/cm^2 was used to carry out TXRF measurements.

4.1.5 Surface Area Measurements

The specific surface areas of alumina (Degussa) and Cabosol (300) SiO_2 were measured on a Quantachrome Monosorb® surface area analyzer using a 30% He-N_2 gas mixture at a pressure of ~20PSIG(1.055 kg/cm^2). The Cabosol SiO_2 used in the study of copper adsorption has an average surface area of 416 m^2/g based on three measurements results of 10.229 g SiO_2.

4.1.6 Electrophoresis Measurements

The zeta potential measurements on particles were carried out using Delsa 440 (Coulter). The zeta potential measurements were performed on a series of SiO_2 systems under different chemical conditions to determine the impacts of isoelectric point shifting with the adsorption of copper on the surfaces.

4.1.7 Titration to Determine Surface Complexation Constants

4.1.7.1 Acid-Base Titration

An acid-base titration method was used to determine the surface acidity constant and the surface site density of the SiO_2 surface. A radiometer (Titralab ABU93) triburette with VIT 90 video titrator was used to complete these measurements. Regent grade HCl (0.00591 M) and KOH (0.0052 M) solutions were used as titrants. The ionic strength employed was 1 M KNO_3, and the initial particle used was 3.633 g/l. The surface acidity constant and surface OH-site density was calculated with the assistance of a FITEQL computer program (Herbelin and Westall, 1996). Titration results are included in Appendix A. (FITEQL in/outputs were used in determining the Cabosil(300) surface acidity constant which has log k = -5.9 and surface site density which is 2 OH site/nm^2).

4.1.7.2 Extraction of Equilibrium Sorption Constants

FITEQL version 3.2, a computer program, was used to determine chemical equilibrium constants from experimental data.

To solve the equilibrium problem at the solid liquid interface using the SCM model, parameters need to be determined. The program used to extract parameters for the SC model is the general nonlinear least square optimization program FITEQL [4.1].

This program yielded best fit parameters to experimental data by adjusting parameters in a chemical equilibrium model [4.2]. Traditional graphical methods may yield biased results due to the approximations required to implement the complicated calculations. In contrast, nonlinear optimization programs are fast and applicable to complex systems over extended ranges. The algorithm used in FITEQL in determining the optimal values of equilibrium constant, site density, and surface binding constants are briefly listed below:

- Define the Chemical Equilibrium Model (Reactions).
- Input the total component concentrations, known K values; guessed unknown K values for the chemical model.
- Input the (titration or adsorption) experimental equilibrium data (total concentrations, free concentrations).
- Compute equilibrium concentrations based on the input K values and the experimental free concentrations.
- Compute the residuals Y_R = Total $_{(cal)}$ - Total $_{(exp.)}$ for all "R" components. The final goal is to minimize the sum of the squares of these residuals.
- Test for convergence.

If convergence is achieved, the optimum parameter values (K values, site density concentration) will be selected. If convergence is not achieved, a designed mathematics approach will be used to get an improved estimate for the unknown K values until convergence is reached.

4.1.8 Surface Complexation Modeling (SC Modeling or SCM)

Surface complexation modeling work of copper contamination onto Cabosol (300) was conducted using Minteqa2/Prodefa2 (version 3.0). The acidic constant used for SiO_2 solid surfaces was extracted based on the acid/base titration results with SiO_2 particles. The Copper binding constants over SiO_2 used in this modeling work were calculated based on a copper adsorption isotherm (see next paragraph for detail).

Adsorption studies to extract the Cu binding constant on SiO_2: To determine the Copper binding constants with SiO_2 surfaces, copper adsorption as a function of pH was conducted. A suspension containing 1 ppm copper, an ionic strength 0.1M (KNO_3), SiO_2 particle 0.5456 g, and Deionized (DI) water 200 ml was used for the experiments. The pH of the solution was monitored constantly, and the free Cu ions in solution were measured using a copper selective electrode (Cole-Parmer). FITEQL computer program was employed to perform the calculation of Copper binding constants based on adsorption results. See Appendix A for FITEQL in/out put.

4.2 Results and Discussion for Cu contamination over SiO_2

4.2.1 Cu contamination over TEOS

4.2.1.1 Solubility of Cu in the Presence of CA

Solubility of $Cu(OH)_2$: Based on the reactions and equilibrium constant K values listed below, the Copper/H_2O speciation diagram was plotted. As shown in Figure 4.1, the solubility of copper is clearly pH dependent. It needs to be noticed that for pH >7.5, less than 1 ppm copper solution can lead to $Cu(OH)_2$ precipitation [4.3].

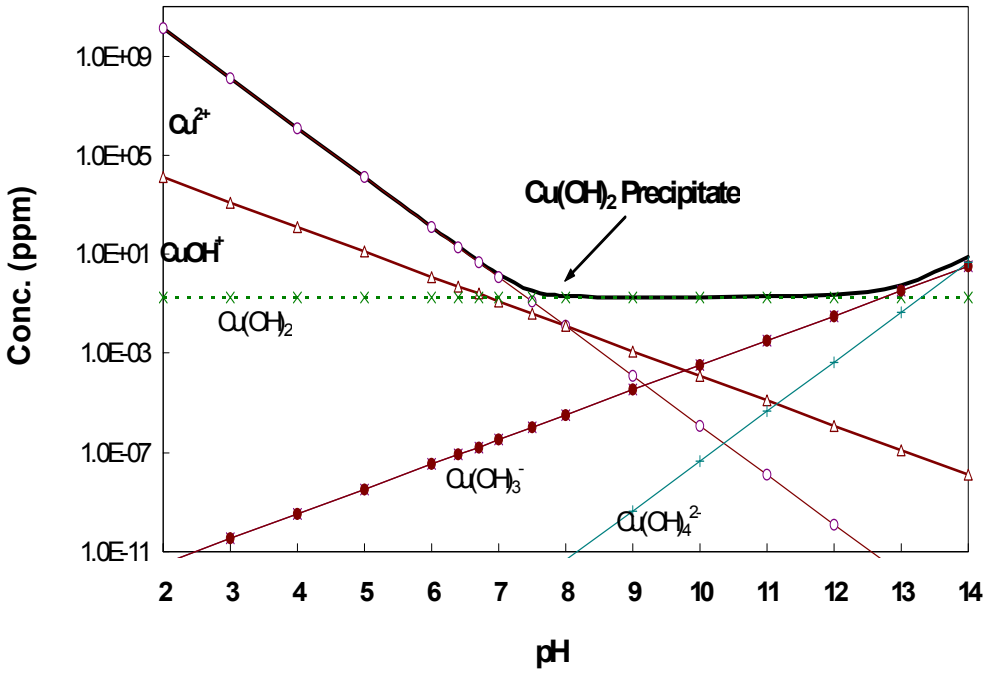

Figure 4.1 $Cu(OH)_2$ solubility as a function of pH

$H^+ + OH^- \leftrightarrow H_2O$ LogK = 14.0

$Cu^{2+} + OH^- \leftrightarrow CuOH^+$ Log K = 7.69

$Cu^{2+} + 2OH^- \leftrightarrow Cu(OH)_2^o$ LogK = 13.68

$2Cu^{2+} + 2OH^- \leftrightarrow Cu_2(OH)_2^{2+}$ LogK = 10.18

$Cu^{2+} + 3OH^- \leftrightarrow Cu(OH)_3^-$ Log K = 26.85

Solubility of $Cu(OH)_2$ in the presence of CA: If 100 ppm CA is added to a copper solution, the solubility of copper in solution ($Cu/CA/H_2O$) will be enhanced greatly as shown in Figure 4.2. This result indicates that the addition of CA to copper polish slurry may prevent the formation of $Cu(OH)_2$ precipitation (a particulate contamination) when polishing is conducted at high pH. The reactions used to make this plot, in addition to the reactions above, are listed below:

$Cit^{3-} + 3H^+ \leftrightarrow H_3Cit$ log K = 14.3

$Cit^{3-} + 2H^+ \leftrightarrow H_2Cit^-$ log K = 11.2

$Cit^{3-} + H^+ \leftrightarrow HCit^{2-}$ log K = 6.4

$Cit^{3-} + Cu^{2+} \leftrightarrow CuCit^-$ log K = 7.2

$Cit^{3-} + H^+ + Cu^{2+} \leftrightarrow CuHCit$ log K = 17.1

$Cit^{3-} + 2H^+ + Cu^{2+} \leftrightarrow CuH_2Cit^+$ log K = 25

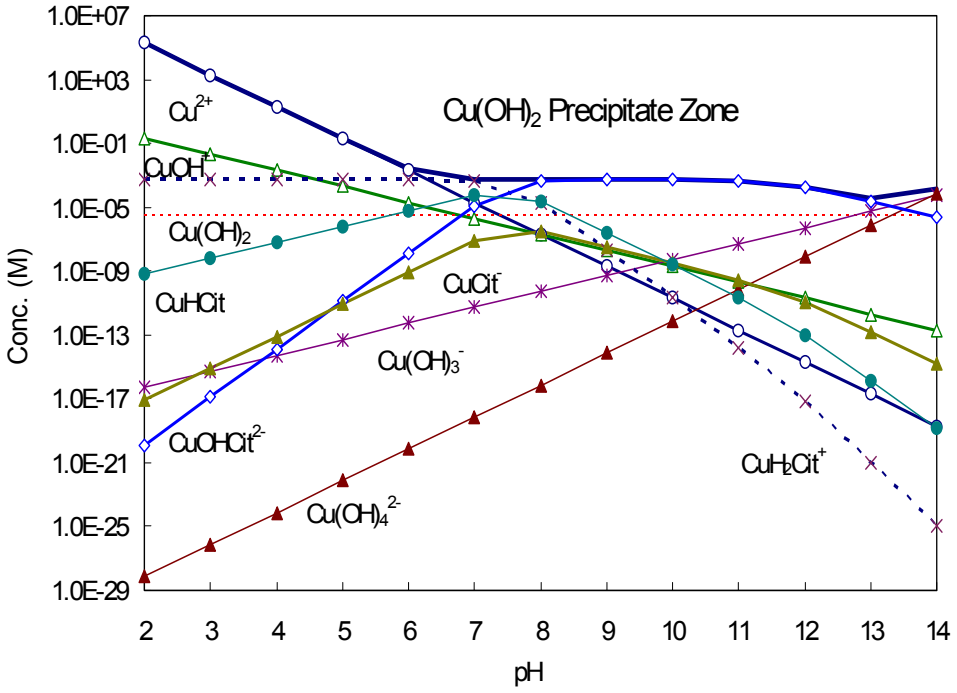

Figure 4.2 $Cu(OH)_2$ solubility in the presence of 100ppm CA

4.2.1.2 Copper Adsorption on TEOS Wafer Surfaces

The extent of copper adsorption on SiO_2 wafer surfaces was measured out by submerging TEOS wafers into copper containing solutions at control pH values. The results showed that the adsorption is both pH and concentration dependent. High pH and high Cu level in the solution led to high copper contamination on the SiO_2 surface. As discussed above, at higher pH, the SiO_2 surface is more negatively charged, and the surface will be more favorable for Cu^{2+} to bind on.

$$\equiv SiOH + Cu_s^{2+} \leftrightarrow \equiv SiOCu^{+} + H^{+}$$

$$2(\equiv SiOH) + Cu_s^{2+} = (\equiv SiO)_2Cu^{o} + H_s^{+}$$

4.2.1.3 Copper Adsorption Kinetics

To understand the copper adsorption mechanism, it is important to know the adsorption kinetics. If copper adsorption is a slow process, the impact it poses to a silicon device may not be as dangerous as we thought. To investigate copper adsorption kinetics, a series of TEOS wafers were dipped into a solution that contained 50 ppm dissolved copper at pH 6. The wafers were removed from the solution and analyzed as a function of time. The results in Figure 4.4 show the copper adsorption on TEOS is kinetically a very fast process. Empirically, equilibrium is reached in < 0.5 minute for a copper level of 50 ppm.

4.2.1.4 Desorption Results

To fully understand copper adsorption mechanisms, desorption experiments were conducted. A series of wafers were initially dipped into a solution that containing 50

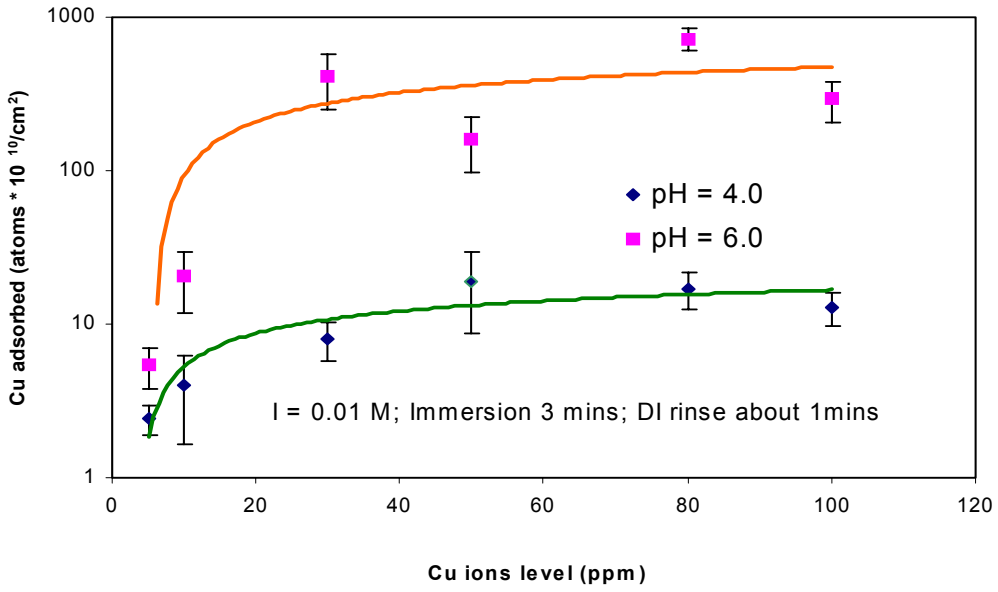

Figure 4.3 Cu adsorption isotherms at pH =4.0 and pH = 6.0
on 6" TEOS-SiO_2 wafer surfaces

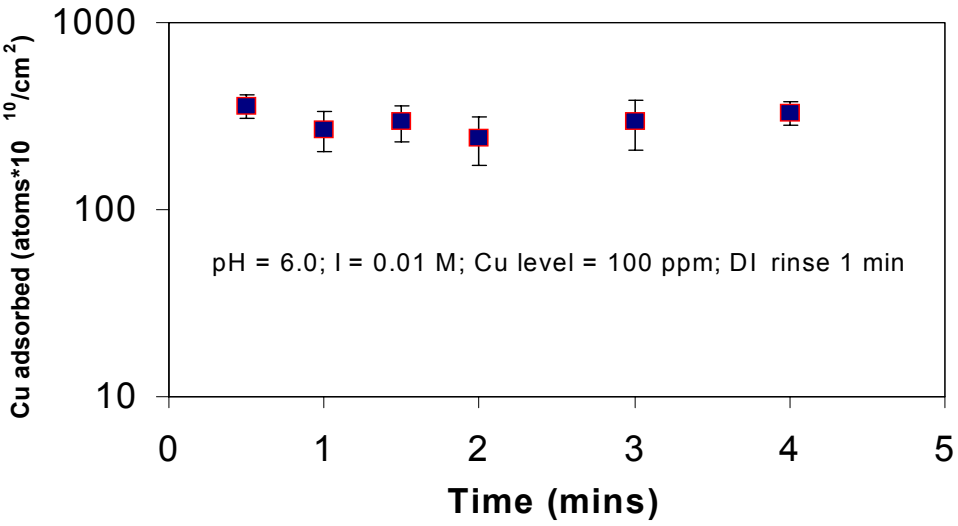

Figure 4.4: Copper adsorption kinetics study

ppm dissolved copper ions with a pH either at 4 or 6 for a dipping time of 1 min. The copper contaminated wafers were then transferred into a water bath with DI water overflowing through the bath for various rinsing times (from 0 to 10 mins). The wafers were taken out of the DI-water bath, spin-dried, and analyzed as a function of time. The surface copper level was analyzed using TXRF technique. As shown in the Figure 4.5, the adsorbed copper on TEOS wafer surface is partially irreversible, especially at pH 6. These results also show that DI water rinsing alone is not sufficient to remove the copper deposited ions (Cu^{2+}) on the wafer surface, especially for polishing conducted at a high pH condition. At a high pH, the surface is more negatively charged and more sites will be available for copper to form double binding over SiO_2 [$(\equiv SiO)_2Cu^o$], which is a stronger bonding than [$(\equiv SiOCu^+$]. It also needs to be noticed that DI rinsing is a very common method used by the electronics Iidustry to clean the device during fabrication. These results indicate that DI water alone is not able to remove the adsorbed copper effectively from SiO_2 surfaces during post-CMP cleaning, especially for polishing conducted at a pH >6.0.

4.2.1.5 Copper Adsorption on TEOS in the Presence of CA

To reduce copper adsorption onto SiO_2 surfaces during CMP wet processing, 100 ppm CA was added to 50 ppm copper containing solution at pH 6.0. The results (Figure 4.6) show that the presence of CA will inhibit the uptake of Copper ions on TEOS-SiO_2 surfaces. Data show that CA alone is able to suppress copper uptake by two orders of magnitude at a pH of 6.0. As shown in the reactions below, the addition of CA will lead

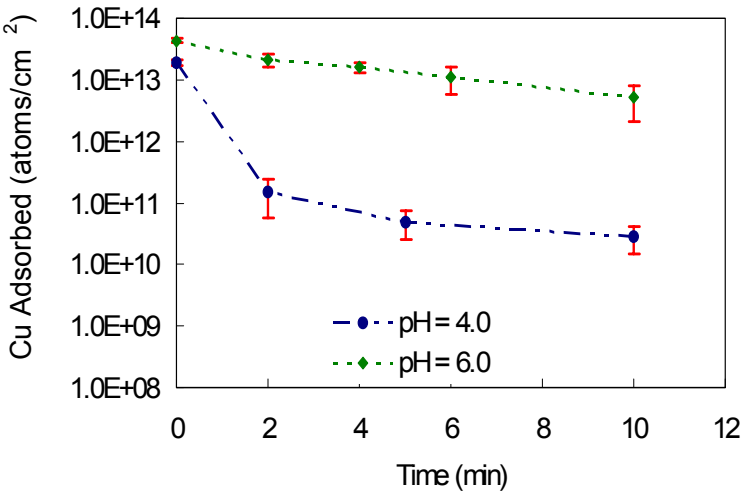

Figure 4.5 Desorption of Cu from silica surface as a function of time at pH = 4.0 and 6.0 respectively

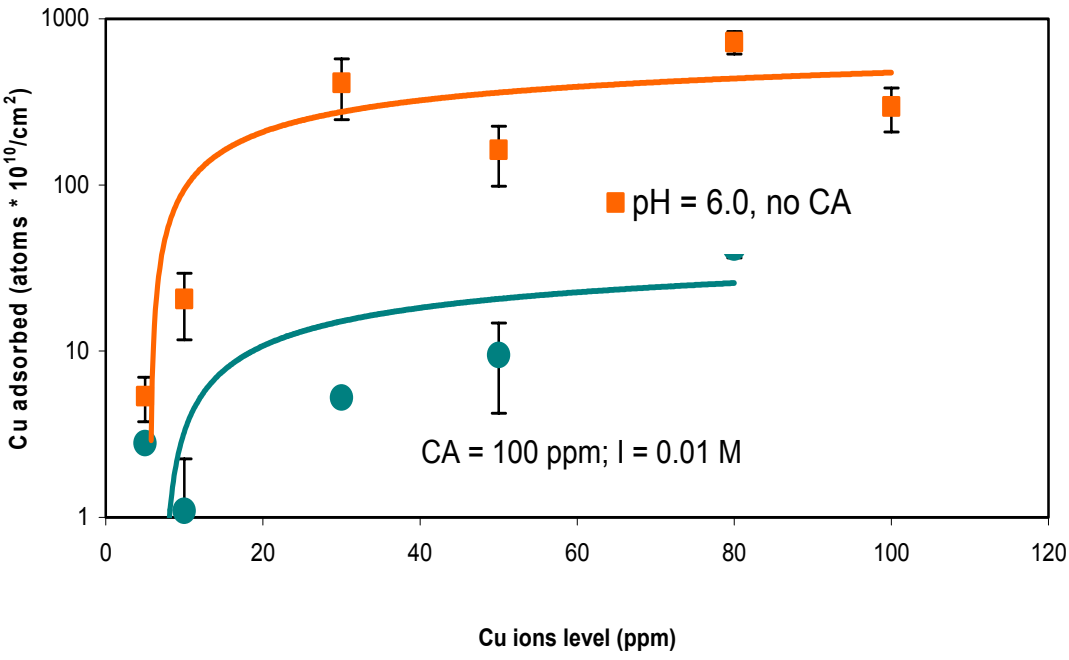

Figure 4.6. Cu adsorption in the presence of CA (I = 0.01 M, Immersion for 3 minutes, DI rinse for 1 minute)

to less free Cu^{2+} ions in the solution (most will be in complex form) and form either neutral charged CuHCit or negatively charged CuCit- at pH = 6.0; as a result, less copper adsorption was seen on SiO_2.

$Cit^{3-} + Cu^{2+} \leftrightarrow CuCit^{-}$ log K = 7.2

$Cit^{3-} + H^{+} + Cu^{2+} \leftrightarrow CuHCit$ log K = 17.1

$Cit^{3-} + 2H^{+} + Cu^{2+} \leftrightarrow CuH_2Cit^{+}$ log K = 25

4.2.1.6 Citric Acid in removing deposited Copper from TEOS-SiO_2 surface

To further test the effectiveness of Citric Acid in Cu-CMP post cleaning, two SC1 cleaned TEOS wafers were dipped into a solution that contained 50 ppm dissolved copper at a pH of 6 for 1 minute. After a DI rinse and spin dry, one wafer was dipped into a DI solution that contained 100 ppm CA. The TXRF results on those two wafers are shown in Figure 4.7. The results clearly indicate that CA can effectively remove deposited copper ions during post Cu-CMP cleaning if applied. As shown in the Figure 4.7 below, ~ 3 orders removal was achieved.

4.2.1.7 Copper Ion Uptake in the Presence of 5% H_2O_2

An oxidant such as H_2O_2, is typically added in a Cu-CMP slurry, either to raise the valence of metal (Cu to Cu^{+}, or Cu^{2+}) or to form oxide films to enhance the mechanical removal rate. The effects of H_2O_2 on copper adsorption on SiO_2 during Cu-CMP were also investigated. The experiments were conducted by dipping pre-cleaned TEOS wafers into a solution containing 5% H_2O_2 and various amounts of copper ions. Solution pH was monitored and maintained at 6 by adding KOH or HNO_3. As depicted

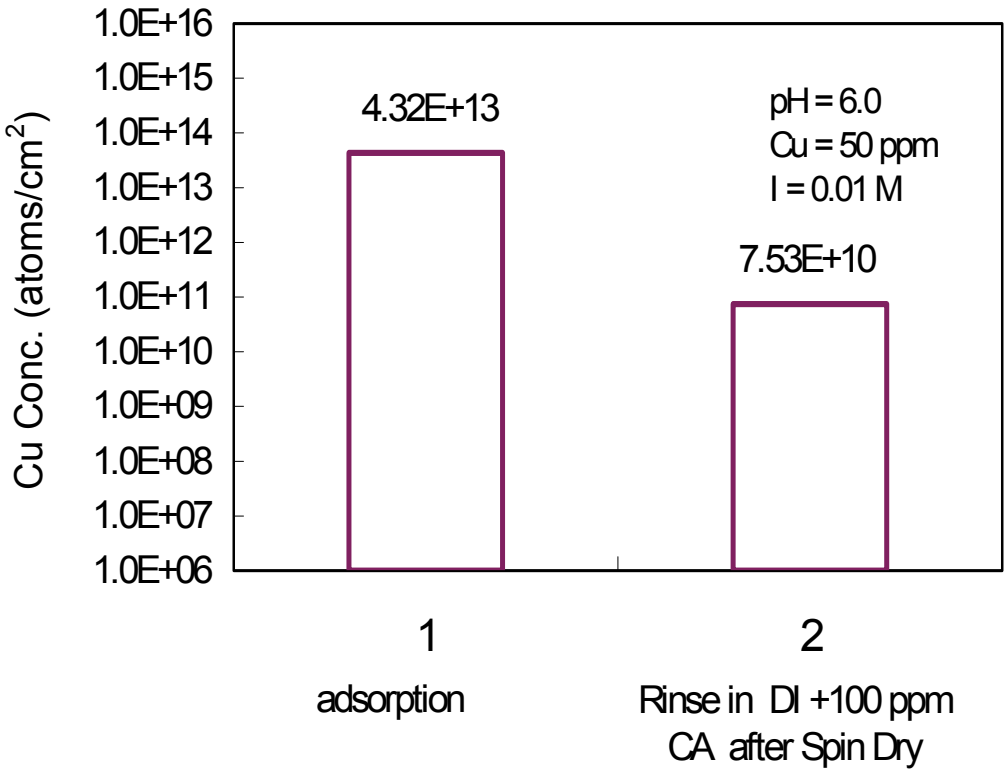

Figure 4.7 Removal deposited copper ions using CA (wafers were immered in 50 ppm copper solution at pH = 6.0 for 1 min, then spin dried and back dipped into DI water containing 100 ppm CA)

in the plot, the addition of 5% H_2O_2 enhances Cu contamination over TEOS.

4.2.1.8 Copper Ion Uptake in the Presence of CA and H_2O_2

To further test CA as an effective method to reduce copper ion deposition onto SiO_2 in the presence of 5% H_2O_2, a set of experiments were carried out using solution that contained 5% H_2O_2, 100 ppm CA and various amount of dissolved copper. The solution pH was maintained at 6.0 by adding diluted HNO_3/KOH. The results clearly show that CA is very effective in reducing copper ion adsorption onto SiO_2, even in the presence of oxidant H_2O_2; the amount of copper adsorbed reduced from ~ 10^{13} atoms/cm^2 to ~10^{10} atoms/cm^2.

4.2.1.9 Copper Uptake in the Presence of BTA, H_2O_2, and CA

Benzotrazole (BTA) is a copper corrosion inhibitor. It is widely used in Cu-CMP slurry to reduce the copper corrosion. The strong oxidant H_2O_2 is also found in most Cu-CMP slurry. It is important to know how these compounds affect copper contamination over SiO_2. In one set of experiments, 0.001 M BTA was added to a copper containing solution. In second set of experiments, 0.001M BTA and 5% H_2O_2 both were added to a copper containing solution. In third one, 0.001 M BTA, 5% H_2O_2, as well as 100CA were added to a copper containing solution. Experimental results are plotted in Figure 4.10. As shown in the plots, the addition of CA and 5% H_2O_2 greatly reduced the amount of copper adsorbed onto SiO_2 surface in the presence of BTA. This may be caused by the formation of CA and copper complexes which are more stable than the copper-BTA complex.

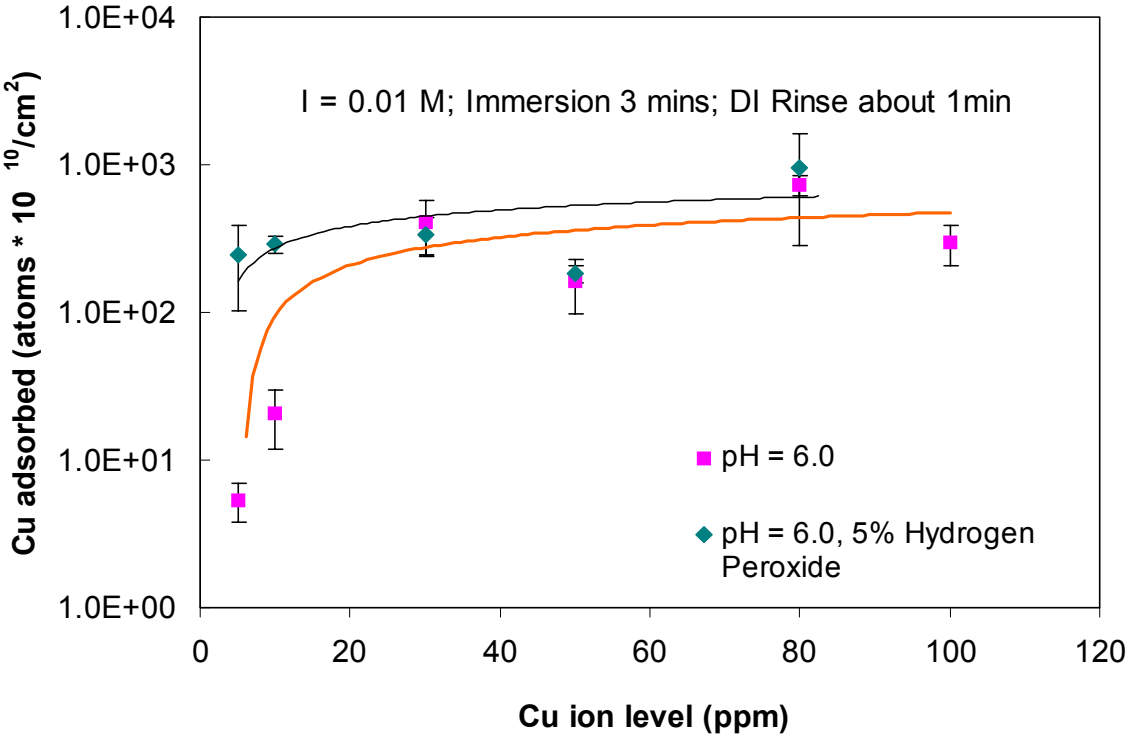

Figure 4.8 Cu adsorption on SiO_2 (TEOS) in the presence of 5% H_2O_2

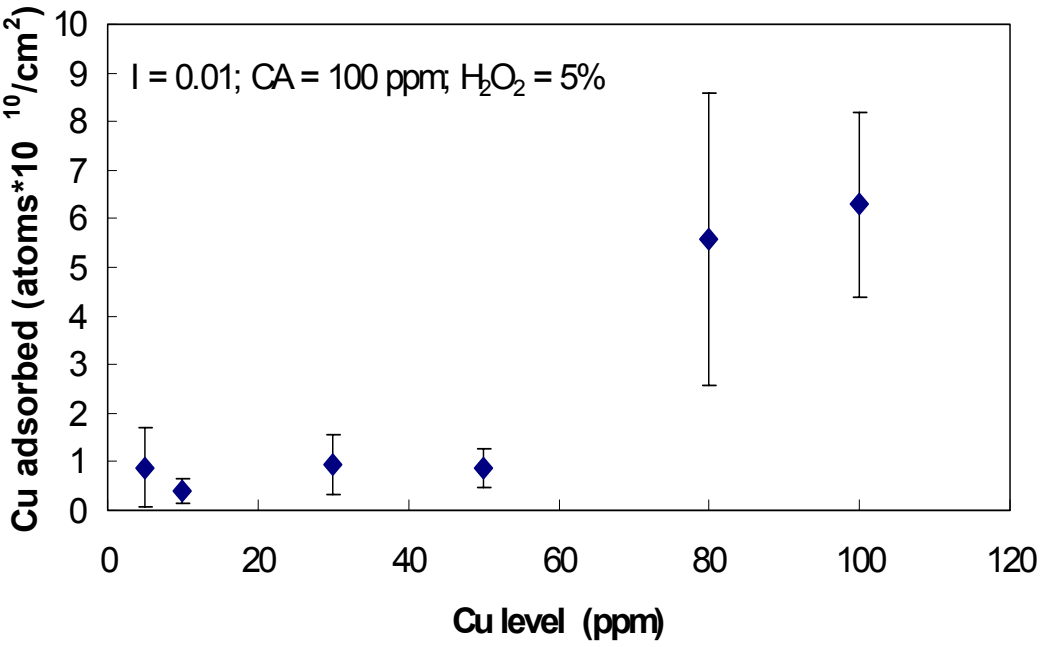

Figure 4.9: Copper adsorption on TEOS-SiO_2 in the presence of 5% H_2O_2 and 100ppm CA at pH = 6.0, I = 0.01M

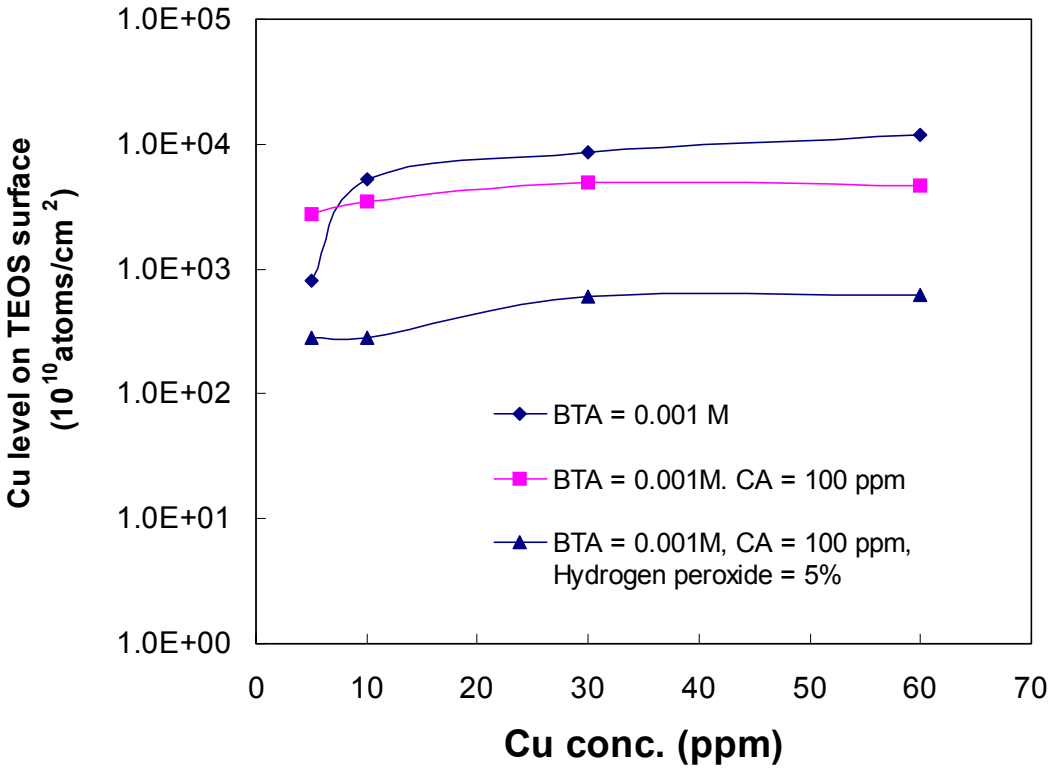

Figure 4.10 Cu adsorption on SiO_2 in the presence of BTA

4.2.2 Results on Cu Interaction with SiO_2 Particles

To study the interaction of Cu^{2+} and SiO_2 thin film, another approach used is to understand the interaction of Cu^{2+} with SiO_2 particles. For particles, there are methods available to measure the surface area, to obtain the surface functional site density. But for a wafer, there is still no available means to measure the surface SiOH site and surface interaction area besides the physical surface area.

4.2.2.1 IEP of SiO_2 Surfaces

To study the copper ions adsorption on SiO_2, electrophoresis was employed. First, 0.4 g SiO_2 was added to a 1 liter solution that contained a dissolved copper level at 0 ppm, 10 ppm, 100 ppm, and 1000 ppm respectively. The pH value was then adjusted using KOH/HNO_3 to the desired pH range. As the results in Figure 4.11 show, SiO_2 has an IEP about 2.5, while $Cu(OH)_2$ has a IEP about 9.5. With the increase of Cu concentration from 10 to 1000 ppm, the electrokinetic behavior of SiO_2 gradually shifted to the behaviors similar to $Cu(OH)_2$. The results indicate that the precipitate $Cu(OH)_2(s)$ formed at high copper concentration and pH level may tend to form a coating over the SiO_2 surfaces and shift the electrophoretic behavior of SiO_2 to $Cu(OH)_2$.

4.2.2.2 Copper Adsorption Isotherms

To study the copper contamination on SiO_2 surfaces, two adsorption isotherms on SiO_2 particles surfaces were obtained. The aqueous phase copper concentration was measured using an AAS. The results indicate that the adsorbed copper at a pH of 6 can reach $\sim 10^{13}$ atoms/cm^2, and at pH 4 $\sim 10^{11}$ atoms/cm^2. The adsorption is strongly pH

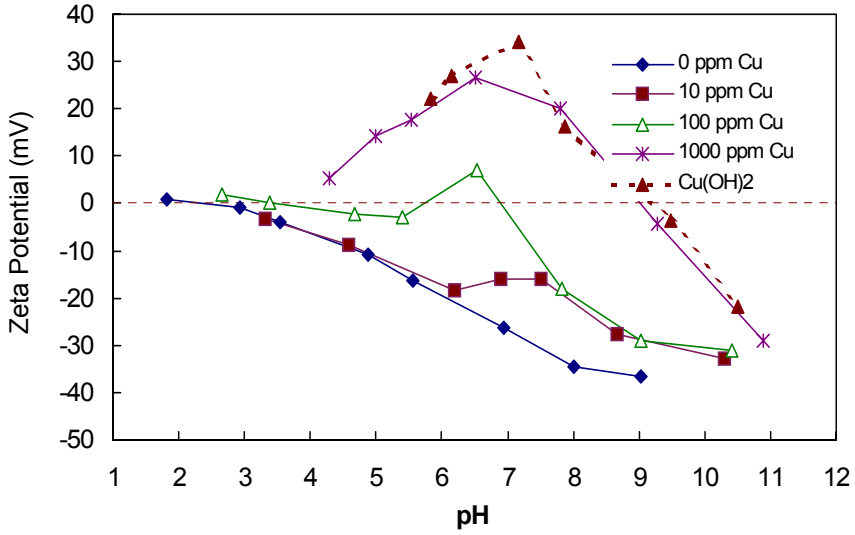

Figure 4.11 Zeta potential of cabsoil silica at different copper level

dependent. In another experiment, 0.8184g of SiO_2 particles was added to a container containing 300 ml DI. ~0.3g KNO_3 was added to the container to have an ionic strength 10^{-2} M. Additionally, N_2 was passed into the solution to keep air from entering the container. The solution also initially contained 1 ppm dissolved copper. The pH value of the solution was adjusted using KOH/HNO_3, and the dissolved copper level was monitored using a copper selective electrode. The results in Figure 4.12 clearly show the pH dependence of copper ion adsorption.

4.2.2.3 Titration Results and Model Parameters

An acid-base titration method was used to determine the surface acidity constant and surface site density of SiO_2 surfaces. A radiometer (Titralab ABU93) triburette with VIT 90 video titrator was used for these measurements. Regent grade HCl (0.00591 M) and KOH (0.0052 M) solutions were used as titrants. The ionic strength employed was 1 M KNO_3, and the initial particle used was 3.633 g/l. The surface acidity constant and surface OH-site density were calculated with the assistance of FITEQL computer program.

To extract the equilibrium constants for Cu adsorption on SiO_2, the FITEQL, a general nonlinear least square optimization program, was used to complete this work. The algorithm used in FITEQL in determining the optimal values of equilibrium constant, site density, and surface binding constants has been discussed briefly above. The results extracted from the titration and Cu adsorption isotherm are summarized in Table 4.1.

4.2.2.4 SCM Prediction of Copper Adsorption Isotherms

Surface complexation modeling was applied to predict the copper uptake levels. The parameters for running SCM are shown in Table 4.1. The model predictions were compared with experimental results and were shown in Figure 4.14 and Figure 4.15. As shown in the figures, the model prediction agrees with experiment results.

4.2.2.5 Distribution Predicted by SCM Model

The SCM model can be used not only to predict the contamination level, but also to predict the species distribution, which helps us better understanding the bond strength of the contamination. The result shown in Figure 4.16 is plotted based on one of the model output. It is shown that at pH greater than 5.5, the dominate adsorbed copper species will be in $(\equiv SiO)_2Cu^0$, which is a stronger bonding (double bonding) over $(\equiv SiOCu^+)$. This result also assists the understanding of the de-sorption result conducted at pH 6.0. That desorption experiment shows that it is much harder to remove the deposited copper adsorbed at pH 6.0 than coppers adsorbed at pH 4.0. Because the adsorbed copper at pH 6.0 is mostly double bonded to the SiO_2 surface, DI alone may not be enough to break the bonding and remove the copper.

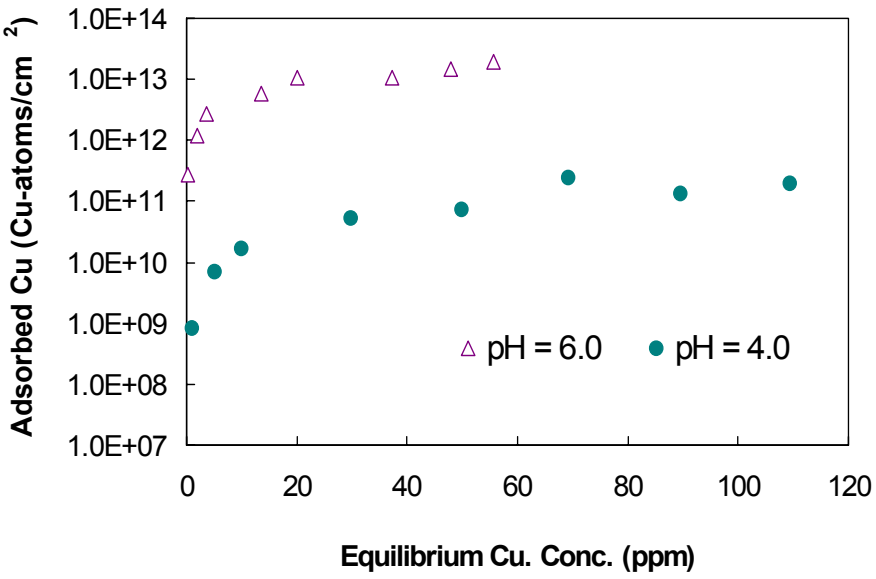

Figure 4.12 Cu adsorption isotherms on silica particles

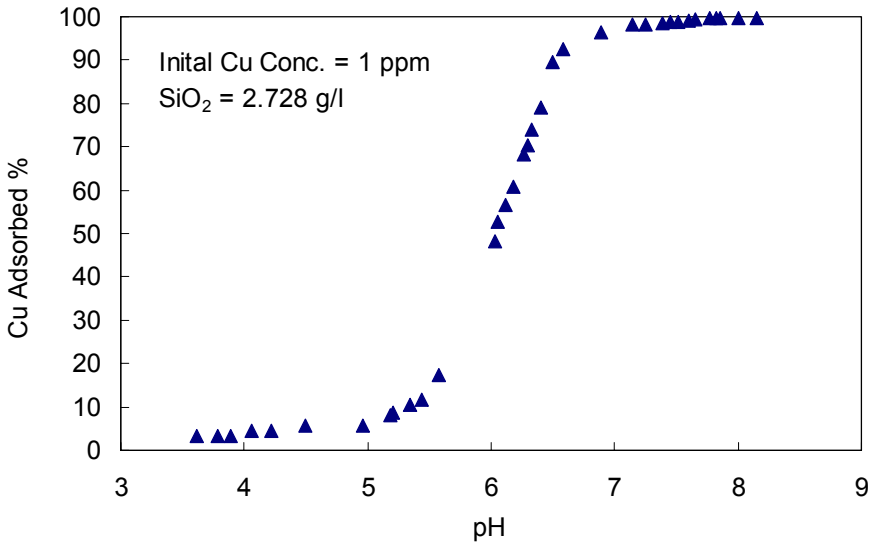

Figure 4.13 Cu adsorption on silica as a function of pH

Table 4.1 Parameters Used in SC Model (the parameters are extracted from Acid-Base Titration data, Cu adsorption data and Surface area measurements)

Parameters	**Values**
Site density (≡SiOH)	2 OH Sites/nm^2
Surface area	416 m^2/g
Solid Conc.	5 g/l
Surface Acidity Constant pK_{A1} $\equiv SiOH \leftrightarrow \equiv SiO^- + H^+$	5.9
Cu Binding Constant pK_1 $\equiv SiOH + Cu_s^{2+} \leftrightarrow \equiv SiOCu^+ + H^+$	4.35
Cu Binding Constant pK_2 $2(\equiv SiOH) + Cu_s^{2+} \leftrightarrow (\equiv SiO)_2Cu^o + 2H_s^+$	8.22

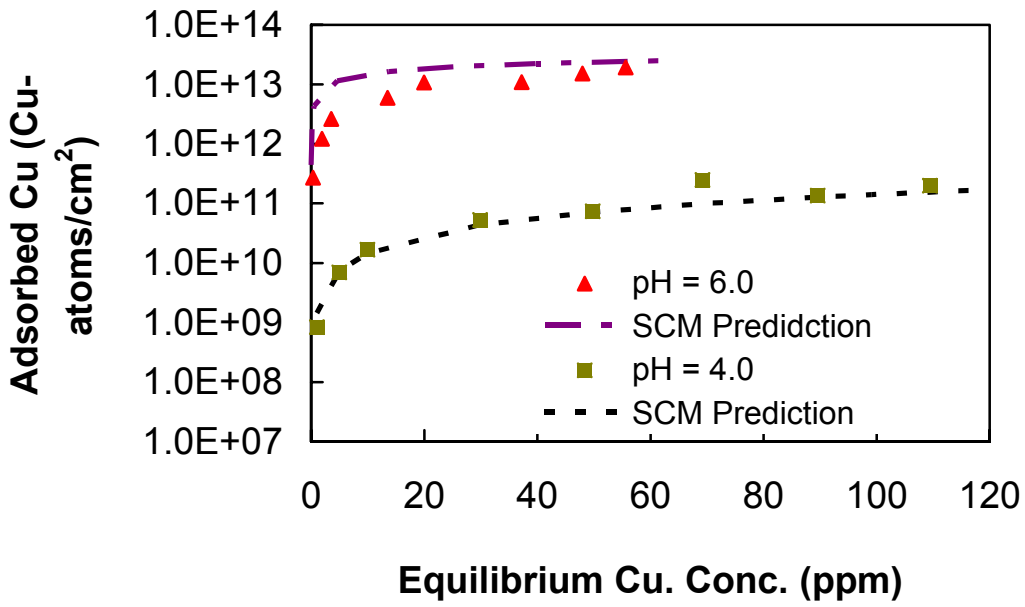

Figure 4.14 Adsorption isotherms and SCM predictions on Cu contamination over SiO_2 particles

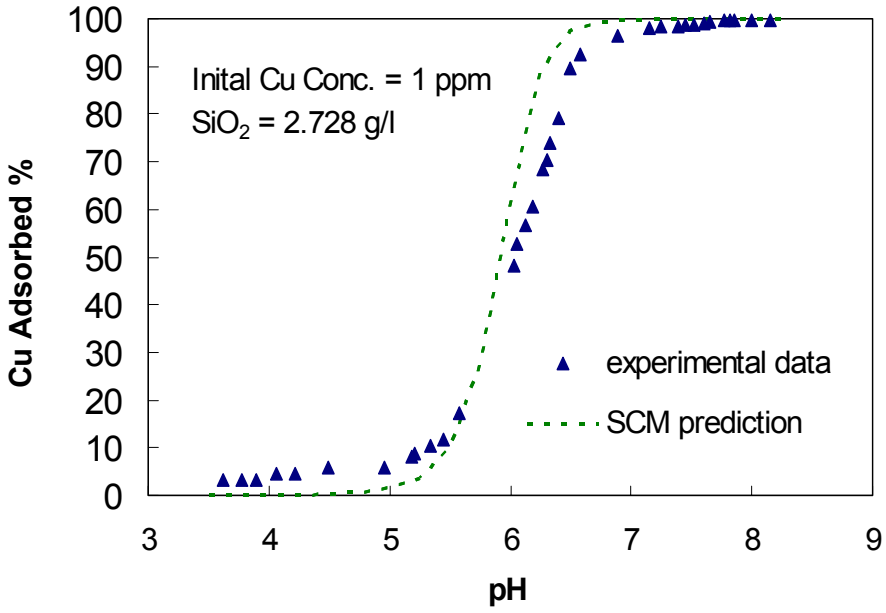

Figure 4.15 SCM modeling result on Cu adsorption

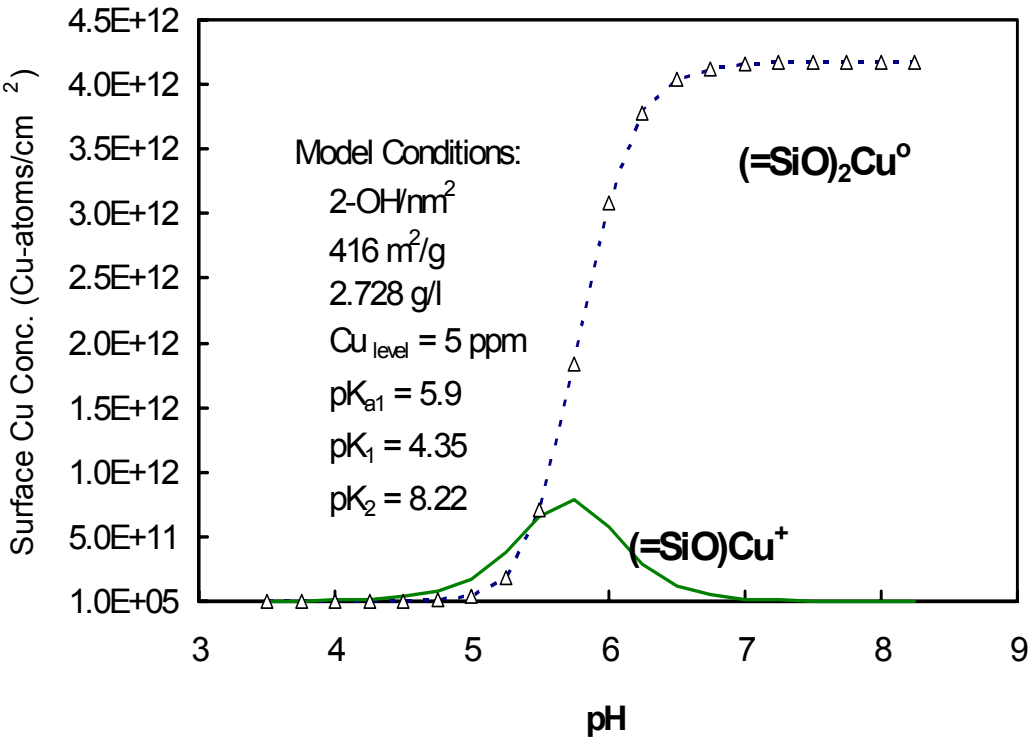

Figure 4.16 SCM prediction on surface bonding species

4.3 Conclusions on Copper Contamination over SiO2 during CMP Polishing

- Copper in the slurry generated during Cu-CMP polishing has a "great opportunity" to contaminate the dielectric SiO_2 surfaces due to the nature of the polishing process; especially, the copper ionic species can contaminate the SiO_2 surface through surface complexing mechanisms.
- The degree of copper contamination on dielectric SiO_2 is pH and copper concentration dependent. For 1 ppm copper in solution, adsorption barely starts at pH = 4.0, and as the pH approaches 7.0, nearly 100% of copper can be adsorbed to SiO_2, given enough surface area for adsorption. The adsorption isotherms of copper on colloidal SiO_2, at both pH = 4.0 and pH = 6.0, follow Langmuir adsorption behavior. Based on this result, choosing the right pH for Cu-CMP polishing to achieve acceptable copper contamination level on dielectric surfaces is critically important.
- From the copper speciation diagram (Figure 4.1), and copper adsorption results at pH=4.0 and pH=6.0, if Cu CMP was conducted at high pH (pH > 6.0), copper not only has a great tendency to be adsorbed on the SiO_2 surface, but also forms $Cu(OH)_2$ precipitate and causes copper-particulate contamination. Based on those results, slightly acidic polishing condition is recommended.
- The copper desorption results show that DI water alone is not able to remove the copper completely from SiO_2 surfaces during ≤10 minutes overflow rinse, especially for adsorption conducted at higher pH, where the dominant Cu-

SiO_2 bonding is bidentate [$\equiv(SO)_2Cu$] and it is well accepted that breaking a bidentate chemical bond requires more energy than breaking a single chemical bond.

- The results with Citric Acid in copper adsorption experiments have proven that Citric Acid is an efficient copper adsorption "suppresser". The addition of complex agents to Cu-CMP slurry or during post Cu-CMP cleaning is recommended to reduce or eliminate copper contamination.
- Surface complexation modeling (SCM), which combines coordination chemistry and a diffusion double layer model, provides a useful tool in predicting Cu and other metal contamination over oxide surfaces. The SCM model not only can predict the contamination level, also can be used to predict the species distribution on solid surfaces, which helps us better understand the bond strength of metal contamination.
- In a real Cu-CMP process, a variety of additives are added to the slurry, such as hydrogen peroxide, Cu corrosion inhibitors, and Cu complexing agents. It is important to consider and understand the impacts of those additives on Cu contamination over SiO_2. The adsorption results have shown that the addition of 5% H_2O_2 or 0.001M BTA will increase the copper contamination over SiO_2, but the addition of Citric Acid with H_2O_2 and BTA will reduce copper contamination significantly.

CHAPTER 5

Cu-CMP EFFLUENTS AND ENVIRONMENTAL REGULATION

The concept of an environmentally friendly manufacturing fab (i.e. GREEN FAB) emphasizes the three Rs – Reduce, Recycle, and Replace --- which translate into reducing chemical usage, recycling water, developing alternative/replacement chemistries that generate less waste and/or being more environmental friendly [5.1, 5.2]. CMP, due to its large consumption of water and slurry/chemicals, and the metal copper content in its Cu-CMP effluents, has attracted the attention from both academia and industries to develop the technologies to facilitate water and copper recycle/reuse [5.3, 5.4]. In this chapter, the physical and chemical characteristics of waste streams generated from Cu-CMP and its potential environmental impacts are discussed.

5.1 Cu-CMP Effluent

The demand for an ever-higher integration and speed has prompted semiconductor manufacturers to shift to copper interconnect technology. The use of the Chemical Mechanical Polishing (CMP) process that was originally developed to planarize interlayer dielectric layers (oxide layers) was expanded to manufacture copper interconnects (Cu CMP). The main consumables in a CMP process are slurry, a polishing pad, and water. Investigations of a 'slurryless' CMP process using fixed abrasive pads has been conducted; however, currently almost all production facilities utilize slurries for planarization. Current CMP operations generate significant amounts of wastes in the semiconductor industry [5.4]. It is estimated that a typical polisher in semiconductor fab can generate ~ 1600ml waste per minute. In addition, slurries used in metal CMP

typically consist of alumina particles or silica particles at a pH of approximately 4-7, it also contains metal ions, organic complexants and corrosion inhibitors.

To comply with ever increasing environmental regulations and meet the International Technology Roadmap for Semiconductor (IRTS) expectation and guidelines, the solids and metal ions need to be removed from the waste slurry stream for safe disposal [5.5, 5.6]. Due to the large volume of water used in CMP, recycling of the processed water is of considerable interest, especially for the fabrication facilities located in an arid environment.

5.1.1 The Characteristics of Copper CMP Wastewater

Wastes from CMP operations are typically very dilute suspensions of colloidal particles and contain certain chemicals. Metal CMP wastes typically contain alumina or silica particles, metal in free ionic form or combined with complexing agents, residual oxidants such as hydrogen peroxide, iodate or ferric nitrate, residual corrosion inhibitors such as benzotriazole, a complexant such as an organic amine, and in all likelihood a buffering agent [5.3, 5.4, 5.7]. Solid concentration in CMP wastes is typically in the range of 0.05 to 0.5%, depending on the amount of water used in and around the tool, tool type and drain segregation. The size of silica particles in the wastes can vary from 70 to 180 nm, depending on whether colloidal or fumed silica particles are used in the slurry. Alumina particles in the wastes show a much broader distribution than silica particles and are roughly in the 100 to 200 nm size range.

Inorganic contaminants are derived from abrading the wafer surfaces, and include metal/semi-metal oxides and low-k hybrid materials. Oxidizers such as peroxide are

commonly present, as are acids and other materials from the cleaning processes. Most of inorganic materials will be in an oxidized from, or if in the form of solids, they will have a surface oxide layer.

Organic materials found in CMP wastewater include pad and adhesive debris, corrosion inhibitors, metal complexing agents, surfactants, stabilizers, dispersing agents, organic acids/bases and other additives. The quantity and type of organic material can vary substantially from one slurry manufacturer to another.

Wastewater pH plays a major role in the relative solubility of the inorganic contaminants. For most metals CMP waste, at pH > 7, insoluble metal oxides or hydroxides are formed. At low pH conditions, transition metals such as copper are highly soluble. The solubility of many organic materials is also pH dependent. Benzotriazole is an example of a copper complexing agent that is soluble at low pH. It serves as a surface corrosion inhibitor in copper plating processes, and helps regulate the rate of copper removal in CMP. Table 5.8.1 below summarizes some chemical species found in Cu-CMP processes and wastewater.

5.1.2 Model System for Cu-CMP Waste Stream

As discussed above, Cu-CMP waste is very unique in character, as it contains dissolved copper ions, complexing agents, oxidizers, inhibitors, and submicron colloidal suspended solids. The industry CMP effluents vary substantially across manufacturers. In this study, the model Cu-CMP waste used to systemically study copper and slurry particle removal is defined as follows:

Table 5.1 List of Chemical Species Found in CMP Wastewater [5.8]

Inorganic Materials
Interconnect: Cu^{2+}, complexed Cu^{2+}, Cu_2O, CuO, $Cu(OH)_2$, WO_3, Al_2O_3, $Al(OH)_3$, Fe^{2+}/Fe^{3+}
Barrier/Liner: Tantalum and Titanium oxides and oxynitrides
Abrasives: SiO_2, Al_2O_3, CeO_2
Oxidizers: Hydroxylamine, $KmnO_4$, KIO_4, H_2O_2, NO_3^-
Strong Acids and weak buffering acids: HF, HNO_3, H_2SO_4, HCL, H_3BO_3, NH_4^+
Strong and weak bases: NH_3, OH^-, TMAH, Choline Base
Organic Materials
Dispersants/surfactants: Poly(acrylic acid), quaternary ammonium salts, alkyl sulfates
Corrosion inhibitors: Benzotriazole, alkyl amines
Metal chelators: EDTA, Ethanol emines, EDA, oxalic and citric acid
Organic Acid: poly(Acrylic), oxalic, citric, acetic, peroxyacetic

- A typical Cu-CMP waste may contain 0.1 – 0.4 w/v% abrasive particles (either alumina or silica)
- 5 – 40 ppm total copper
- From the large amount of the complex agents, Ethylenediamine (EDA) was selected as the complexing agent from the model Cu-CMP waste stream.

In this study, a suspension containing alumina or silica particles, copper ions, Ethylenediamine (EDA), and water were used to simulate waste generated from a copper CMP process.

5. 2 Environmental Regulations and Their Impacts on Cu-CMP Process

Industrial water consumption and plant discharges are closely monitored by regulatory agencies at all levels which are constantly demanding reduced water consumption and lowered contaminant levels in discharged wastes. Copper CMP waste streams need to be treated to remove copper levels below local regulatory levels, which typically range from 0.1 to 5 ppm in the USA, although some countries impose a mass-based rather than concentration based limits [5.9]. It has been recently ruled that copper CMP wastes do not fall under the category of plating wastes and are not regulated by federal standard 40 CFR 433.13 (Metal Finishing Point Source Category). Developing cost-effective strategies for the removal of suspended solids and dissolved copper from CMP waste stream is an area of great importance to fabrication facilities.

It is important to discuss the environmental regulations to understand the impacts of Cu-CMP generated waste streams in order to develop the treatment options to meet the

local regulations. In this analysis, the focus will be on the environmental regulations impact on copper CMP, on the wafer effluents generated by the copper CMP process regulated under the Clean Water Act (CWA), and on the disposal of sludge generated by wastewater treatment either at the semiconductor plant or at the Publicly Owned Treatment Works (POTW) regulated under the Resource Conservation and Recovery Act (RCRA). One should also note that if the semiconductor manufacturing effluents are discharged into a POTW, mandates to regulate what comes into its collection and treatment system are issued by an enforcement authority.

5.2.1 Environmental Impacts of Heavy Metal

Trace quantities of heavy metals, such as nickel (Ni), manganese (Mn), lead (Pb), chromium (Cr), cadmium (Cd), zinc (Zn), copper (Cu), iron (Fe), and mercury (Hg), are important constituents of most waters. Heavy metal and nonmetallic wastes, and/or organic compounds may enter the wastewater system and have a detrimental effect upon the treatment system, particularly in biological treatment processes. Heavy metals such as copper, zinc, nickel, lead, cadmium, and chromium can react with microbial enzymes to retard or completely inhibit metabolism [5.10]. Regulating the discharge of heavy metals, including Cu from fabrication facilities, is therefore important to protect biological systems in our environment.

5.2.2 The Clean Water Act (CWA or FWDCA)

The Clean Water Act or Federal Water Pollution Control Act was enacted in 1948, and was subsequently amended in 1965, 1972, 1977 and 1987. The CWA is meant to control point source discharges into navigable waters of the US, and states that any

point-source discharge of pollutants is illegal unless it is covered under the terms of National Pollutants Discharge Elimination System (NPDES) permit, which needs to be renewed each year. This applies to all industrial facilities as well as POTWs. Pollutants are classified as conventional pollutants [see Table 5.2], toxic pollutants [see Table 5.3] and non-conventional pollutants which are neither categorized as conventional or toxic, such as ammonia, chemical oxygen demand (COD) and some organic chemicals such as pesticide residues. Copper and its compound are listed in the toxic pollutant category [5.11, 5.12, 5.13]. A semiconductor manufacturing plant can fall into two separate situations with respect to its waste stream management; it can discharge effluents directly into a body of water (e.g. the IBM Burlington, Vermont plant which discharges into the Winooski river) or into a POTW (e.g. Motorola Oak Hill factory in Austin, Texas which discharges into the South Austin POTW).

In the case of IBM Burlington, the semiconductor manufacturer has to obtain an NPDES permit issued by the state or by the EPA. The effluent limits are then determined by an analysis of the environmental impact of the discharge. The receiving water body is surveyed by the state to calculate the Total Maximum Daily Load (TMDL) acceptable for that body of water according to 40 CFR 130, the NPDES permit limits. The National Recommended Water Quality Criteria for Copper are listed in Table 5.4. The criteria are are not legally binding. States may have different and potentially more stringent criteria.

Additionally, the EPA has defined categorical (industry-specific) effluent limits, such as 40 CFR 433 for metal finishing operations and 40 CFR 469 for semiconductor manufacturing operations (see Table 5.5).

Table 5.2: The Five Conventional Pollutants (defined in 40 CFR 401.16)

Biological Oxygen Demand (BOD)	Total Suspended Solids (TSS)	pH
Fecal Coliform	Oil and Grease	

Table 5.3: The 65 Toxic Pollutants or Classes of Pollutants (defined in 40 CFR 401.15)

1. Acenaphthene	35. Fluoranthene
2. Acrolein	36. Haloethers (other than those listed elsewhere; includes chlorophenylethers, bromophenylphenyl ether, bis(dichloroisopropyl) ether, bis-(chloroethoxy) methane and poly-chlorinated diphenyl ethers)
3. Acrylonitrile	
4. Aldrin/Dieldrin	
5. Antimony and compounds	
6. Arsenic and compounds	37. Halomethanes (other than those listed elsewhere; includes methylene chloride, methychloride, methylbromide, bromoform, dichlorobromomethane
7. Asbestos	
8. Benzene	
9. Benzidine	38. Heptachlor and metabolites
10. Beryllium and compounds	39. Hexachlorobutadiene
11. Cadmium and compounds	40. Hexachlorocyclhexane
12. Carbon tetrachloride	41. Hexachlorocyclopentadiene
13. Chlordane (technical mixture and metabolites)	42. Isophorone
14. Chlorinated benzenes (other than dichlorobenzenes)	43. Lead and compounds
	44. Mercury and compounds
15. Chlorinaed ethanes (including 1,2-dichloroethane, 1,1,1-trichloroethane, and hexachloroethane)	45. Naphthalene
	46. Nickel and compounds
16. Chloroalkyl ethers (chloroethyl and mixed ethers)	47. Nitrobenzene
	48. Nitrophenols (including 2,4-dinitrophenol, dinitrocresol)
17. Chlorinated naphthalene	49. Nitrosamines
18. Chlorinated phenols (other than those listed elsewhere: includes trichlorophenols and chlorinated	50. Pentachlorophenol

cresols) 19. Chloroform 20. 2-chlorophenol 21. Chromium and compounds ***22. Copper and compounds*** 23. Cyanides 24. DDT and metabolites 25. Dichlorobenzenes (1,2-, 1,3-, and 1,4-di-chlorobenzenes) 26. Dichlorobenzidine 27. Dichloroethylenes (1,1-, 1,2-dichlorothylene) 28. 2,4-dichlorophenol 29. Dichloropropane and dichloropropene 30. 2,4-dimethylphenol 31. Dinitrotoluene 32. Diphenylhydrazine 33. Endosulfan and metabolites 34. Endrin and metabolites ethylbenzene	51. Phenol 52. Phthalate esters 53. Polychlorinated biphenyls (PCBs) 54. Polynuclear aromatic hydrocarbons (including benzanthracenes, benzopyrenes, benzofluoranthene, chrysenes, dibenz-anthracenes, and indenopyrenes) 55. Selenium and compounds 56. Silver and compounds 57. 2,3,7,8-tetrachlorodibenzo-p-dioxin (TCDD) 58. Tetrachloroethylene 59. Thallium and compounds 60. Toluene 61. Toxaphene 62. Trichloroethylene 63. Vinyl chloride 64. Zinc and compounds

Table 5.4: National Recommended Water Quality Criteria for Copper (listed in the Federal Register under 62FR42160)

	Freshwater		Saltwater	
	CMC (µg/l or ppb)	CCC (µg/l or ppb)	CMC (µg/l or ppb)	CCC (µg/l or ppb)
Copper	13	9	4.8	3.1

Table 5.5: Metal Finishing and Semiconductor Industry Effluent Limits as Defined in 40 CFR 433 and 40 CFR 469.

Pollutant or pollutant property	Maximum for any 1 day (mg/l except for pH) (2)		Monthly average shall not exceed (mg/l except for pH) (2)	
	Metal finishing	Semiconductor	Metal Finishing	Semiconductor
Cadmium	0.69		0.26	
Chromium	2.77		1.71	
Copper	3.38	none	2.07	none
Lead	0.69		0.43	
Nickel	3.98		2.38	
Silver	0.43		0.24	
Zinc	2.61		1.48	
Cyanide	1.20		0.65	
Total Toxic Organics (1)	2.13	1.37	---	----
Oil and Grease	52		26	
TSS	60		31	
PH	6.0-9.0	6.0-9.0	6.0-9.0	6.0-9.0
Fluoride	----	32	----	17.4

(1) The list of TTOs is not the same for the Metal Finishing and the semiconductor industries.
(2) Best Practical Technology (BPT), best Achievable Technology (BAT) and Pretreatment Standards for Existing Sources (PSES) limits are the same.

In Motorola's case, not only must they comply with federal and local regulations, categorical limits, sewage sludge disposal or use standards, but they must also abide by the standards (local limits) set by the receiving POTW.

An additional point that needs to be clarified is that when two types of industrial processes are discharged on the same site, they are subject to these limits separately, i.e. they cannot be tested for pollutants after mixing (the so-called 'dilution is no solution' rule) if dilution makes a pollutant for one process non-detectable.

This was obviously an issue for semiconductor manufacturers because the electroplating and copper CMP processes were categorized as metal finishing processes (see document EPA/310-R-95-002: Profile of the Electronics and Computer Industry, 1995, p94). This meant that the Cu concentration in effluents of electroplating and copper CMP should follow the metal finishing end-of-process effluent limits as defined in 40 CFR 433, as 2.07 mg/l monthly average and 3.38 mg/l maximum for one day. However, the semiconductor industry is regulated under the 40 CFR 469, which does not have an effluent limit for copper. Upon request for clarification by the semiconductor industry, the EPA issued a letter on April 21, 1998, which ruled that the electroplating and copper CMP processes would be regulated under the semiconductor industry effluent standards, which set no limit on copper.

5.2.3 National Pretreatment Program for Indirect Dischargers

The national pretreatment program was enacted on June 26, 1978, and is found in the Code of Federal Regulations at 40 CFR 403. Its purpose is to provide the regulatory

framework to ensure that non-domestic point sources do not discharge any pollutant into a POTW collection system that may interfere with the operation of the POTW (including sludge operations), thus pushing it out of compliance of its NPDES permit and affect the ambient water quality of the receiving water body [5.14, 5.15].

The purpose of the pretreatment program is to control the discharge of 126 priority pollutants (including copper) into POTWs. All large POTWs (≥5 MGD) and smaller POTWS with significant industrial discharges are required to establish a local pretreatment program. Essentially, the POTW will analyze its wastewater treatment pollutant removal performance data, and from the data determine how much pollutant can be accepted from industrial users so as to be compliant and to avoid plant fouling.

The local limits are not only dependent on the technology being used or the portion of the influent that comes from industry, but also strongly on the receiving water body. As a result, local limits for copper can vary considerably from one POTW location to another (Table 5.6)

5.2.4 Regulation on Sewage Sludge Use and Disposal

Most of the POTWs use their sludge to make fertilizer that is either sold in bulk or packaged and distributed. The use of sewage sludge is regulated under the CWA in 40 CFR 503 that specifies some federal limits for metal contents in 40 CFE 503.13. For example, the monthly average concentration of copper allowed under 40 CFR 503.13 is 1500 mg/kg. Additionally, states may impose stricter limits (EPA WEB) [5.16].

Table5.6: Local Limits at Several POTWs [5.9]

	Capacity/ Average Flow MGD (1)	Water Quality Criteria for copper (mg/l or ppb)	POTW dilution credit	POTW discharge limit	POTW annual discharge limit	Industrial discharge local limit for copper
Deer Island, MA	1080/370	4.8 mg/l (acute) 3.1 mg/l (chronic)	70:1	None	None	1.5 mg/l (2)
Clinton, MA	3/2.4	3.9 mg/l (acute) 2.7 mg/l (chronic)	2:1	6.0 mg/l (max) (3) 4.6 mg/l (average) (3)	None	1.5 mg/l (4)
Austin, TX Walnut Creek	60/42			10 mg/l		1.9 mg/l
Sunnyvale, CA	29.5/15		1:1	8.6 mg/l (5)	715	0.7 mg/l (6) 0.5 mg/l (7)

(1) MGD = Million Gallons per Day
(2) Under revision, will probably be 1.0 mg/l
(3) Expected, currently under discussion
(4) Under revision, will probably by 1.0 mg/l or lower
(5) 1-Day Average
(6) Maximum Concentration, 'Grab' sample
(7) Maximum concentration, composite sample

5.2.5 The Resource Conservation and Recovery Act (RCRA)

Congress enacted the Resource Conservation and Recovery Act (RCRA) in 1976 as the primary regulatory vehicle to ensure that hazardous waste is properly managed from the point of its generation to its ultimate disposal or destruction, i.e., "from cradle to grave." RCRA establishes a very complex and comprehensive set of requirements to define the materials that are subject to hazardous waste regulation. The act also describes the responsibilities of anyone who generates, transports, stores, treats, disposes of or otherwise manages hazardous waste (EPA WEB).

Listed Hazardous Waste include wastes from non-specific sources, such as a specific industrial operation with an unspecified technology used to perform the operation (list defined in 40 CFR 261.31). It also includes waste from specific sources, such as a specific technology (the K-list defined in 40 CFR 261.32) and discarded commercial chemical products.

Among the Listed Hazardous Wastes, F-006 contains wastewater treatment sludge from electroplating operations except from the following processes: (1) sulfuric acid anodizing of aluminum; (2) tin plating on carbon steel; (3) zinc plating (segregated basis) on carbon steel; (4) aluminum or zinc-aluminum plating on carbon steel; (5) cleaning/striping associated with tin, zinc and aluminum plating on carbon steel; and (6) chemical etching and milling of aluminum. The implication for waste generated by the copper interconnect process is that if rinse water from the copper electroplating process finds its way to the semiconductor factory waste treatment facility, the sludge generated

becomes a Listed Hazardous Waste under F-006, no matter how little copper the sludge contains.

5.2.6 The Superfund Act (CERCLA)

The Comprehensive Environmental Response, Compensation and Liability Act (CERCLA), known as the Superfund Act, was enacted on December 11th 1980. It established a regulatory framework to pay for the clean-up of abandoned hazardous waste sites and authorized EPA to recover the fund from the Potentially Responsible Party (PRP) for the clean-up cost. Among the PRPs are the generators of the substances such as the metal polishing industry and semiconductor industry.

Sludge generated from a semiconductor facility must be converted to solid waste before it can be disposed of in a landfill. Provided it has not been in contact with electroplating rinse effluents and that it does not exhibit any hazardous characteristics (Ignitability, Corrosively, Reactivity and Toxicity), such solid waste can be disposed of in a non-hazardous landfill. Nonetheless, the semiconductor manufacturers remain liable for damages due to the waste under RCRA's principle of "liability from cradle to grave." Thus, there remains a possibility that in the distant future, the receiving landfill may leach copper and be listed as a superfund site requiring clean-up (EPA WEB).

5.3 Trends in Environmental Regulation and Its Implication for Cu-CMP Process

Several factors influence the evolution of environmental regulations. As more scientific evidence is gathered, a certain chemical may be recognized as toxic and new laws may limit its use or disposal. Additionally, as waste treatment technology improves, the EPA may require more stringent discharge limits. Public opinion and increased

awareness of environmental issues always pushes for a reduction of certain categories of waste. Locally, new environmental conditions (such as population growth) or the increase of certain categories of pollutants in industrial or domestic waste streams may force POTWs to revise their local limits so as to remain in compliance with the specifications of their NPDES permit to maintain ambient water quality. Currently, several new regulations relevant to copper discharge are under discussion.

The first item currently under discussion between the semiconductor industry and the EPA is the de-classification of sludge that has been exposed to electroplating rinse water from the F-006 listing. De-classification would incur significant savings for the semiconductor manufacturers since disposing of hazardous waste costs typically $500 per ton whereas disposing of non-hazardous sludge costs $50 per ton. On the other hand, there is currently a debate as to whether the copper CMP sludge, seen as a follow-up of the electroplating process, should justify an F-006 rating.

The second item concerns possible new categorical limits for the Metal Plating and Machining (MP&M) industry. After surveying 2000 metal plating and machining sites, the EPA has determined that the Best Achievable Technology (BAT) economically feasible is capable of achieving an effluent level for copper of 0.6 mg/l and for Total Suspended Solids (TSS) of 38 ppm. That limit, much stricter than any previous one, could be applied to new and existing sources. It remains to be clarified whether it would apply to the CMP effluent process [5.9].

In summary, one must consider that, Copper CMP is a mainstream technology. The increased load of copper and TSS into effluents may require the receiving POTW to

decrease the local limits of copper. It is necessary at this point to develop a technology for removing copper from Cu-CMP effluents in compliance with future, possibly more stringent, environmental regulations. Options must be sought for the semiconductor industry to find a more cost effective method of either treating or managing its Cu-CMP effluents.

CHAPTER 6

ELECTROCOAGULATION

The two major issues from the effluents generated by the Cu-CMP process are copper content in the effluents which needs to be removed to meet the local discharge or dispose limit, and the content of abrasive colloidal particles (Al_2O_3 or SiO_2 based) that needs to be removed to reclaim the large quantity of water that is consumed during the CMP process. In this chapter, the treatment options, especially Electrocoagulation technique (EC), are discussed.

6.1 Removal of Suspended Slurry Particles and Copper from CMP Waste Steam

6.1.1 Particle Surface Charge

To understand how particles are brought together, it is important to understand the surface charge of colloid particles. An important factor in the stability of colloids is the presence of the surface charge. It develops in a number of different ways, depending on the chemical composition of the medium and the colloid. Regardless of how it is developed, this stability must be overcome if these particles are to be aggregated (flocculated) into larger particles with enough mass to settle easily.

When the colloid or particle surfaces become charged, some ions of the opposite charge (known as counter ions) become attached to the surface. They are held together by electrostatic and van der Waals forces to overcome thermal agitation. Surrounding this fixed layer of ions is a diffused layer of ions, which is prevented from forming a compact double layer by thermal agitation. This is illustrated schematically in Figure 3.3. As shown, the double layer consists of a compact layer (Stern) in which the potential drops

from Ψ_0 to Ψ_s and a diffuse layer in which the potential drops from Ψ_s to 0 in the bulk solution [6.1, 6.2].

If a particle, as shown in Fig. 3.3, is placed in an electrolyte solution and an electric current is passed through the solution, the particle, depending on its surface charge, will be attracted to one or the other of the electrodes, dragging with it a cloud of ions. The potential at the surface of the cloud (called the surface of shear) is measurable. The measured value is often called the zeta potential ς. Theoretically, the zeta potential should correspond to the potential measured at the surface enclosing the fixed layer of ions attached to the particle.

6.1.2 DLVO theory

The DLVO theory [6.3, 6.4] is the central work on colloid stability. The theory considers the balance of attractive London-van der Waals forces and repulsive electrostatic interactions between two proximate surfaces. DLVO theory is based on the concepts of an electric double layer. As two surfaces of like charge are brought together, their electric double layers interact, resulting in an electrostatic repulsion. Electrostatic repulsion is countered by van der Waals force to produce an energy barrier that may contain two minima, or positions of selective stability (primary minimum and secondary minimum; Figure 6.1). The energy profile in Figure. 6.1 is a strong function of the ionic strength of the system and the surface charge characteristics of colloidal surfaces. At high ionic strength, the electric double layer is very thin, resulting in a relatively small repulsion force and elimination of the repulsive energy barriers. As a result, particles will coagulate.

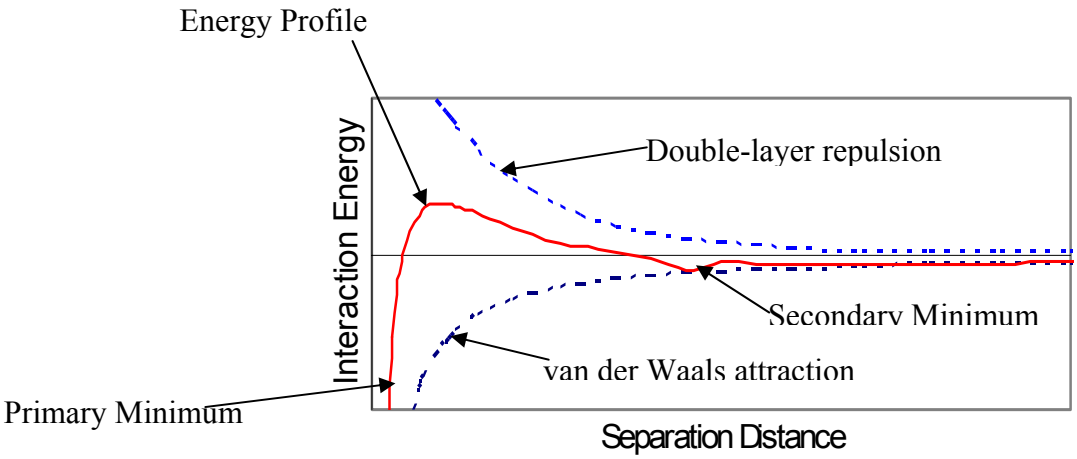

a

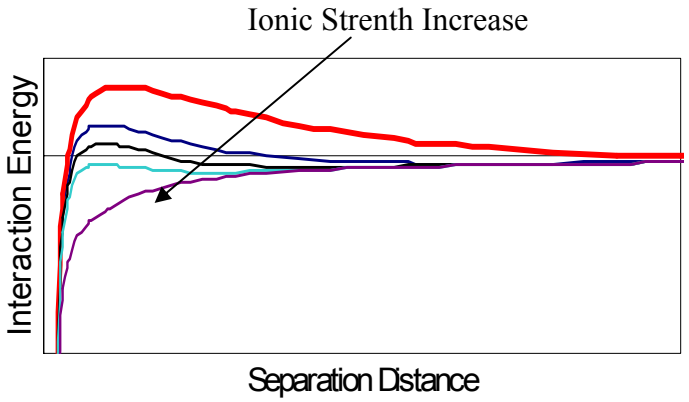

b

Figure 6.1 a. Schematic representative of total energy of interaction verses separation distance – bases on DLVO Interaction. b. Energy profile verses separation distance with increase of solution ionic strength.

6.1.3 Techniques of Removing Suspended Slurry Particles

There are several ways to remove particles from their suspension: Aggregation/Flocculation, Flotation, Chemical Precipitation, Filtration, Electrodecantation, and Electrocoagulation.

Aggregation/Flocculation: To bring particles together, steps must be taken to reduce particle charge or to overcome the effect of this charge. The effect of the charge can be overcome by (1) the addition of potential-determining ions, which will be taken up by or will react with the colloid surface to reduce the surface charge, or the addition of electrolytes, which will reduce the thickness of the diffuse layer and thereby reduce the zeta potential, (2) the addition of long-chained organic molecules (polymer), whose subunits are ionizable and are therefore called polyelectrolyte, which bring about the removal of particles through adsorption and bridging, and (3) the addition of chemicals that form hydrolyzed metal ions [6.5] or change the system pH to bring particles to its iso electric point (IEP).

Flotation: Flotation is a unit operation used to separate solid or liquid from a liquid phase. Separation is achieved by introducing fine gas (usually air) bubbles into the liquid phase. The bubbles attach to the particulate matter, and the buoyant force of combined particle and gas bubbles is great enough to cause particles to rise to the surface. Particles that have a higher density than the liquid can thus be made to rise.

Chemical Precipitation: In wastewater treatment, it is the addition of chemicals to the system that alters the physical state of dissolved and suspended solids and facilitates their removal by sedimentation. The chemical added to wastewater interact

with substances that are either normally present in the wastewater or added for this purpose. The typical chemicals used are alum, lime, ferrous sulfate and lime, and ferric chloride.

Filtration: Filtration uses a membrane as the physical barrier to remove the particle from the system. For small colloidal particles, ultrafiltration is selected to remove the fine particles out of the waste system. Crossflow-microfiltration was used for large volume effluent treatment, but membrane fouling is a big concern with its application in treating CMP waste. Combined with pre-treatment, the overall treatment efficiency can be improved significantly.

- ***Ultrafiltration****:* Silica particles in oxide slurry can range in size from 20 to 80 nm, far too small to be retained by microfilters alone. Ultrafiltration membranes have pore sizes substantially smaller than the silica particles in slurries, and thus can provide an absolute barrier to all suspended particles regardless of concentration and flow conditions. Using an UF system to treat CMP wastewater has helped semiconductor industries to meet local effluent discharge limits with regard to total suspended solids [6.5].
- ***Crossflow-microfitration:*** The use of crossflow microfiltration in wastewater treatment is limited because of membrane fouling as a result of the colloidal fraction. A large part of this colloidal fraction can be converted into a settleable particulate fraction through a pretreatment such as electrocoagulation [6.6] (Figure 6.2).

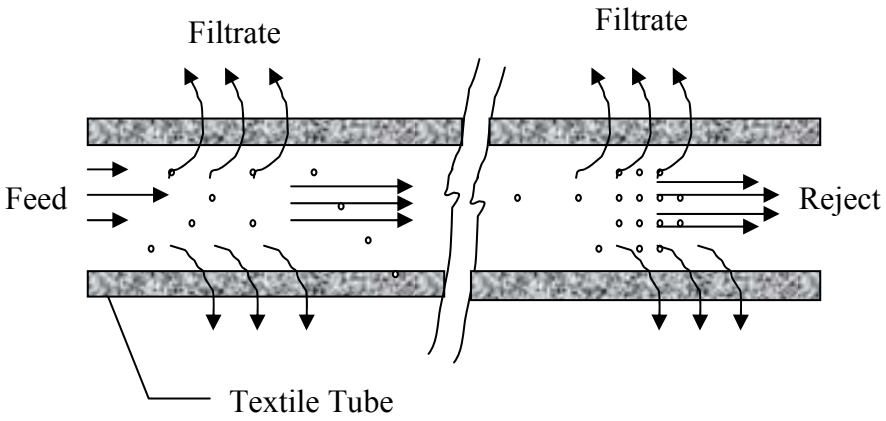

Figure 6.2: Illustration of Cross-Flow filtration

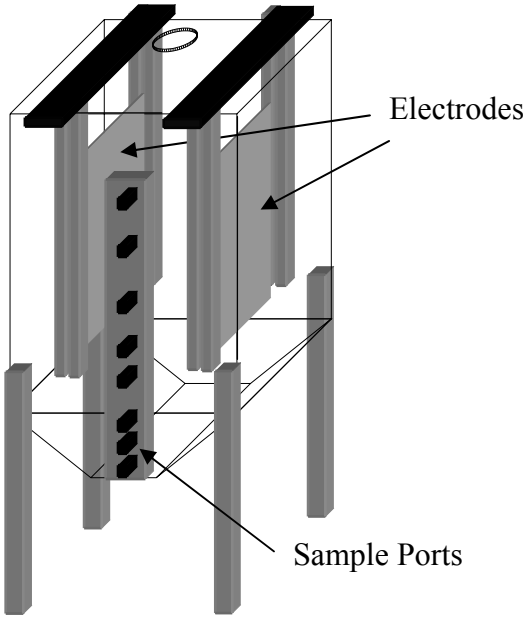

Figure 6.3 Illustration of Electrodecantation [6.7]

***Electrodecantation*:** When a current is passed through a suspension of charged particles, the charged particles migrate electrophoretically toward the electrode of opposite charge. The accumulation of particles around that electrode increases the density locally and thus the particle-enriched suspension sinks to the bottom of the vessel. At the opposite electrode, a colloid-depleted region develops and rises. The stratification or decantation process is stabilized against mixing by the resultant vertical density gradients [6.7].

6.1.4 Techniques of Removing Copper from CMP waste suspension

Copper removal technologies have been used for decades by printed circuit board (PCB), electronics, and metal finishing industries. These include precipitation (lime precipitation for example), ion exchange, electrodialysis and other electrolytic processes.

Newer technologies have also been investigated specifically for the treatment of CMP effluents, which present more challenges because they contain strong oxidizers, suspended particles of very small size, and copper that may be strongly complexed. Such technologies are proposed by companies such as Kinetico (electrowinning) and US filters of Microbar (filtration).

6.2 Electro-Coagulation (EC)

6.2.1 Application of EC

One technique that can be used to concentrate the submicron sized particles suspended in a liquid is Electrocoagulation. Electrocoagulation has been exploited in a wide range of industrial and laboratory scale water treatment application. It has been

employed to remove solids from waste waters containing food, oil, textile, mining, electroplating, and various other suspended particulates treatment [6.8, 6.9, 6.10, 6.11, 6.12]. This technique involves the application of an electric field to a suspension to enhance the particle–particle contact required for coagulation. The coagulated solids then settle out leaving behind clarified liquid. A considerable advantage of this approach is the capability to simultaneously remove suspended matter, petroleum products, bacterial contamination, and metal ions.

The potential application of Electrocoagulation in treating CMP wastes has started to attract attention from different research institutes [6.13]. Factors such as type of electrode and electrode surface area that enhance copper and organic removal from CMP waste during electrocoagulation have been studied [6.14, 6.15]. When adding the chemical complexity from CMP waste stream into the suspended system, the fundamental removal mechanisms of copper and different type colloidal systems during EC need to be further and more fully understood in order to apply this technology effectively and successfully in treating the Cu-CMP waste effluents.

6.2.2 Removal Pathways of Copper Species and Colloidal Particle during EC

6.2.2.1 The Removal Pathways of Copper under EC

The dissolved copper contained in the Cu-CMP effluents can be removed by electroplating directly on cathodic electrode via:

$$Cu^{2+} + e^- + H_2O = Cu_2O + H^+ \qquad (1)$$

$$Cu^{2+} + 2e^- = Cu^o \qquad (2)$$

Another pathway for Cu^{2+} to leave the suspension is via in-situ precipitation, which can be achieved by increasing the pH in cathodic chamber:

$$Cu^{2+} + OH^- = Cu(OH)_2 \qquad (3)$$

Additionally, any dissolved metal ions in the complexed and uncomplexed form contained in the waste dispersion may be electrolytically removed under suitable conditions. In the case of a CMP waste containing dissolved copper and complexing agent ethylenediamine (EDA), copper removal is possible through additional pathways discussed above and as listed below:

$$Cu(EDA)^{2+} + 2e^- \rightarrow Cu^o + EDA \qquad (4)$$

$$Cu(EDA)^{2+} + e^- + H_2O \rightarrow Cu_2O + EDA + H^+ \qquad (5)$$

$$Cu(HEDA)_2^+ + 2e^- \rightarrow Cu^o + 2HEDA \qquad (6)$$

Reactions (1)-(2) and (4)-(6) represent the removal of uncomplexed and complexed copper ions by electrolytic reduction. Since hydroxide (OH^-) ions are produced in the cathodic chamber ($2H_2O + 2e^- \rightarrow H_2 + 2OH^-$), copper ions may also be hydrolyzed to form insoluble copper hydroxide ($Ksp = 2 \times 10^{-19}$) precipitates [6.16]. The solubility of $Cu(OH)_2$ (s) is plotted in Figure 4.1 as a function of solution pH. It can be seen that the precipitation of $Cu(OH)_2$ is thermodynamically favorable at solution pH values greater than 7 for dissolved copper concentrations greater than 1 ppm.

6.2.2.2 Solids Removal Pathways under EC

There are several mechanisms that can make particles separated from the suspension during electrocoagulation due to the reactions on electrodes. They are as follows:

- Iso-Electro Point (IEP) mechanisms due to pH change during EC
- Chemical induced coagulation due to pH increase in anode chamber
- Electrodecantation due to electrophoretic migration of charged particles towards the electrode of opposite charge
- Ionic strength induced coagulation due to the release of ionic species from anode.

IEP Mechanisms:

The point of zero charge (PZC) is where the surface charge is zero. The isoelectric point is where the electrical mobility of particles is zero. For most colloidal systems, when the system is brought to IEP it will coagulate immediately (e.g. Al_2O_3 colloidal system). During EC, the pH at cathode and anode area will change due to the reactions on the electrodes which may bring the colloidal particles to its IEP and lead to particle coagulation.

Ionic Strength Mechanisms

The basic principals of stabilization by the ionic double layer around particles were developed by Derjaguin, Landau, Verwey, and Overbeek [6.3], hence the "DLVO" theory. It has been specifically applied to spherical particles. By increasing the ionic strength of the system, due to cathodic and anodic reactions, the repulsion force will be reduced and at a certain point it will lead to particle coagulation. Al_2O_3 colloidal system follows this theory very well.

Electrodecantation (ED)

As mentioned earlier, electrodecantation results from the electrophoretic migration of charged particles towards the electrode of opposite charge. As a result, the suspension will have a locally particle-enriched and colloidal-depleted regions around electrodes respectively. The particle-enriched region will sink to the bottom due to higher density while the colloidal-depleted region will rise up. The stratification or decantation process is achieved via the resultant vertical density gradients [6.7].

Adsorption and Precipitation by Hydrous Oxides

Iron will be released from the anodic chamber during EC if the anode material is stainless steel. Silica, both soluble and colloidal, can be removed from water to very low levels in neutral or slightly alkaline solution through co-precipitation with insoluble metal hydroxides in situ or by adsorption with the addition of freshly formed hydroxides to the suspension [6.17, 6.18].

CHAPTER 7

EXPERIMENTS AND RESULTS FOR Cu AND ABRASIVE PARTICLE REMOVAL

In this chapter, the materials, methods, and experimental design used to remove copper and abrasive particles are discussed. The results of electrocoagulation to remove both Cu and abrasive Al_2O_3 and SiO_2 particles simultaneously will also be presented and discussed.

7.1 Materials and Methods

7.1.1 Experimental Setup

Figure 7.1 depicts the experimental set up used to remove copper ions while simultaneously separating the solids. The electrodes were made from 316 stainless steel and were placed 2.9 cm apart. The inner electrode was submerged 7 cm into the suspension and a DC field of 3.5 V/cm was applied. A Hewlett Packard 6634A system DC power supply was used to provide the power. The membrane separating 100 ml of water and 225 ml of suspension consisted of regenerated cellulose dialysis tubing with molecular weight cut off of 12-14,000 (Spectra/Por). To understand the particle removal mechanisms, the electrode polarity was swapped and the inner electrode material was changed to a graphite carbon electrode in some experiments.

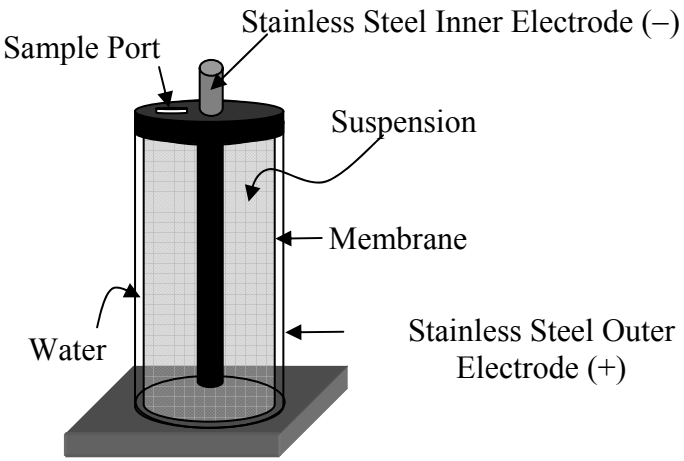

Figure 7.1 Electrocoagulation setup

7.1.2 Suspension Preparation

Colloidal alumina (Al_2O_3) or silica (SiO_2) suspensions were prepared at concentrations of 0.1–0.4w/v% by dispersing high purity α-alumina (Degussa) or Klebosol (1498-50) in deionized (DI) water. Copper nitrate was added to the suspensions to achieve a final copper ion concentration of ≈ 40ppm along with equimolar amounts of ethylenediamine (EDA). The conductivity of the suspension was adjusted to ≈1300μS/cm by adding the appropriate amount of KNO_3. The suspensions were sonicated for 1 minute using a model W-375 sonicator/cell disruptor (Heat Systems-Ultrasonics Inc.) to break up aggregates and help disperse the solids. An Orion 122 handheld conductivity meter with a standard probe and an Orion 701A digital pH meter were used for conductivity and pH measurements, respectively.

7.1.3 Copper and Fe Concentration Level Measurement

Copper and iron concentration of the liquid located in the both inner and outer chambers were measured using a Perkin-Elmer atomic absorption spectrophotometer, model 2380. The copper and iron standard solutions required for calibration were prepared with 1000 ppm Weiss Research copper nitrate or iron nitrate standard solution, respectively.

7.1.4 Solid Concentration Measurement Using Turbidity Meter

The solid abrasive concentration in the suspension was measured using a turbidity meter (model: Hach Ratio/XR Turbidimeter). Principally, a particle suspension is placed in a spectrophotometer curette and the “absorbance” is measured by the detector. For a

colloidal system, light is not adsorbed by the solution, but is scattered in all directions and does not reach the detector. This quantity is regarded as “absorbed.”

The apparent absorption obeys an equation analogous to Beer's Law over some limited range of concentration:

$$\text{"A"} = \log_{10}(P_o/P) = kbc \qquad (7)$$

where A is the apparent absorbance, P_0 is the radiant power of the applied light, P is the radiant power of emergent light, k is a constant, b is the path of length, and c is the concentration of precipitate, the value of k is determined empirically with a series of standards. The solid concentration will be proportional to the amount of absorbance of the suspension.

7.1.5 Standard Calibration Curve for Al_2O_3 and SiO_2 Slurry System

To measure the solid concentration in a suspension system using a turbidity meter, varied amount of Al_2O_3 and SiO_2 particles were suspended into 100ml ultra pure water with or without chemical additives in the solution. After sonication to break up the particles, the suspension was characterized with the turbidity meter to get the turbidity reading. The plots (Figure 7.1 and Figure 7.2) below show a linear correlation of turbidity reading vs. solid concentration in the suspension for both Al_2O_3 and SiO_2 colloidal systems. For suspension with chemical additives of dissolved 40 ppm copper and EDA, the linear correlation stays closely the same.

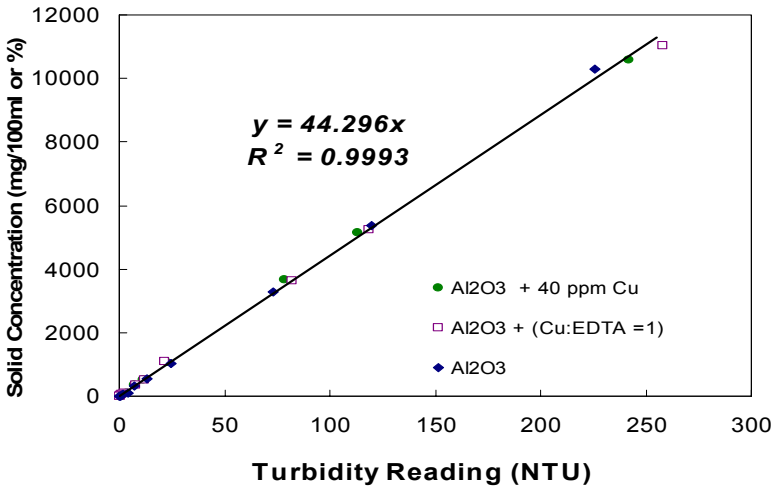

a. Solid Concentration of Al_2O_3 vs. Turbidity Reading

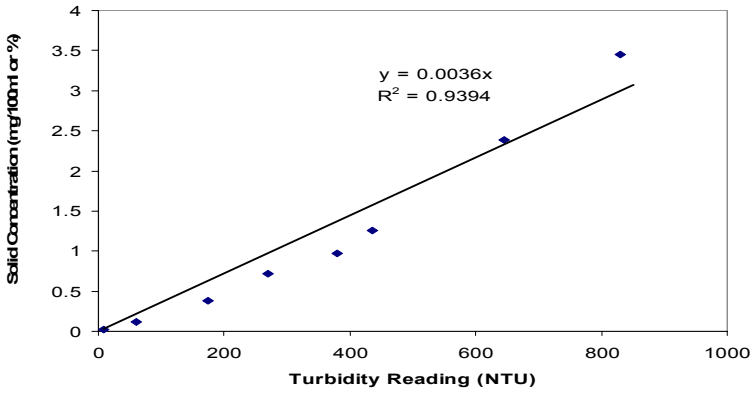

b. Solid Concentration of SiO_2 vs. Turbidity reading

Figure 7.2 Al_2O_3 and SiO_2 turbidity reading and solid concentration calibration curves. a. Solid concentration of Al_2O_3 vs. turbidity reading; b. Solid concentration of SiO_2 vs. turbidity reading

7.1.6 Membranes Used in Electrocoagulation

Both dialysis, and positive and negative surface charged membranes were used in this study to understand the impacts of membrane surface charge on copper and particle removal during electrocoagulation. A dialysis membrane is made of cellulose and has pore diameters of 1-5 nm. Small molecules can diffuse through these pores, but large molecules (such as proteins or colloids) cannot. This type of membrane was used in most of the experiments unless otherwise stated.

Three types of membranes were provided by Pall Corporation: two of them had positively charged membrane surfaces, and one is negatively charged, based on the information provided by the company:

- Positively (+) charged: MWO#: 4ES-C9228-6 (Catalog number: 2005351; Par #: NW2-DD). This membrane has a quaternary ammonium group on nylon 6.6 polymer and isoelectric point of pH 9.
- Negatively (–) charged: PN#: 80528(Catalog #: 88852). The membrane is amphoteric, and has carboxyl and amine on nylon 6,6 polymer
- Positively (+) charged; P/N: 80552(Super-Q30). The membrane has a quaternary ammonium group on polyethersulfone polymer.

7.1.7 Particle Size Analyzer:

The mean particle size distribution in suspension was characterized using a Coulter N4 particle size analyzer.

7.1.8 Zeta Potential Measurements

Electrophoretic mobility measurements were conducted using a Coulter Delsa 440SX electrophoretic light-scattering apparatus. The pH of the suspensions was adjusted by adding small amounts of KOH/HNO_3.

7.1.9 TEM for SiO_2 Particle Crystal Structure Analysis

A Hitachi H-8100 high resolution transmission electron microscope (TEM) was used to analyze the structure of coagulated SiO_2. Suspensions of SiO_2 were collected at different stages of electrocoagualtion; each suspension was then oven-dried and subjected to TEM for structure analysis.

7.1.10 X-ray Diffraction for Cathodically Deposited Cu Structure Analysis

To examine and characterize the copper deposited on the cathode, X-ray diffraction analysis was performed using a Sigmens D500 diffractormeter with Cu-Kα radiation.

7.2 Results and Discussion

7.2.1 pH Change in Anodic and Cathodic Chambers during EC:

To understand copper and suspended particle removal during electrocoagulation with the typical electrocoagulation setup described in section 7.1.1 (stainless steel electrodes, dialysis membrane, 3.5V/cm power supply), the pH in both anodic and cathodic chambers was monitored as a function of current application time. The results of the cathodic chamber depicted in Figure 7.3 indicate a pH increase from 6 to 11 in 5 minutes; concurrently, the pH in the anodic chamber decreases from 6 to ~2. No differences in pH were observed when the 0.1 M KNO_3 solution was replaced with a

waste stream that contained 0.4% Al_2O_3, 40 ppm copper and equimolar EDA. The increase of pH in the cathodic chamber and the decrease of pH in the anodic chamber were due to reactions:

Anode/oxidation:

$$2H_2O \rightarrow 4H^+ + 4e^- + O_2 \quad (8)$$

Cathode/reduction:

$$2H_2O + 2e^- \rightarrow H_2 + 2OH^- \quad (9)$$

7.2.2 Eh-pH Diagram of Cu/H_2O System

The Eh-pH diagram (Figure 7.4) shown below is for the system of Cu/H_2O. The species considered in the diagram are: Cu, Cu^+, Cu^{2+}, $HCuO_2^-$, CuO_2^{2-} , $Cu(OH)_2$(s), Cu_2O (s), CuO(s) $Cu(OH)_2$(aq). This diagram shows that the copper oxidation state is a function of pH. The reduction of Cu^{2+} at higher pH (>5.0) is Cu and Cu_2O, which is consistent with our X-ray results based on the sample collected from the cathode during EC (X-ray results indicate that Cu and Cu_2O were deposited on the cathode during EC with Cu-CMP waste that contains 40 ppm copper, 0.4% Al_2O_3).

7.2.3 Electro Kinetic Behavior of Al_2O_3

It is important to understand the electrokinetic behaviors of alumina particles as a function of pH in the presence of Cu ions in order to effectively remove alumina particles and Cu ions from CMP waste streams simultaneously. In this study, 0.4% Al_2O_3 was

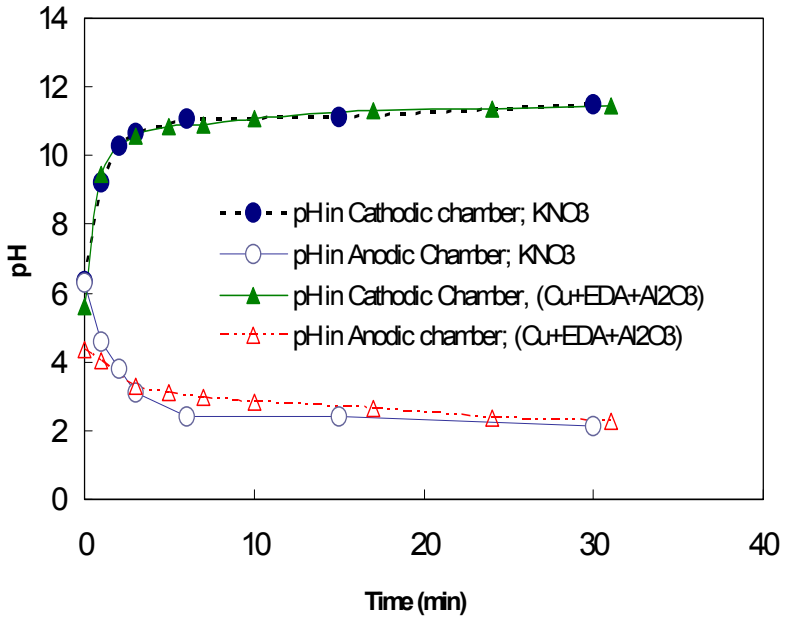

Figure 7.3 pH change in both cathodic and anodic chambers during EC

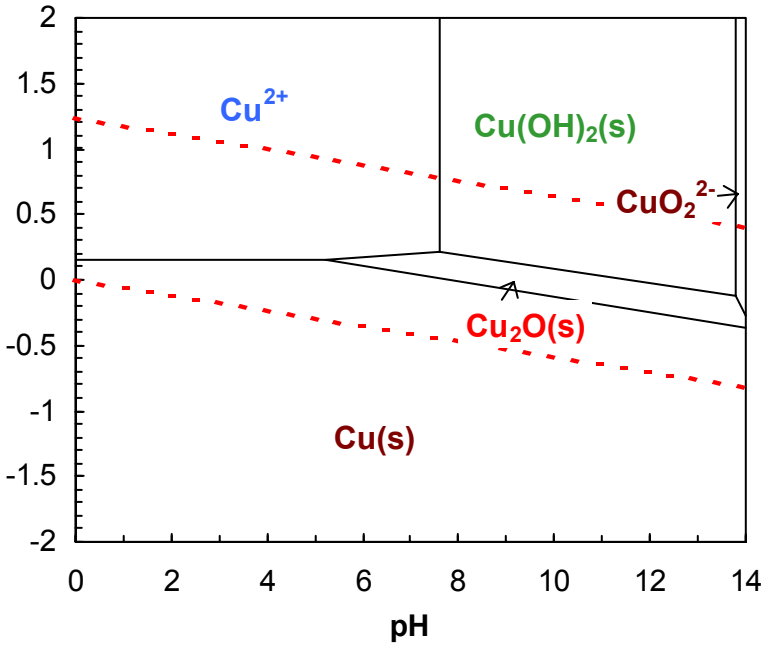

Figure 7.4 Eh-pH diagram for Cu/H_2O system

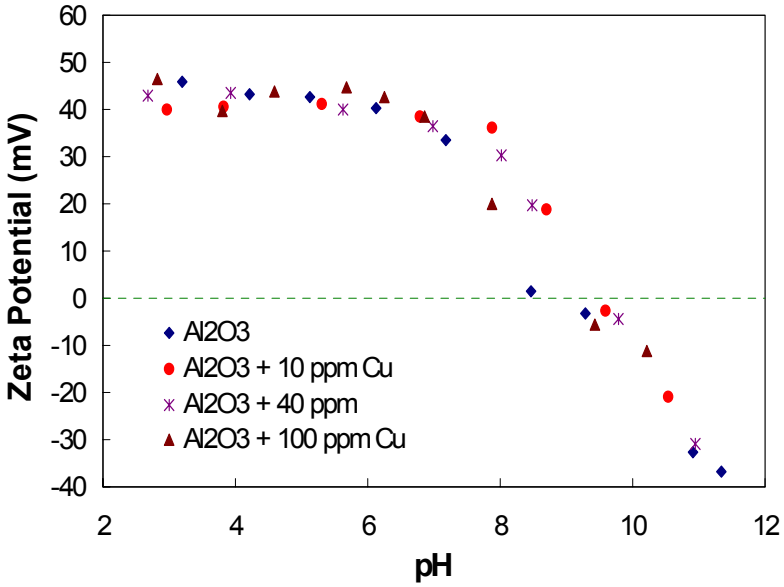

Figure 7.5 Electrokinetic behaviors of Al_2O_3 (Degussa) in the presence of different copper level as a function of pH

suspended in solutions that contained 0, 10, 40, 100 ppm copper, respectively. The electrophoresis measurements of each solution were conducted using Delsa 440 at various pH values. As shown in Figure 7.5, the presence of Cu ions in Al_2O_3 systems ranging from 0-100ppm does not shift the alumina IEP significantly and the IEP of Degussa alumina is approximately at pH ~ 9.0.

7.2.4 Copper and Alumina Removal

7.2.4.1 Copper Removal under EC

The suspensions containing ~ 40 ppm dissolved copper and ~40ppm copper with 0.4w/v% Al_2O_3 were put in a cathodic chamber (the anodic chamber was filled with deionized water) and tested under EC respectively with an electrical current gradient of 3.5 V/cm. The concentration of copper on the top surface of the suspension was monitored during EC as a function of time. As shown in Figure 7.6, the total copper removal on top of the suspension reaches to ~90% after 2 hours exposure under EC. The removed copper either deposits on the cathode or precipitates out from the system. There is no significant difference in total copper removal with or without the presence of Al_2O_3 particles in the suspension.

7.2.4.2 Cu and EDA Molar Ratio and Its Impacts on Copper Removal

To understand the role that the complexing agent plays during copper removal, various amount of EDA were added to the suspension system that contains 40 ppm copper and ~0.4% Al_2O_3 to form a Cu:EDA molar ratio of 2:1, 1:1, 1:2 and 1:3. The suspension has initial pH 6.0, counductivity of 1.3mS/cm and a current supply of 3.5V/cm during EC. The results in Figure 7.7 and 7.8 show that the molar ratio of

Cu:EDA plays a critical role in copper removal through cathodic deposition, but has no significant impact on Al_2O_3 removal. For the system containing Cu:EDA molar ratio = 1:2, up to 80% of 40ppm copper can be removed through electrodeposition.

Cu^{2+} and EDA form strong complexes; as the EDA concentration increases from Cu:EDA = 2:1 to Cu:EDA=1:2, the complex will shift from $Cu(EDA)^{2+}$ to $Cu(EDA)_2^{2+}$ as shown in reaction (10) and (11). $Cu(EDA)_2^{2+}$ is a more stable form than $Cu(EDA)^{2+}$ complex (see K value). This positively charged stable complex is able to prevent copper from precipitating and cause it to migrate to the cathode for plating reactions to take place. As the EDA concentration approaches Cu:EDA=1:3, the extra EDA, based on the reduction reaction on cathode, might shift the reduction reactions [(12) – (14)] to the opposite direction and reduce the amount of copper being plated out. Clearly, the results indicate that the chemistry of the solution plays a critical role in cathodic copper removal.

$$H_2NCH_3\text{-}CH_3NH_2 + Cu^{2+} \xrightarrow{K = 10^{10.5}} H_2N\text{-}CH_3\text{-}CH_3\text{-}NH_2 \quad (10)$$

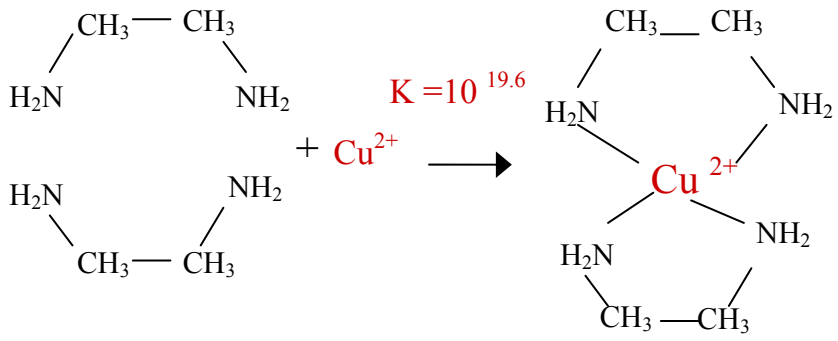

(11)

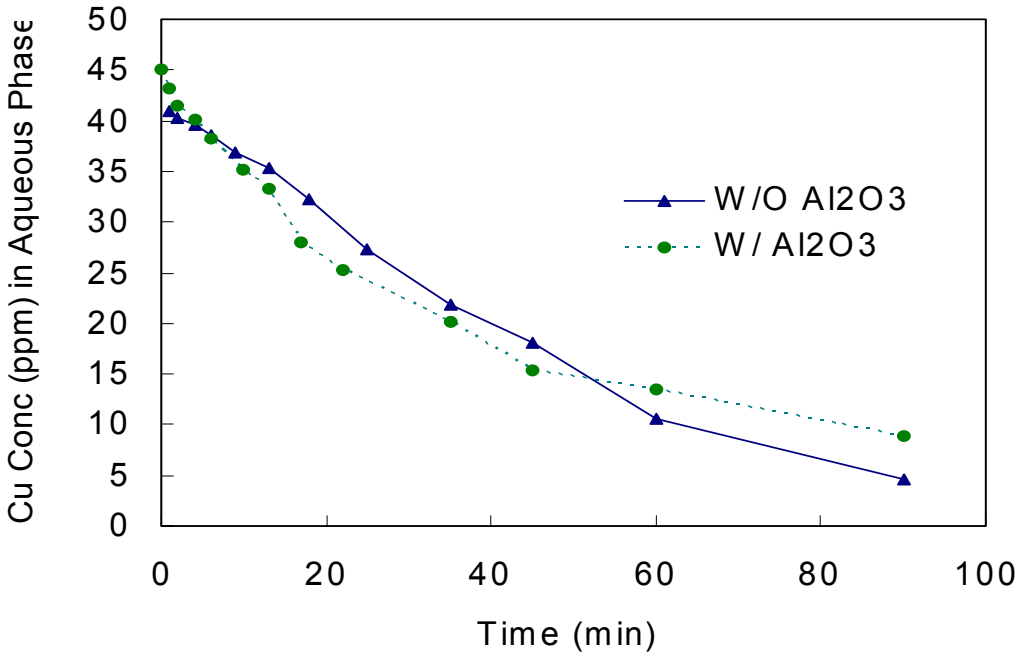

Figure 7.6. Copper concentration change on top of the suspension as a function of time during EC in the presence and absence of Al_2O_3

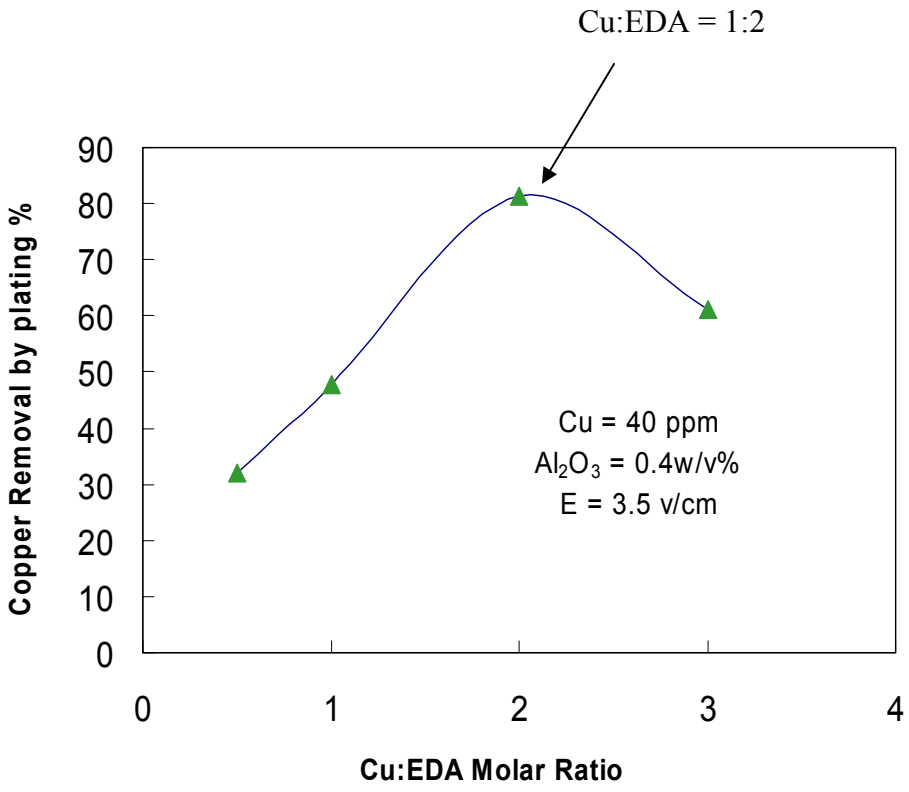

Figure 7.7 The impact of Cu:EDA molar ratio on copper removal through cathode plating

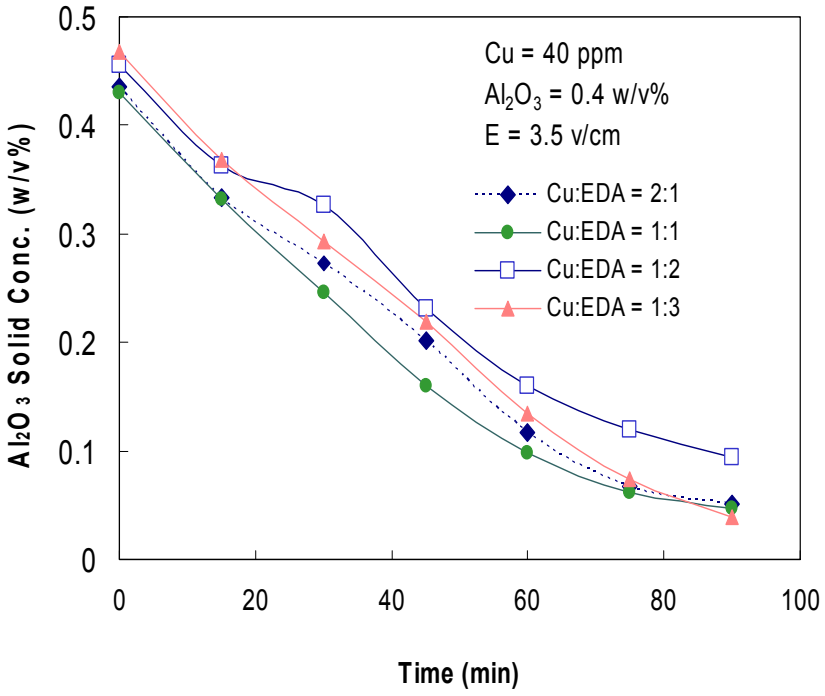

Figure 7.8. Al_2O_3 removal during EC at different Cu:EDA molar ratio in the suspension

$$Cu(EDA)^{2+} + 2e^- \rightarrow Cu^o + EDA \quad (12)$$

$$Cu(EDA)^{2+} + e^- + H_2O \rightarrow Cu_2O + EDA + H^+ \quad (13)$$

$$Cu(HEDA)_2^{+} + 2e^- \rightarrow Cu^o + 2HEDA \quad (14)$$

7.2.4.3 The Effects of Current Duration on Cu and Particle Removal during EC

To study the impact of current duration on cathodic copper deposition and Al_2O_3 removal from the top of the suspension, a 10V current was supplied to the suspension containing 0.4% Al_2O_3, 40 ppm dissolved copper and 38 ppm EDA (initial pH of the suspension is ~6.0 and conductivity ~1.3mS/cm). Two different modes of current were used in this study; one is a non-stop continuous current application for 2 hours, while the other is intermittent: 5 minutes on and 10 minutes off over 2 hours of EC. As shown in Figure 7.9, the non-stop current application yields more copper deposition on the cathode (47.7%) than the one with the intermittent current application (31.8%), with no significant difference on Al_2O_3 removal. The results indicate that a continuous current supply is needed for better copper cathodic removal. As shown in the reactions below, a continuous electron supply is needed to move the reaction forward, as long as Cu^{2+} is available in the solution.

$$Cu^{2+} + e^- + H_2O = Cu_2O + H^+$$

$$Cu^{2+} + 2e^- = Cu^o$$

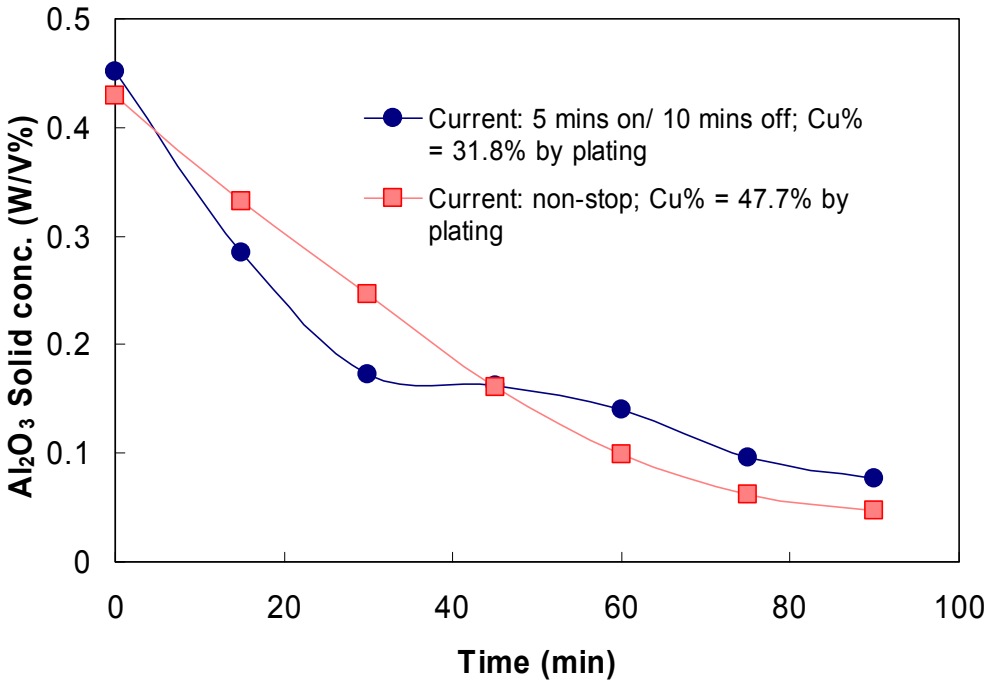

Figure 7.9 The effects of current supply on the copper and particle removal

7.2.4.4 Effects of Membrane Type on Al_2O_3 and Cu removal

Four different types of membranes were used in the EC setup. Among the four membranes, one is a cellulose dialysis membrane with molecule weight cut off of 12-14,000. The other three are provided by Pall Corporation with different surface charges (2 are positively charged and one is negatively charged). The suspension used in the experiment contains ~40 ppm Copper, ~38 ppm EDA (Cu:EDA = 1:1 molar ratio) and 0.4% Al_2O_3. The results in Figure 7.10 and Figure 7.11 show that cathodic copper removal is significantly higher (up to ~80%) for the set up using positive charged membranes coupled with the electrocoagulation cell. The negatively charged membrane not only yields poor copper removal (~28% on cathode depostion), but also poor Al_2O_3 removal. One possible reason is that the negatively charged membrane surfaces adsorb or attract positively charged copper species and positively charged Al_2O_3 (at the beginning of EC), preventing them from migrating to the cathode to be removed through electrical deposition (for copper) or getting concentrated at the cathode area (for particle removal).

7.2.4.5 The impact of Different Complex Agents on Copper Removal

To explore the impact of complexing agents on copper and Al_2O_3 removal in 0.4% Al_2O_3 suspension system, Citric Acid (CA) and EDA are added to the suspension separately in a typical EC set up. The results show that there are no significant particle removal differences (Figure 7.12), but copper deposition on a cathode differs significantly. For a suspension containing 40 ppm copper and Cu:CA = 1:1 molar ratio, only ~2% copper is removed through cathode deposition versus ~48% copper cathode

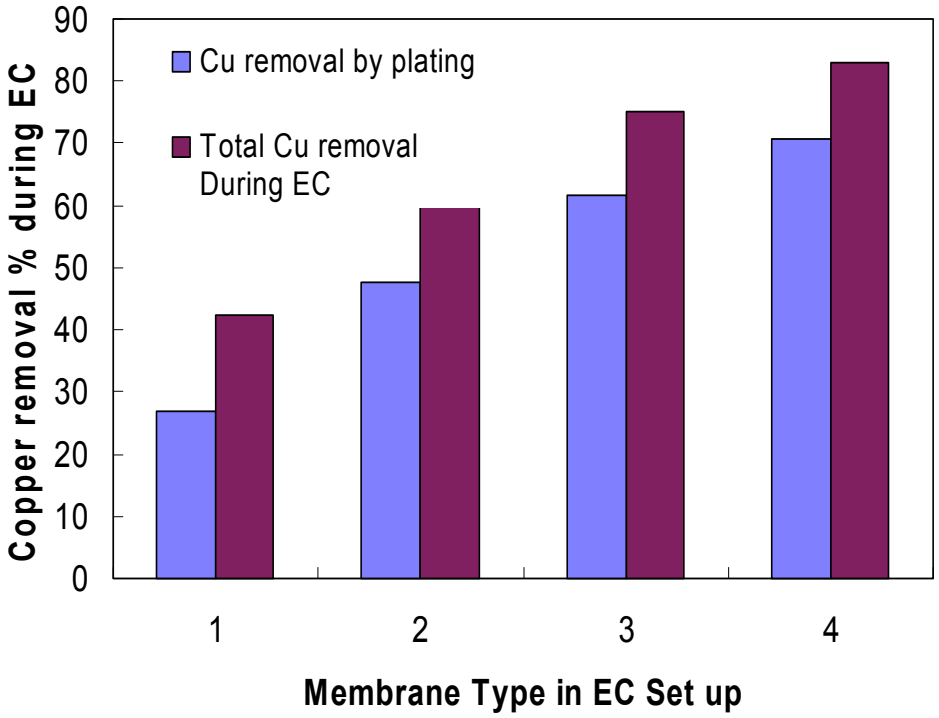

Figure 7.10 The effects of membrane type on copper removal during EC (1 – negative charged; 2- dialysis membrane, 3 – positive charged, 4 – positive charged)

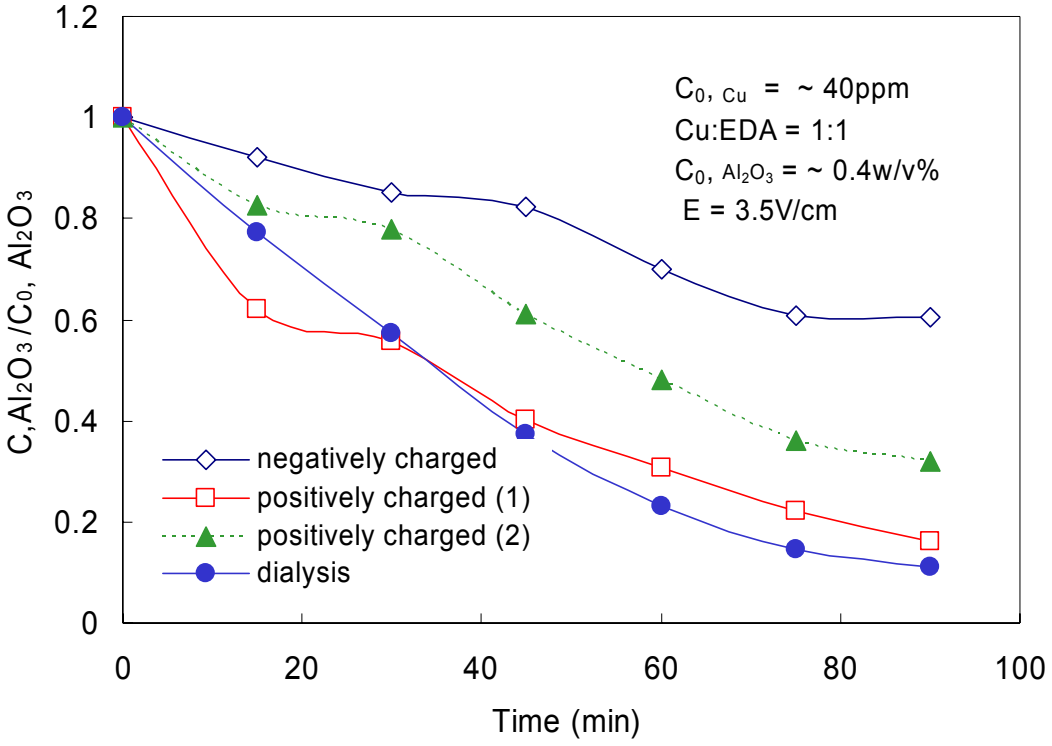

Figure 7.11 The effects of membrane on Al_2O_3 particle removal during

deposition for Cu:EDA = 1:1 suspension. The difference in copper removal is due to the charges formed for Cu-EDA and Cu-CA complexes. As discussed earlier, Cu and EDA form stable positively charged complexes, which will prevent copper from precipitating and move copper to the cathode for deposition during EC. As for citric acid, as shown in the reactions below, Cu and citric acid form negatively, neutral and positively charged complexes. Under an electrical field, the positively charged complex will be driven to the cathode for copper deposition. The negatively charged complexes will be driven away from the cathode and the neutral charged complexes will not be moved to or concentrated at the cathode. As a result, both negatively and neutral charged copper-CA complexes will significantly reduce the "opportunity" for copper to deposit onto the cathode. In addition, the OH^- formed at the cathodic chamber will react with H^+ (see reaction below) and shift the Cu-CA complex reaction to the opposite direction which will free Cu^{2+} for precipitation instead of electro-deposition.

Cu/EDA reactions: $Cu^{2+} + EDA \leftrightarrow Cu(EDA)^{2+}$

$Cu^{2+} + 2EDA \leftrightarrow Cu(EDA)_2^{2+}$

Cu/CA reactions: $Cit^{3-} + Cu^{2+} \leftrightarrow CuCit^-$

$Cit^{3-} + H^+ + Cu^{2+} \leftrightarrow CuHCit$

$Cit^{3-} + 2H^+ + Cu^{2+} \leftrightarrow CuH_2Cit^+$

$H^+ + OH^- \leftrightarrow H_2O$

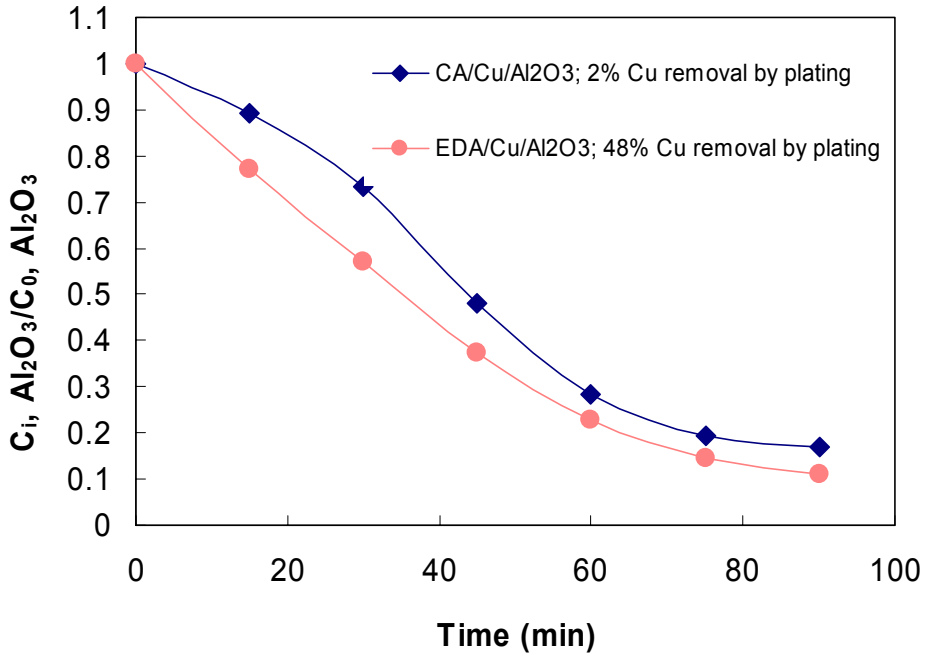

Figure 7.12 The impacts of CA and EDA on Al_2O_3 particle and copper cathodic

7.2.4.6 The Initial Copper Level Impact on Cu Removal over Cathode Deposition

To study the impact of the initial Cu concentration on the amount of copper plating on the cathode in a typical EC set up, three different copper concentrations ranging from 0.5 ppm copper to 40 ppm copper were selected in the presence or absence of 0.4% Al_2O_3. The results (Figure 7.13) show that higher copper concentration in the suspension results in a higher percentage of copper plating out on the cathode. The absence of Al_2O_3 enhances copper removal significantly at all three concentration levels. One explanation is that the initial positively charged Al_2O_3 reaches the cathode surface and prevents copper from reaching the cathode for deposition. Another reason might be copper adsorption on Al_2O_3 which would reduce the level of free dissolved copper in the suspension for electro-deposition in the presence of Al_2O_3.

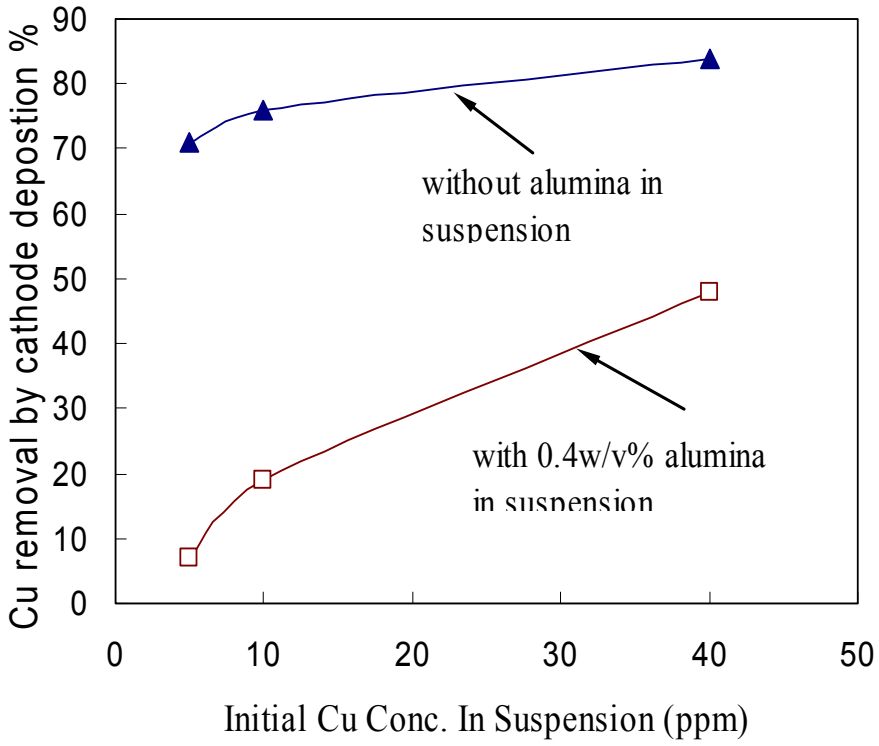

Figure 7.13 The impact of Cu initial level and Al_2O_3 solid concentration on copper removal during EC

7.2.5 Cu and SiO_2 removal under EC

7.2.5.1 Zeta Potential of SiO_2 Based Suspension

To make an "artificial waste" that would be representative of a silica based Cu-CMP process, which contains abrasive silica solid, copper ions, and certain copper complexing agent, 0.1% klebosol silica (1498-50), 20 ppm copper ions, and 19 ppm EDA were mixed together to form a colloidal suspension. The electro-kinetic behavior of the model system is presented in Figure 7.14. The slight increase in zeta potential for a suspension system containing 20 ppm copper, and a suspension containing 19 ppm EDA with 20 ppm copper in pH region 3 to 7, was caused by adsorption of either copper ions or Cu-EDA complexes on SiO_2 surfaces, and for pH region 7 to 9, the increases of zeta potential were caused by the precipitation $Cu(OH)_2$ in the colloidal system. As shown in Figure 7.14 , the presence of EDA alone has no significant adsorption to either shift the IEP or change the magnitude of zeta potential on silica.

7.2.5.2 Copper and SiO_2 Removal

For the simulated SiO_2 based Cu-CMP waste system, which contains 0.1% Klebosol (1498-50) abrasive particles, 20 ppm Cu ions, 19 ppm EDA, pH 6.0, and conductivity of 1.3 mS/cm, a study of the Cu removal kinetics was conducted. The samples were collected over time from the top of the suspension in the electrocoagulation cell and were acidified using HNO_3, after which they were analyzed using AAS. As shown in Figure 7.15, the copper level at top of the suspension decreases significantly as a function of time. Approximately 85% of copper ions were removed from the suspension after 2 hours EC at an electric field of 3.5 V/cm, and approximately 73% of

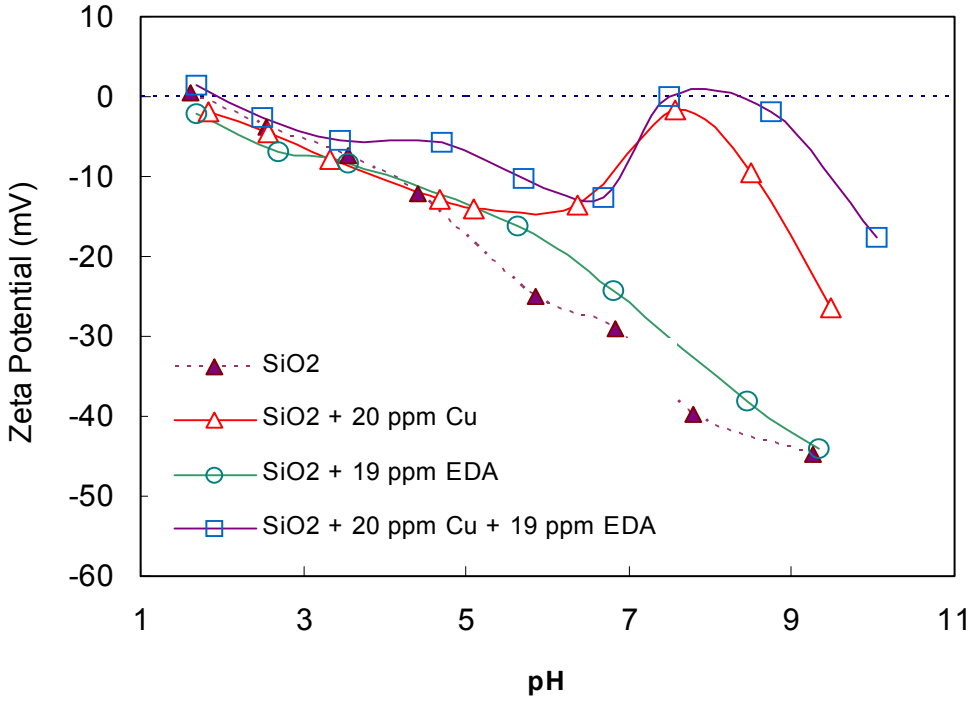

Figure 7.14 Zeta potential of silica systems under different Copper and EDA level

copper is removed from the system by plating out on the cathode. For silica particles, the final removal can reach to ~80% from the top of the suspension. The increase in particle concentration at ~ 20 minutes of EC in silica suspension was caused by iron hydroxyl formation in the cathode chamber (more discussion in Chapter 8 for the causes). As shown in the reactions below, the iron species were formed in the anode chamber due to oxidation reaction on the anode. The positively charged Fe^{2+} and Fe^{3+} will migrate toward the cathode, where a large quantity of OH^- was generated, and the formation of $Fe(OH)_2\downarrow$ and $Fe(OH)_3\downarrow$ will occur naturally due to its poor solubility causing particle concentration to increase temporarily (Figure 7.16).

For stainless steel anode:

$$Fe \rightarrow Fe^{2+} + 2e^-$$

$$Fe \rightarrow Fe^{3+} + 3e^-$$

$$2H_2O \rightarrow 4H^+ + 4e^- + O_2\uparrow$$

For cathode and in cathode chamber:

$$2H_2O + 2e^- \rightarrow H_2\uparrow + OH^-$$

$$Fe^{2+} + 2OH^- \rightarrow Fe(OH)_2\downarrow$$

$$Fe^{3+} + 3OH^- \rightarrow Fe(OH)_3\downarrow$$

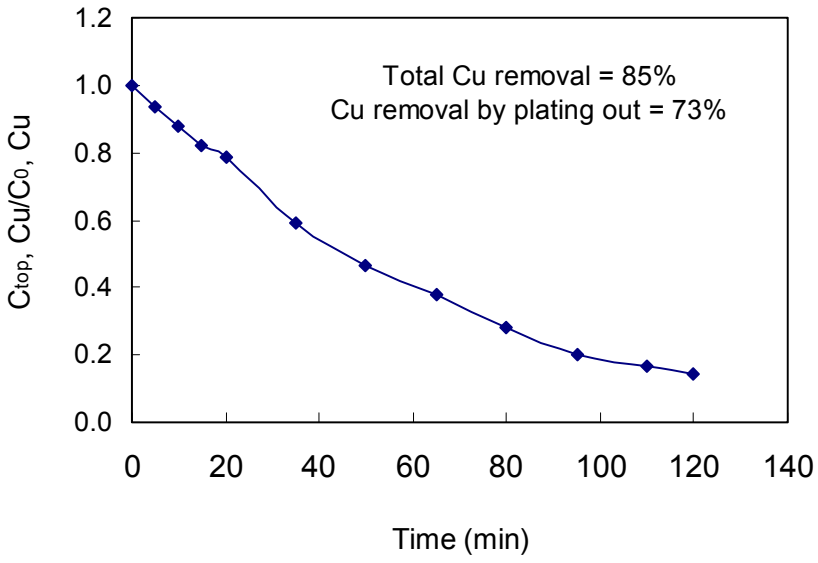

Figure 7.15 Cu removal from silica suspension during EC

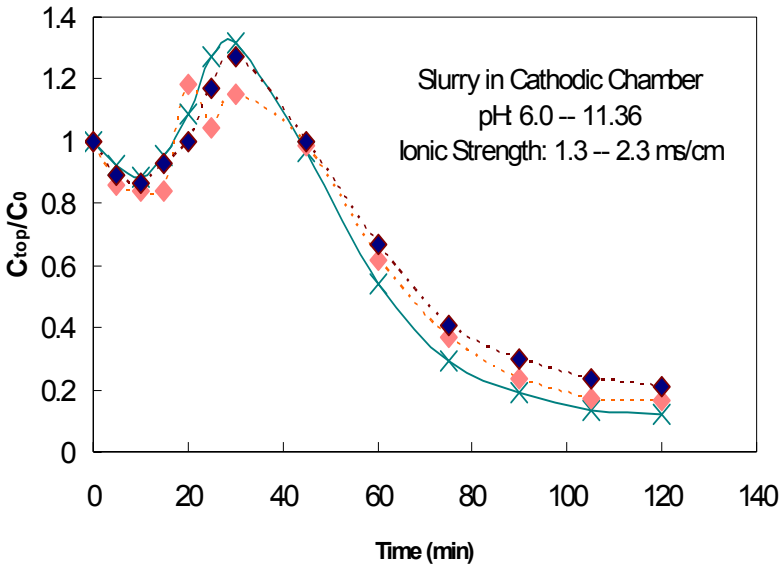

Figure 7.16 SiO_2 removal during EC as a function of time

CHAPTER 8

THE REMOVAL MECHANISMS OF ALUMINA AND SILICA USING ELECTROCOAGULATION

In this chapter, the removal mechanisms of Al_2O_3 and SiO_2 under EC will be discussed via experimental observation.

8.1 Electrode Reactions and $Fe(OH)_x$ Formation

When a current is applied to stainless steel electrodes, electrochemical reactions take place on both the anode and cathode. For a waste stream containing alumina and silica colloidal particles without other chemical species and additives, the reactions for stainless steel electrodes are as follows:

At the anode chamber:

$$2H_2O \rightarrow \quad 4H^+ + 4e^- + O_2$$

$$Fe \rightarrow Fe^{2+} + 2e^-$$

$$Fe^{2+} \rightarrow \quad Fe^{3+} + e^-$$

At the cathodic chamber:

$$2H_2O + 2e^- \leftrightarrow \quad H_2 + 2OH^-$$

Clearly, the reaction at the anode will cause pH decrease due to the formation of H^+, while at the cathode, the pH will increase due to the generation of OH^- at the chamber. The iron species formed at the anode chamber will migrate through a dialysis membrane to the negatively charged cathode, driven by both current and concentration

gradients. Due to elevated concentrations of OH^- at the cathode chamber, migrated iron species quickly form into iron hydroxide species through the reactions listed below.

$$Fe^{2+} + 2OH^- \rightarrow Fe(OH)_2\downarrow$$

$$Fe^{3+} + 3OH^- \rightarrow Fe(OH)_3\downarrow$$

The solubility diagram of $Fe(OH)_3$ is shown in Figure 8.1. The solubility of $Fe(OH)_3$ is strongly pH dependent and is poor in neutral pH range (5-8). The *Ksp* for $Fe(OH)_3 = 1.6\times10^{-39}$ (at 25^oC).

The Fe level in both anodic and cathodic chambers was monitored as a function of time during EC. As shown in Figure 8.2, significant amounts of Fe are produced in both chambers. Fe^{3+} is a good coagulant and has been widely used in waste water treatment systems to remove colloidal particles from waste streams. It is logical to expect that the Fe^{3+} produced during EC may be one of the mechanisms that lead to Al_2O_3 or SiO_2 removal.

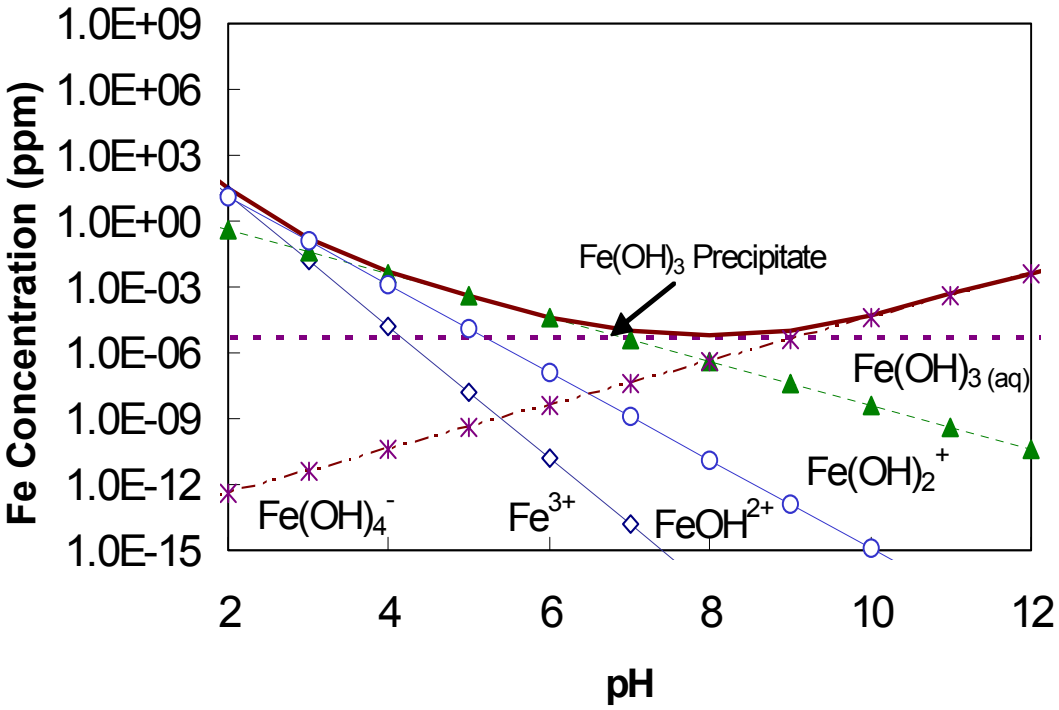

Figure 8.1 Speciation diagram of $Fe(OH)_3$

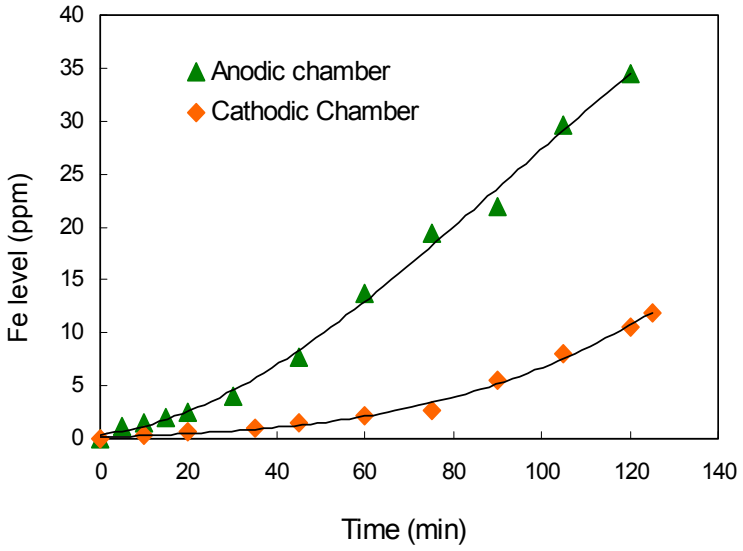

Figure 8.2 Total Fe levels in both anode and cathode chambers during EC

8.2 Alumina Removal Mechanisms

As discussed in earlier chapters, there are three possible mechanisms that can lead to alumina removal during electrocoagulation: IEP mechanism (due to the pH change to reach to Al_2O_3 IEP point), ionic strength, and iron hydroxyl species induced coagulation. To better understand these mechanisms, experiments were designed and conducted to ultimately determine the dominant mechanism that removes alumina from waste suspension during EC.

8.2.1 Carbon Anode

To understand the impact of iron hydroxyl $Fe(OH)_x$ species on Al_2O_3 removal, an experiment employing a graphite anode was conducted. The graphite carbon material was used as the anode and placed at the center of the EC set up. The stainless steel cylinder was used as the cathode and a 0.1% Al_2O_3 (Degussa) slurry suspension was used to fill the cathode chamber. The turbidity change on top of the suspension in the cathodic chamber was measured and the results are shown in Figure 8.3. The final pH of the slurry system after 2 hours at 3.5 V/cm current supply was ~8.3. The concentrated particles at the bottom of suspension were collected and particle size was measured using N4 plus particle analyszer; it was found that the average diameter is 13970.3 nm. The result indicates that coagulation took place during EC and this coagulation is independent of iron hydrolyzed species formation in the cathodic chamber.

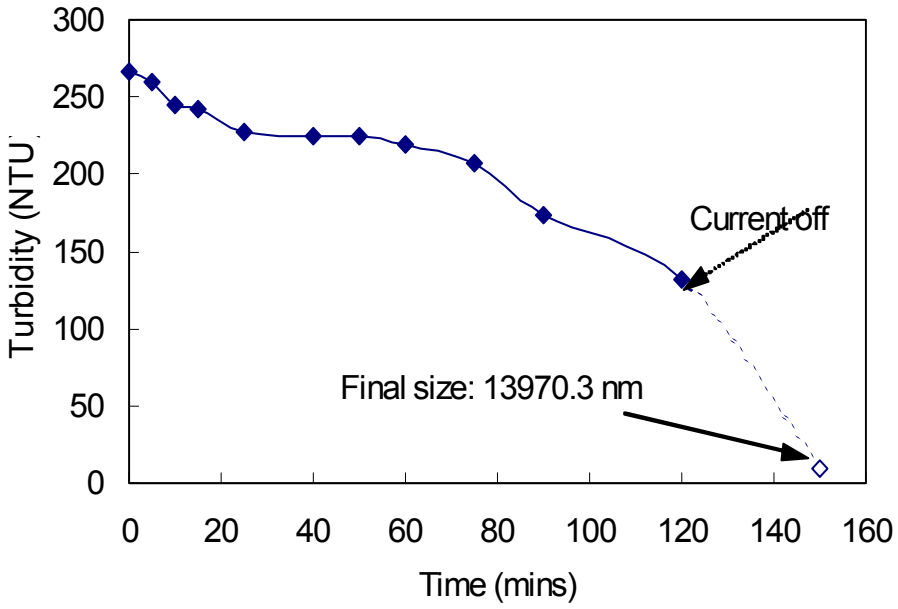

Figure 8.3 Top suspension turbidity change during EC for 0.1% Al_2O_3 with graphite anode

8.2.2 Alumina Removal Mechanism ---Duration of Current

To understand the impact of current application on Al_2O_3 removal mechanisms, 2 minutes and 90 minutes magnitude of current were applied to a 0.4% Al_2O_3 suspension (initial pH ~6.0 and 1.3 mS/cm conductivity) on a typical EC set up. As shown in Figure 8.4, compared with a 90 minute current application, particle removal with 2 minutes of current supply is faster. As discussed earlier, Al_2O_3 (Degussa) has an IEP around pH = 9.0. After the application of current for 90 minutes, the pH in the suspension increased to 11.53; during 2 minutes of current application, the suspension pH was brought to ~10, which is closer to the IEP of Al_2O_3. The electrostatic repulsion between particles was reduced when suspension is close to its IEP and particle coagulation takes place. This result indicates that the fastest way to remove Al_2O_3 from waste suspension is to bring Al_2O_3 suspension to a pH value that is close to its IEP.

8.2.3 Stability of Al_2O_3 Suspension

To understand the Al_2O_3 removal mechanism under EC, it is important to understand the stability of Al_2O_3 as a function of ionic strength. In this experiment, the pH of 0.2% Al_2O_3 suspension is adjusted to ~6.0 and KNO_3 was added to bring the suspension conductivity to various values (0.06 mS/cm to 12.97mS/cm). As shown in Figure 8.3, by simply increasing the salt content in the suspension to achieve a conductivity greater than 2.78 mS/cm, Al_2O_3 destabilization will occur. Due to the electrode reactions during EC, the ionic strength in both chambers increases dramatically (up to 2.3 mS/cm in cathodic chamber), suggesting the increase of ionic strength is a

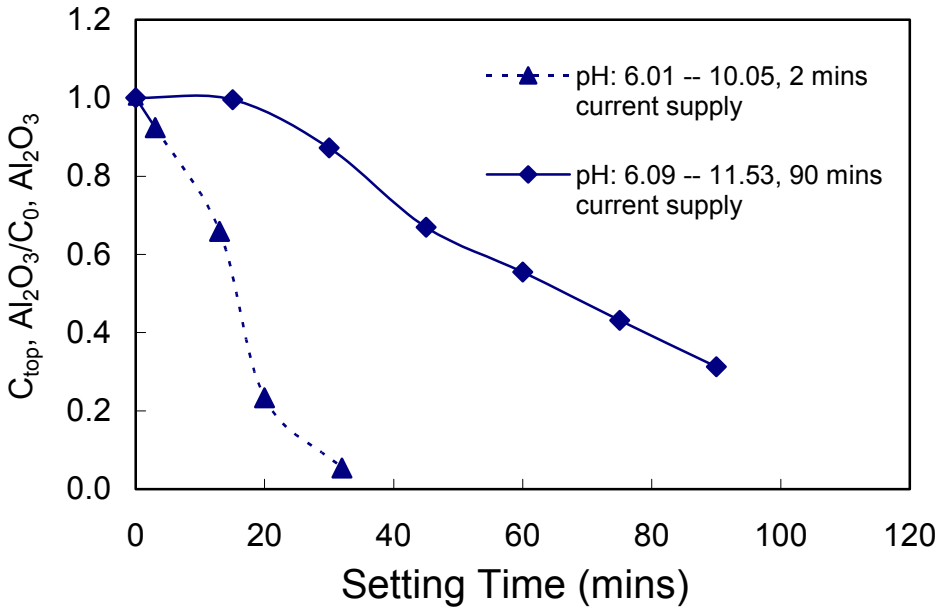

Figure 8.4 The impact of current supply duration on Al_2O_3 reremoval during EC

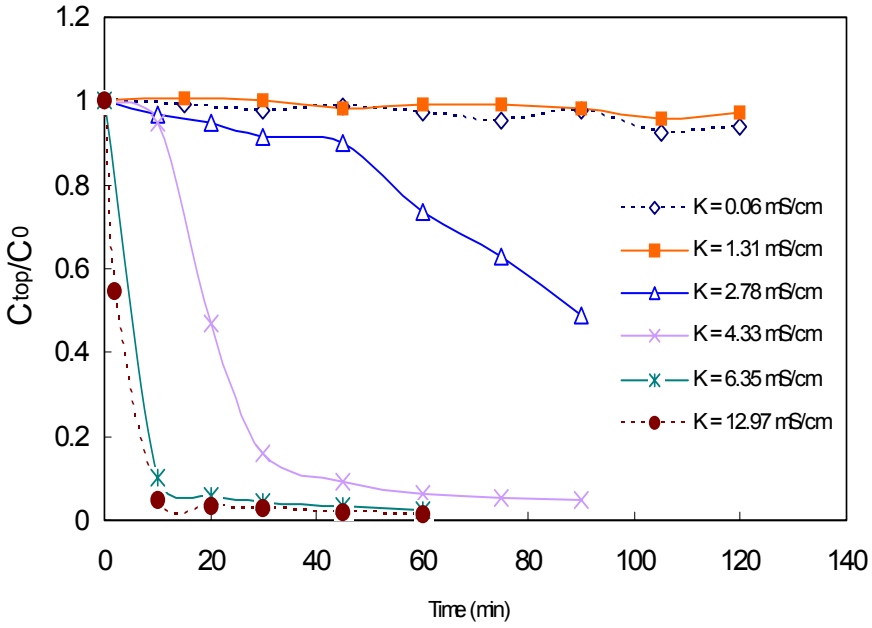

Figure 8.5 Al_2O_3 suspension stability as a function of ionic strength for 0.2% Al_2O_3 (Degussa) suspension

possible mechanism responsible for the destabilization and ultimately the removal of Al_2O_3 during EC.

8.2.4 Removal of Alumina Particles Under Electric Field in Both Chambers

Simulated CMP slurry containing 0.1% alumina with a pH 6.0 and conductivity of 1.3 mS/cm was put into both cathodic and anodic chambers in a typical electrocoagulation set up that had a 3.5 V/cm electric field. The solid concentration at the top surface of both chambers was monitored using a HACH RATIO/XR Turbidimeter. As shown in Figure 8.6, the alumina particles could be removed from the suspension by either cathodic (pH increase) or anodic (pH decrease) processes. However, particles in the anodic chamber were removed faster than particles in the cathodic chamber. This is because the anodic chamber is very acidic (pH = ~2). In addition, there will be more dissolved ionic species in the anodic chamber than in the cathodic chamber (which is highly alkaline). As a result, the ionic strength in the anodic chamber (conductivity ~ 4.0 mS/cm) is higher than in cathodic chamber (conductivity ~ 2.3 mS/cm), leading to faster Al_2O_3 coagulation and removal.

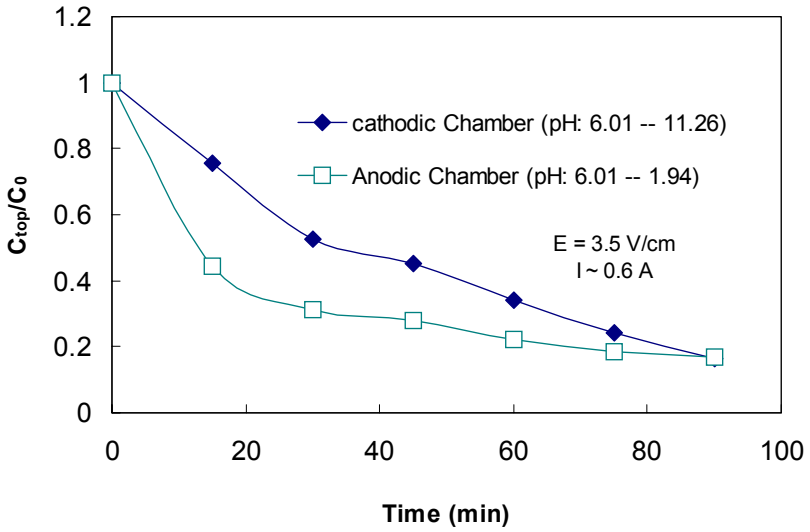

Figure 8.6 Al_2O_3 removal in both chambers during EC

8.3 Fundamental Removal Mechanisms of Silica during EC

To understand SiO_2 removal mechanisms during EC, a series of electrocoagulation experiments were conducted. Factors such as pH, ionic strength, duration of current supply, and a graphite anode were studied to support the hypothesis that the removal mechanisms of SiO_2 during EC are induced by hydroxyl iron species {$Fe(OH)_3$ $Fe(OH)_2$; FeOH} formed from anode stainless steel dissolution and OH^- generated by the cathode.

8.3.1 The Impact of Ionic Strength on SiO_2 Slurry Stability

Based on the double layer theory, the double layer will be compressed with the increase of ionic strength, which will reduce the distance of colloidal particles and enhance particle coagulation. In this experiment, different amounts of KNO_3 were added to the SiO_2 slurry system. As shown in Figure 8.7 and 8.8, as conductivity increased to ~8-12 mS/cm the 0.2% silica based slurry remained stable for suspension at a pH ~6.0 and ~ 2.0 during the test. Empirical results indicate that it may not be feasible to bring SiO_2 particle out the suspension simply by increasing the ionic strength. Results also show that during the 2 hours of electrocoagulation, the increase of ionic strength (from 1.3mS/cm to 2.3mS/cm in cathode chamber) is not the major cause of SiO_2 removal.

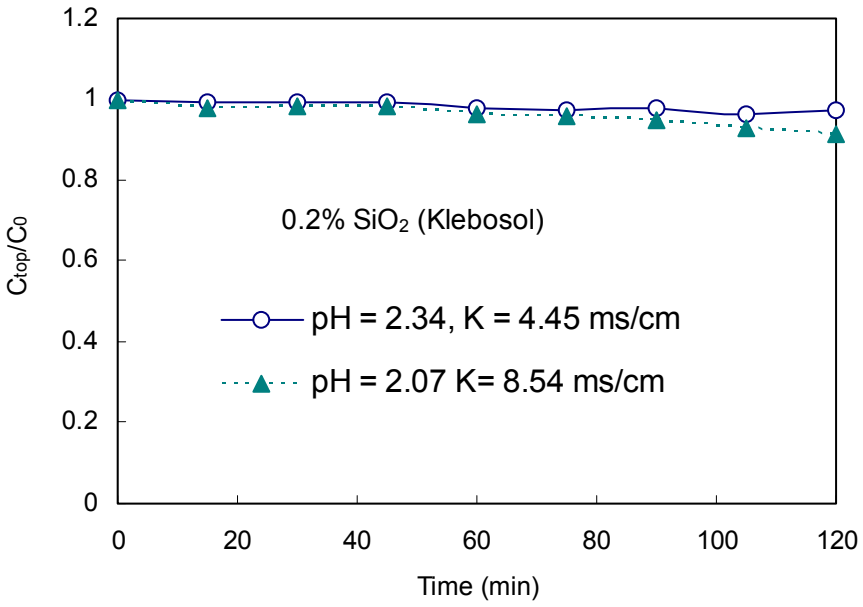

Figure 8.7 SiO_2 stability study at pH = 2.0 as a function of ionic strenghth

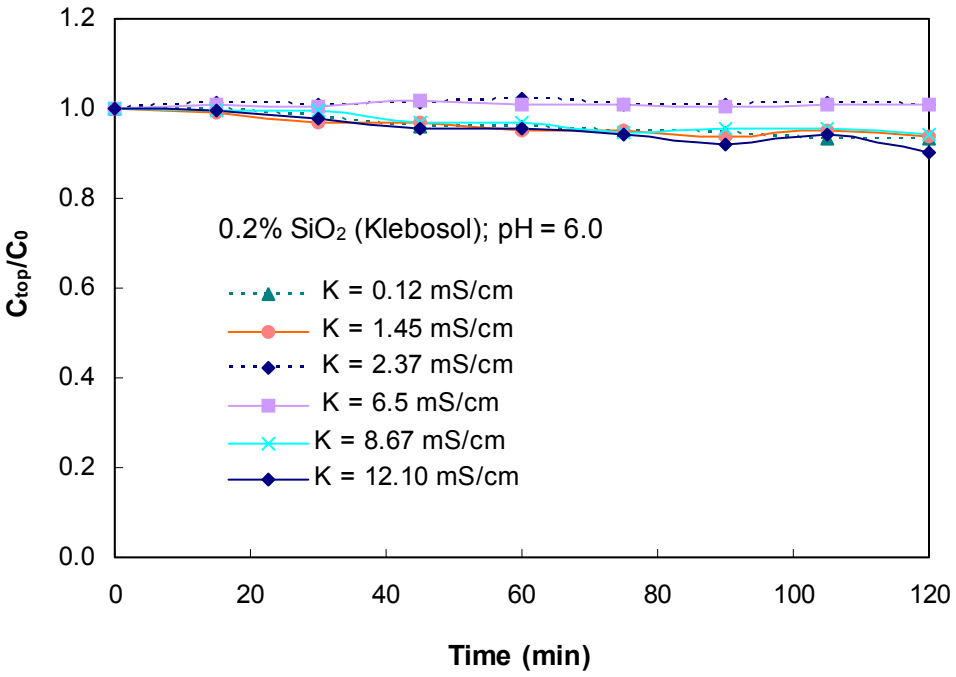

Figure 8.8 SiO_2 stability study at pH = 6.0 as a function of ionic strength

8.3.2 Understanding the IEP Impact on SiO_2 Removal during Electrocoagulation

SiO_2 has an IEP of ~2.0, and previous work has shown that the pH in an anodic chamber will reach pH ~ 2.0 in 5 minutes and will stay at this value for the remainder of the 2 hours EC. Thus, if SiO_2 is placed in an anode chamber during EC, the SiO_2 will be brought to its IEP. In this experiment, the simulated 0.4 % klebosol SiO_2 (1498-50), was put into the anode chamber with a 3.5 V/cm electric field. The same type of suspension was also put into the cathodic chamber for particle removal evaluation. As shown in Figure 8.9, the klebosol particle in the anodic chamber that was brought to its IEP (~2.0) has no apparent solid concentration change. However, the same type of slurry suspension was put into the cathodic chamber, a significant concentration change was observed during 120 minutes EC. These results indicate that the removal of SiO_2 from the bulk suspension during EC was not caused by the IEP mechanism.

8.3.3 The Effect of Current Supply Duration on SiO_2 Particle Removal

In these experiments, the only variable was the duration of current supply on stainless steel electrodes. The 0.1% klebosol SiO_2 slurry with pH ~6.0 and conductivity of 1.3 mS/cm was put in a cathodic chamber with a current supply of 0.5 hour, 1hour, and 2 hours respectively during EC; The turbidity of the suspension at the top layer was measured as a function of time. As shown in Figure 8.10, during 2 hours of current supply on the cathodic chamber, the particle removal was the fastest and ~12 ppm total Fe was found in the cathodic chamber. To achieve the same level of particle removal for the 1 hour duration of current supply, an additional 6 hours sitting time was required. For

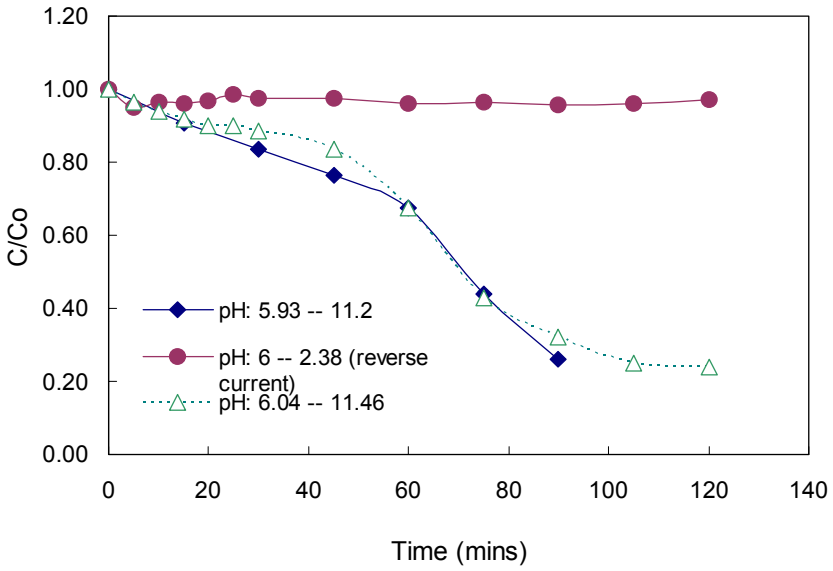

Figure 8.9 SiO_2 removal in both chambers during EC

the 0.5 hour duration of current supply, a much longer sitting time was required to achieve particle removal level that was seen with 2 hours EC. The Fe contents in the cathodic chamber were ~2.5 ppm and ~1ppm respectively for 1 hour and 0.5 hour EC. Previous pH measurements have shown that the pH reaches ~11 in 5 minutes in the cathodic chamber and stays at this value during EC. Empirically, the major modulator for particle removal differences is not pH, but rather, it is the Fe content in the cathodic chamber.

8.3.4 Using Graphite Anode to Study the Removal Mechanisms of SiO_2

To fully understand the role that Fe plays during EC of SiO_2 and whether SiO_2 removal is triggered by the release of iron species from a stainless steel anode, a comparison experiment between stainless steel and graphite carbon electrodes was conducted. The employed graphite anode was ~ 0.6cm in diameter and was placed at the center of the EC setup; the stainless steel cylinder was used as the cathode, and the current supply was 3.5V/cm. The 0.1% klebosol silica slurry was then put into the cathode chamber. The top layer turbidity was measured and plotted as shown in Figure 8.11. The carbon graphite anode, which does not generate iron species, the solid concentration on top layer was unaltered during the period of testing (2 hours EC). Under similar conditions, the use of a stainless steel anode shows a ~80% reduction of the solid concentration on the top layer. Those results indicate that the hydrolyzed iron species in the suspension play an essential role in SiO_2 removal during EC with stainless steel as the anode.

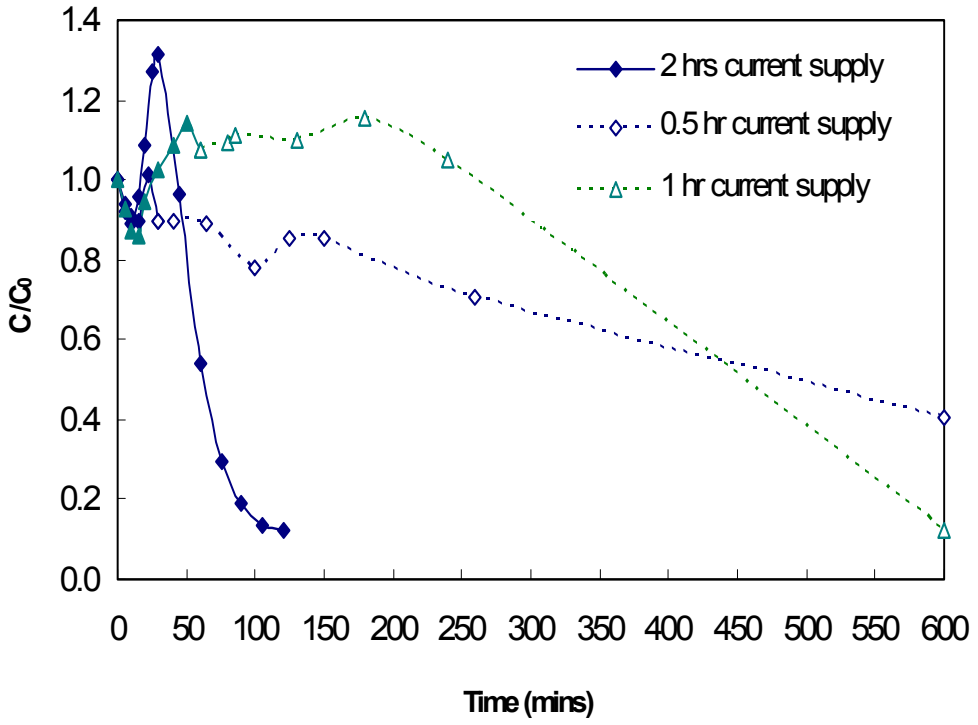

Figure 8.10 The effects of current supply duration on silica removal

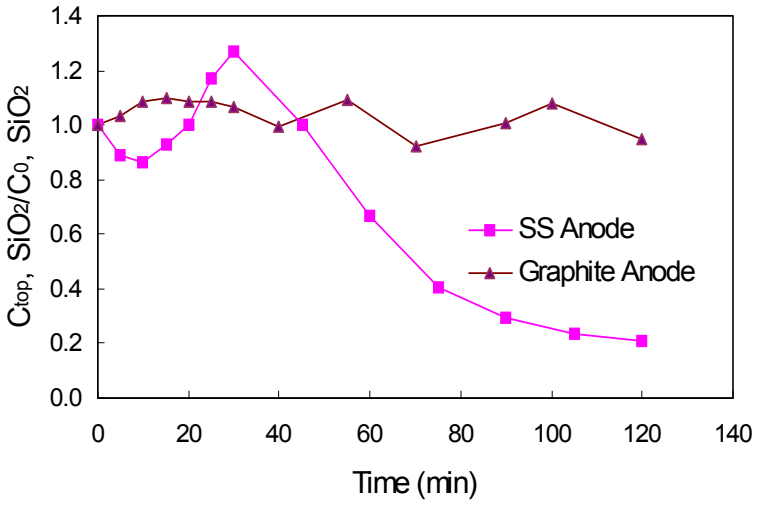

a

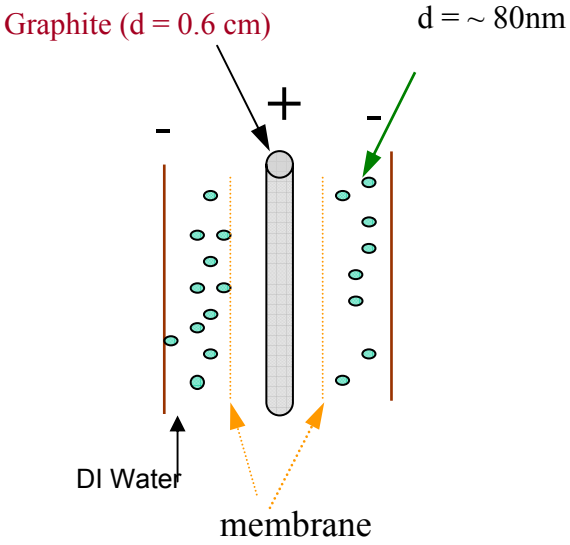

b

Figure 8.11 SiO_2 removal as a function of anode materials. a. SiO_2 removal as a function of time for graphite and stainless steel; b. Illustration of EC using graphite anode

8.3.5 TEM study of the SiO_2 removal mechanisms during EC

The 0.1% SiO_2 based slurry suspension was collected at times of 0, 45, 120 minutes during a typical EC setup experiment and analyzed with TEM. As shown in Figure 8.12 , SiO_2 is very spherical, uniform particle initially. As the EC progresses, at a time of 45 minutes, Figure 8.13 shows that some small particles start to form, which corresponds to the turbidity increase of the solution (see Figure 8.10). At time of 120 mins, Figure 8.14 shows that tiny particles are either adsorbed onto SiO_2 surface or bridge SiO_2 particles together. These three figures further demonstrate that the removal mechanism of SiO_2 from the suspension during electrocoagulation is due to coagulation induced by iron hydrous species [FeOH, $Fe(OH)_3$] (see Figure 8.15 for illustration).

Early work conducted by James and Healy [8.1] for the adsorption of polyvalent metal ions on silica has proven that Fe^{3+} is adsorbed on SiO_2 increasingly with rising pH, first neutralizing the charge on silica, then nucleating the metal hydroxide on the silica surface, and finally covering the surface with hydroxide.

d = ~ 80nm

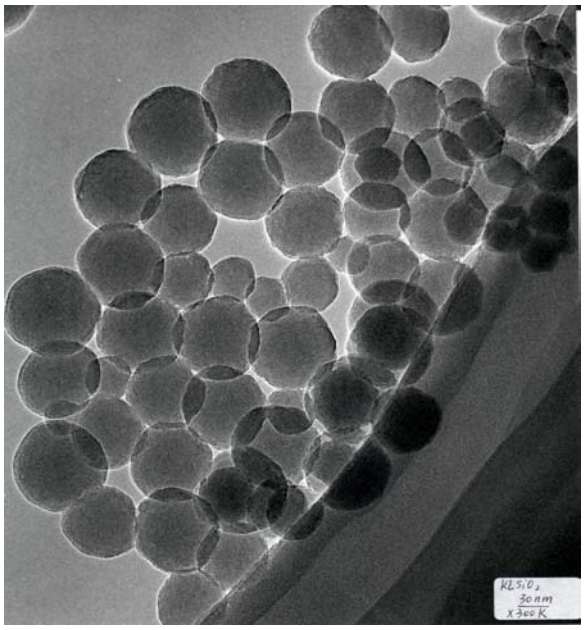

Figure 8.12 TEM Picture of Klebosol SiO_2 (t = 0 min)

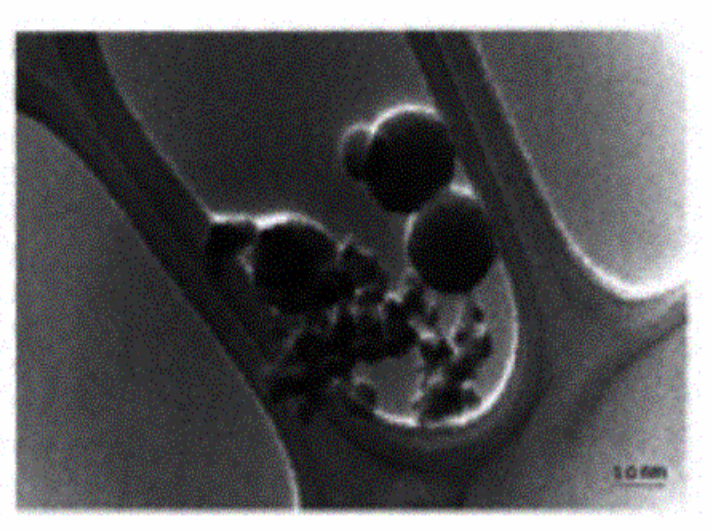

Figure 8.13 TEM of silica suspension particle at t = 45 mins during EC.

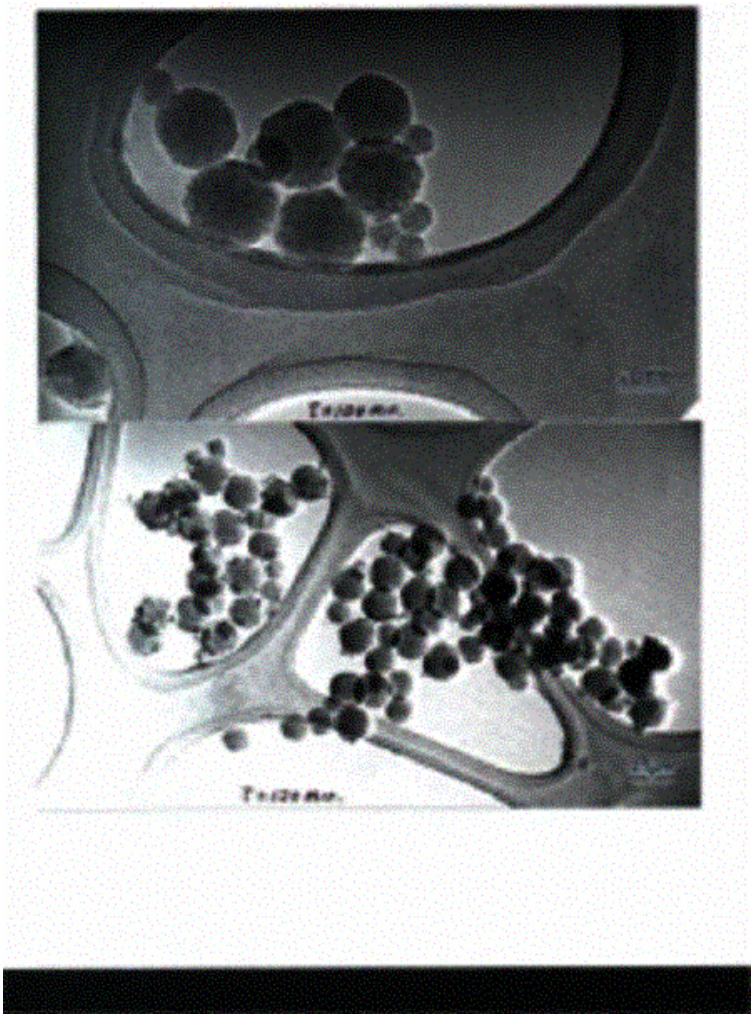

Figure 8.14 TEM of silica suspension particle at t = 120 mins during EC

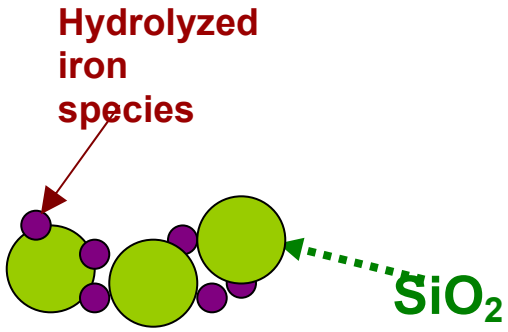

Klebosol SiO_2 at t = 120 mins

Figure 8.15 Illustration of Fe(OH)x adsorbing on or bridging the SiO_2

CHAPTER 9

CONCLUSIONS ON COPPER AND PARTICLE REMOVAL DURING ELECTROCOAGULATION

1. Electrocoagulation is able to remove both copper and particles (Al_2O_3 and SiO_2) simultaneously from simulated Cu-CMP waste suspension.
2. Removal of copper through cathode electroplating is a function of appliced charge duration, solid content in the suspension, the type and amount of the complexing agents, and the membrane surface charges. With appropriate selection of membrane type (positively charged membrane surfaces) and complexing agents (EDA), up to 80% copper can be electroplated out from a suspension containing 40 ppm copper and 0.4% Al_2O_3 under 3.5V/cm current supply for a duration of 2 hours EC.
3. SiO_2 removal mechanism under EC is induced by the generation of iron species from a stainless steel anode. The dissolved iron species from the anode forms hydroxyl species [$Fe(OH)_2$, $Fe(OH)_3$] in an alkaline cathodic chamber and functions as a coagulant leading to SiO_2 removal.
4. Al_2O_3 particles have a different removal mechanism during EC. Al_2O_3 suspension can be de-stabilized by increasing the ionic strength in the suspension, or by bringing the suspension to its IEP. Unlike SiO_2, it is not necessary to have Fe(OH)x formation to induce or accelerate Al_2O_3 removal during EC. The fastest way to remove Al_2O_3 from a suspension is to bring Al_2O_3 to its IEP.

APPENDIX A

Extract Cabsoil(300) Surface Acidity Constant and Surface OH Site Density Using FITEQL Program Based on Acid-Base Titration Data

Titration Results on Cabosil SiO_2:

Ionic Strength: 1M (KNO_3)
Surface Area of SiO_2: 416 m^2/g
V_{H2O}= 310 ml
W_{SiO2} = 1.1263g
C_{HCl} = 0.01773 M
C_{KOH} = 0.0156M

Total KOH (ml) added	Total Acid Added HCl (ml)	pH	Dilution Factor
0	0	2.01	0.0000
31.029	0	2.5	0.91
53.1945	0	3.5	0.85
56.713	0	4.5	0.84
58.6154	0	5.5	0.84
62.0698	0	6.5	0.83
67.9157	0	7.5	0.82
72.1908	0	8.0	0.81
76.4837	0	8.4	0.80
80.5407	0	8.7	0.79
85.9741	0	9.0	0.78
93.847	0	9.3	0.76
105.0497	0	9.6	0.74
120.8893	0	9.9	0.71
149.9999	0	10.2	0.67
204.0497	0	10.5	0.60
254.0497	0	10.7	0.55

FITEQL32.EXE
INPUT:

Table 1 Set Up Chemical Equilibrium Problem
Table1.1 Components (initial input)

#	ID	Component	X	logX	T	Type
1.	1	XOH	1.000D-03	-3.0000	1.000D-03	I -T
2.	160	PSI	1.000D-01	-1.000	0.000D+00	I-T
3.	50	H[+]	1.000D+00	0.000	0.000D+00	II –T, X

Table 1.2: Species, log K, and Stoichiometry matrix

#	ID	Name	logK	XOH	PSI	H[+]
1	50	H[+]	0.000	0.000	0.000	1.000

2	100	OH[-]	-13.800	0.000	0.000	-1.000
3	1	XOH	0.000	1.000	0.000	0.000
4	1100	XO[-]	-6.000	1.000	-1.000	-1.000

Table 1.3: Electric Double Layer Model
Gouy-Chapman Model

$S(m^2/g)$ = 4.160D+02 A (g/l) = 3.633D+00
Electrolyte Concentration (mol/L) = 1.000D +00
Electrolyte Valence = 1.000D+00

Table 1.4 Optimize K for species:
1100 XO[-]

Table 1.5 Optimize T for components:
1 XOH

Table 2: Input Data for Verification -- Serial data and Estimated Standard Deviation

Table 2.1 Total Concentration for components

#	H[+]
1	-2.674D-03
2	-2.880D-03
3	-3.026D-03
4	-3.169D-03
5	-3.302D-03
6	-3.475D-03
7	-3.717D-03
8	-4.046D-03
9	-4.481D-03
10	-5.200D-03
11	-6.315D-03
12	-7.200D-03

Table 2.2 Free Concentration for Components

#	Log H[+]
1	-6.500D+00
2	-7.500D+00
3	-8.000D+00
4	-8.400D+00
5	-8.700D+00
6	-9.000D+00

7	-9.300D+00
8	-9.600D+00
9	-9.900D+00
10	-1.020D+01
11	-1.050D+01
12	-1.070D+01

Table 2.3 Dilution Factors:

1	8.300D-01
2	8.200D-01
3	8.100D-01
4	8.000D-01
5	7.900D-01
6	7.800D-01
7	7.600D-01
8	7.400D-01
9	7.100D-01
10	6.700D-01
11	6.000D-01
12	5.500D-01

Table 2.4 Standard Deviation of Total Concentration

Component	Relative	Absolute
H[+]	1.000D-02	1.000D-06

Table 2.5 Standard Deviation of Free Concentration

Component	Relative	Absolute
H[+]	2.303D-02	0.000D+00

Table 3: Values of Adjustable Parameters at Each Iteration

	LogK	T	
	XO[-]	XOH	WSOS/DF
0	-6.000D+00	1.000D-03	69.49495
1	-5.624D+00	4.734D-03	76.25436
2	-5.718D+00	4.958D-03	74.40329
3	-5.789D+00	5.016D-03	74.09549
4	-5.831D+00	5.053D-03	73.96157
5	-5.858D+00	5.076D-03	73.89812
6	-5.876D+00	5.091D-03	73.86587
7	-5.888D+00	5.101D-03	73.83876
8	-5.896D+00	5.108D-03	73.84854

9	-5.902D+00	5.113D-03	73.83299
10	-5.905D+00	5.116D-03	73.82947
…….			
21	-5.913D+00	5.123D-03	73.82307

***** Optimization Procedure Converged *****

21.	-5.913D+00	5.123D-03	73.82307

Based on the program results:

Acidity constant for SiO_2 surface: Logk = -5.913

Total surface SiOH site = (5.123×10^{-3} mole $\times 6.02 \times 10^{23}$ OH-site/mole)/[L $\times$(3.63g/L) $\times(416\times10^{4}$ cm^2/g)] = 2-OH site/nm^2

APPENDIX B

Extract Copper Binding Constant on Cabsoil Silica using FITEQL Program Based on Copper Adsorption Data

Table 1: Chemical Equilibrium Problem

Table 1.1 Components

#	ID	Components	X	LogX	T	Type
1	160	X-Psi	1.000D-01	-1.000	0.000D+00	I -T
2	2	Cu[2+]	1.574D-05	-4.803	1.574D-05	I -T
3	3	XOH	3.767D-03	-2.424	3.770D-03	I -T
4	5	Cu(ads)	1.000D+00	0.000	0.000D+00	II -T, X
5	6	H[+]	1.000D+00	0.000	0.000D+00	III -X

Table 1.2.1: Species, Log K, and Stoichiometry Matrix

#	ID	Name	LogK	X-Psi	Cu[2+]	XOH	Cu(ads)	H[+]
1	1	H[+]	0.000	0.000	0.000	0.000	0.000	1.000
2	2	OH[-]	-13.78	0.000	0.000	0.000	0.000	-1.000
3	3	Cu[2+]ag	0.000	0.000	1.000	0.000	0.000	0.00
4	4	CuOH[+]ag	-8.220	0.000	1.000	0.000	0.000	-1.000
5	5	Cu(OH)2ag	-14.32	0.000	1.000	0.000	0.000	-2.000
6	6	Cu(OH)3ag	-26.8	0.000	1.000	0.000	0.000	-3.000
7	7	XOH	0.000	0.000	0.000	1.000	0.000	0.000
8	8	XO[-]	-5.900	-1.000	0.000	1.000	0.000	-1.000
9	9	XOCu[+]	-4.350	1.000	1.000	1.000	1.000	-1.000
10	13	(XO)2Cu	-8.220	0.000	1.000	2.000	1.000	-2.000

Table 1.3 Electric Double Layer Model

Gouy-Chapman Model
$S(m^2/g)$ = 4.160D+02; A(g/L) = 2.728D+00
Electrolyte Concentration (mol/L) = 1.000D-01
Electrolyte Valence = 1.000D+00

Table 1.4 Optimize K for species:

9	XOCu[+]
13	(XO)2Cu

Table 2: Input Data for Verification – Serial Data and Estimated Standard Deviation

Table 2.1 Total Concentration for Components

#	Cu(Ads)	Log H[+]

1	5.215D-07	-3.89
2	7.175D-07	-4.06
3	7.175D-07	-4.22
4	9.109D-07	-4.49
5	9.109D-07	-4.96
6	1.290D-06	-5.18
7	1.384D-06	-5.21
8	1.660D-06	-5.34
9	1.841D-06	-5.44
10	2.713D-06	-5.49
11	7.570D-06	-5.85
12	8.278D-06	-5.94
13	8.925D-06	-6.05
14	9.556D-06	-6.08
15	1.075D-05	-6.28
16	1.106D-05	-6.30
17	1.163D-05	-6.33
18	1.244D-05	-6.45
19	1.410D-05	-6.51
20	1.454D-05	-6.75
21	1.515D-05	-7.08
22	1.544D-05	-7.25
23	1.546D-05	-7.30
24	1.549D-05	-7.39
25	1.553D-05	-7.45
26	1.555D-05	-7.52
27	1.559D-05	-7.60
28	1.563D-05	-7.65
29	1.567D-05	-7.77
30	1.567D-05	-7.82
31	1.568D-05	-7.85

Table 2.4 Standard Deviation of Total Concentration

Component	Relative	Absolute
Cu(ads)	1.000D-02	1.000D-06

Table 2.5 Standard Deviation of Free Concentration

Component	Relative	Absolute
H[+]	2.303D-02	0.000D+00

Table 3: Values of Adjustable Parameters at Each Iteration

#	Logk XOCu[+]	LogK (XO)2Cu	WSOS/DF
0	-4.350	-8.220	0.26614
1	-4.348	-8.219	0.26605
2	-4.347	-8.225	0.26605
3	-4.347	-8.221	0.26605
4	-4.347	-8.224	0.26605
……			
21	-4.347	-8.223	0.26605
22	-4.347	-8.223	0.26605

**** Optimization Procedure Converged ****

22	-4.347	-8.223	-0.26605

Based on the program calculation. The two acid constants on =SiOH surfaces are:

Logk1 = -4.347

Logk2 = -8.223

APPENDIX C

Modeling Input and Output of Cu Adsorption on SiO_2 Surfaces at Different pH Using MINTEQA2/PRODEFA2 Program

Inputs:
Temperature(Celsius): 25.00
Units of concentration: Molal
Ionic strength: 0.010 molal; fixed
If specified, carbonate concentration represents total inorganic carbon. Precipitation is allowed only for those colids specified as allowed in the input file (if any).
The maximum number of iterations is: 40
The method used to cmpute activity coefficients is: Davies equation
Intermediate output file
Adsorption model: Diffuse Layer
Number of adsorbing surfaces: 1
Complexation reactions:
811330 =SO1- 0.0000 -5.9000 0.0000 0.0000 -1.00 0.00 0.00
0.00 3 1.000 811 -1.000 330 -1.000 813 0.0000 0 0.000 0 0.000 0

8112310 =SO1Cu+ 0.0000 -4.3500 0.000 0.000 1.00 0.00 0.00
0.00 5 1.000 811 -1.000 330 1.000 813 1.000 231 1.000 2 0.000 0

8112311 (=SO)2Cu 0.0000 -8.2200 0.000 0.000 0.00 0.00 0.00
0.00 4 2.000 811 1.000 231 -2.000 330 2.000 330 0.000 0 0.000 0

The input data will be used in a series of sweeps
The input parameters for each sweep will be indentical to this initial listing except that:
-- The fixed equilibrium pH in successive sweeps will be:

3.50 3.75 4.00 4.25 4.50 4.75
5.00 5.25 5.50 5.75 6.00 6.25
6.50 6.75 7.00 7.25 7.50 7.75
8.00 8.25

Output (just list one output that is at pH =6.0):
Type I – components as species in solution

ID	Name	Cal Mol	Activity	Log actvty	Gamma	New logK
330	H+1	1.110E-06	1.000E-06	-6.0000	0.9011	0.045
231	Cu+2	9.389E-06	6.191E-06	-5.2083	0.65939	0.181
410	K+1	1.000E-01	9.011E-02	-1.0452	0.90113	0.045
492	NO3-1	1.000E-01	9.011E-02	-1.0452	0.90113	0.045
811	ADS1TYP1	3.296E-03	3.296E-03	-2.4820	1.0000	0.000

Type II – Other species in solution or adsorbed

ID	Name	Calc Mol	Activity	Log actvty	Gamma	New Logk
8112311	(=SO)2Cu	5.820E-05	5.820E-05	-4.2351	1.0000	-8.220
2313303	Cu(OH)4 -2	2.326E-21	1.534E-21	-20.8142	0.6594	-39.419
2313304	Cu2(OH)2+2	2.529E-09	1.667E-09	-8.7779	0.6594	-10.178
3300020	OH-	1.111E-08	1.001E-08	-7.9995	0.9011	-13.953
2313300	CuOH +	6.847E-08	6.170E-08	-7.2097	0.9011	-7.955
2313301	Cu(OH)2 AQ	1.282E-07	1.285E-07	-6.8912	1.0023	-13.681
2313302	Cu(OH)3-	8.581E-15	7.732E-15	-14.1117	0.9011	-26.854
8113301	=SO-	2.463E-04	3.463E-04	-3.4605	1.000	-5.900
8112310	=SO1Cu+	1.089E-05	1.089E-05	-4.9631	1.000	-4.350

REFERENCES

Chapter 1

[1.1] IRTS 1998, *International Technology Roadmap for Semicondutor*, http://www.irts.net/

[1.2] Singer, P.H. (1992) *Semiconductor International*, P44, March.

[1.3] Rosenberg, R. (1994) *MRS Symp. Proc*., 337, 33.

[1.4] Murarka, S.P., (1993) *Metalization Theory and Practice for VLSI and ULSI*, Butterworth-Heinemann, Boston, P15.

[1.5] Sze, S.M. (1981) *Physics of Semiconductor Devices*, John Wiley & Sons, Inc, New York.

[1.6] Ramappa, D.A. and Henley, W.B. (1999) "Effects of copper contamination in silicon on thin oxide breakdown" *Journal of the Electrochemical Society*, 146(6), 2258-2260.

[1.7] Browne, S., Krygier, V., O'Sullivan, J., and Sandstrom, E.L. (1999) "Treating Wastewater from CMP Using Ultrafiltration" *Micro*, March, P77.

[1.8] IRTS 2005, *International Technology Roadmap for semiconductor* . http://www.irts.net/

Chapter 2

[2.1] Warnock, J. (1991) *J. Electrochem. Soc*., 138, 2398

[2.2] Bhushan, M, Rouse, R., and Lukens, J.E. (1995) *J. Electrochem. Soc*., 142, 3845.

[2.3] Fury, M.A. (1997) *Solid State Technology*, P81, May.

[2.4] Staigerwald, J.M., Murarka, S.P., and Gutmann, R.J. (1997) *Chemical Mechanical Planarization of Microelectronic Materials*, John Wiley & Sons, NY.

[2.5] Colloins, R.J., and Williams, G. (1995) *Solid State Technology*, May.

[2.6] Fury, M.A. (1995) *Solid State Technology*, April, p47.

[2.7] Smith, W.L., Kruse, K., Holland, K., and Harwood, R. (1996) *Solid State Technology* Jan. p77.

[2.8] Jairath, R., Desai, M., Stell, M., Stell, M., Telles, R., and ScherberBrewer, D. (1994) Mat. Res. Soc. Symp. Proc. 337, 121.

[2.9] Sivaram, S., Leggett, R., and Maury, A. (1991) in *Proc*. 3rd *Int. Symp. On ULSI Science and Technology*, eds. J.M. Andrews and G.K. Celler, p606, The Electrochem. Soc., Inc

[2.10] Singer, P. (1998) *Semiconductor International*, P.91, June

[2.11] Wang, S., and Guatam, G. (2002) " Integrating Cu/ultra-low-k with CMP." *Solid State Technology*, Sep. Supplement, Vol. 45 Issue 9, p7.

[2.12] Wang, S., and Guatam, G. (2002) " Integrating Cu/ultra-low-k with CMP." *Solid State Technology*, Sep. Supplement, Vol. 45 Issue 9, p7.

[2.13] Ryu, C., Lee, H., Kwon, K.W., Loke, A.L.S., and Wong, S. (1999) "Barriers for copper Interconnects" *Solid State Technology*, Apr., pp.53-56.

[2.14] Lee, D.N., 1996. *MRS Symp. Proc*., 427, 167

[2.15] Dubin, V.M., Shacham-Diamand, Y., Zhao, B., Vasudev, P.K., and Ting, C.H. (1996) *MRS Symp. Proc*., 427, 179.

[2.16] Singer, P. (1998) *Semiconductor International*, P.91, June

[2.17] Raghunath, C. Ph.D. Dissertation, University of Arizona (1997)

[2.18] Zhang, L. Ph.D Dissertation "Contamination and Galvanic Corrosion in Metal Chemical-Mechanical Planarization" University of Arizona, 1998

[2.19] Dornisch, D., Li, G., and Brongo, M. (2000). "Cu contamination control for advanced interconnect manufacturing." *Solid State Technology*, May, Vol. 43 Issue 5, p137,

[2.20] Runnels, S.R. (1994), *J. Electrochemical Society*, 141, 1900

[2.21] Runnels, S.R., and Eyman, L.M. (1994) *J. Electrochem. Soc*., 141, 1698.

[2.22] Nanz, G., and Camilletti, L.E. (1995) *IEEE Trans, Semi. Manuf*., 8, 382.

[2.23] Runels, S. R. (1996) *Journal of Electronic Materials*. 25, 1574

[2.24] Tseng, W.-T., and Wang, Y.-L. (1996) *J. Electronic Materials*, 25, 1574

[2.25] Cook L.M., (1990) *J. Non-cryst. Solids*, 120, 152.

[2.26] Tomozawa, M., Yang, K., Li, H., and Murarka, S.P. (1994) *MRS Symp. Proc*., 337, 89.

[2.27] Tomozawa, M. (1997) "Oxide **CMP** mechanisms" *Solid State Technology*, Jul, Vol. 40 Issue 7, p169.

[2.28] Kaufman, F.B., Thompson, D. B., Broadie, R.E., Jaso, M.A., Guthrie, W. L., and Pearson, D. J., Morinaga, H., Aoki, M., Maeda, T., Fujisue, M., Tanaka, H., and Toyoda, M. (1997) *MRS Symp, Proc*., 477, 35.

[2.29] Zhang, F., and Busnaina, A.(1999) "Submicron particle removal in post-oxide chemical-mechanical planarization (**CMP**) cleaning." *Applied Physics A: Materials Science & Processing*, Vol. 69 Issue 4, p437.

[2.30] IRTS 2005, *International Technology Roadmap for semiconductor* . http://www.irts.net/

[2.31] Syverson, W.A., Fleming, M.J., and Schubring, P.J. (1992) in Proc. 2nd International Symp. *Cleaning Technology in Semiconductor Device Manufacturing, eds., J*. Ruzyllo and R.E. Novak, The Electrochemical Society, Inc., NJ.

[2.32] Krusell, W.C., de Larios, J. M., and Zhang, J. (1995) "Mechanical brush scrubbing for post-CMP clean" *Solid State Technology*, 109, June.

[2.33] Wang, Y.-L., Liu, C., Feng, M.-S., and Tseng, W.-T. (1998), *Materials Chemistry and Physics*, 52, 23.

[2.34] Morinaga, H., Aoki, M., Maeda, T., Fujisue, M., Tanaka, H., and Toyoda, M. (1997) *MRS Symp. Proc*., 477, 35

[2.35] Pohl, M.C. and Griffiths, D.A. (1996), "The importance of particle size to the performance of abrasive particles in the CMP process" *Journal of Electronic Materials*, Vol.25, No. 10.

[2.36] Schmidt, D.N. ed., (1994) "Contamination Control and Defect Reduction in Semiconductor Manufacturing", *Proceedings, Symposium of Electrochemical Society*.

[2.37] Noguchi, J., Konishi, N., and Yamada, Y. (2005) "Influence of Post-**CMP** Cleaning on Cu Interconnects and TDDB Reliability" *IEEE Transactions on Electron Devices*, May, Vol. 52, Issue 5, p934-941.

Chapter 3

[3.1] Zhang, L. Ph.D Dissertation "Contamination and Galvanic Corrosion in Metal Chemical-Mechanical Planarization" University of Arizona, 1998

[3.2] Schindler, P.W. (1981) "Surface comlexes at oxide-water interfaces" In *Adsorption of Inorganics at Solid-Liquid Interfaces*, Anderson, M.A. and Rubin, A.J. Eds. Ann Arbor Science, Ann Arbor, Michigan

[3.3] Bolt, G.H., and Riemsdijk, W.H. (1982) "Iron adsorption on inorganic variable charge constituents: in *Soil Chemistry*, vol. Bolt, G.H. Eds, Elsevier, Amsterdam.

[3.4] Stumm, W. (1992) *Chemistry of the Solid-Water interface*. John Wiley & Sons, New York, NY.

[3.5] Vysotskii, Z.Z., and Strazhesko, D.N., (1974) "Adsorption and adsorbent." In Strazhesko. D.N. Ed , Wiley, New York, 1974, p.55.

[3.5] Dzombak, D.A., and Morel, F.M.M. (1990) *Surface Complexation Modeling*, John Wiley & Sons, New York, NY.

[3.6] Stumm, W., and Morgan, J.J. (1981) *Aquatic chemistry*. John Wiley & Sons, New York, NY.

[3.7] Morinaga, H., Aoki, M., Maeda, T., Fujisue, M., Tanaka, H., and Toyoda, M. (1997) *MRS Symp. Proc*., 477, 35

[3.8] Awaya, N., Inokawa, H., Yamamoto, E., Okazaki, Y., Miyake, M., Arita, Y., and Kobayashi, T. (1996) *IEEE Trans. Electron Devices,* 43, 1206 (1996)

[3.9] Lee, W., Torek, K.J., Palsulich, D.A., Weston, L. 1997. "The Adsorption-Desorption of Cations at the Silica-water interface and Its implication in wafer-cleaning efficacy" *Mat. Res. Soc. Symp. Proc*, Vol. 477.

[3.10] Davis, J.A. (1977) "Adsorpton of trace metals and complexing ligands at the oxide/water interface." Ph.D. thesis, Stanford University, Stanford, California.

[3.11] Dzombak, D.A. (1986) " A general model for predicting sorption of inorganics on hydrous oxides"

[3.12] Hunter, R.J. (1981) *Zeta Potential in Colliod Science: Principles and Applications*. Academic press, New York

[3.13] Overbeek, J. Th.G. (1952) " Electrochemistry of the double layer" In: H.R.Kruyt (Editor), *Colloid Science*, Vol. I, Elservier, Amsterdam.

[3.14] David, S.B., and Allison, J.D. (1988) MINTEQA2, An equilibium metal speciation model: User's Manual, Environmental Research laboratory, U.S. Environmental Protection Agency, Atehns, Georgia.

[3.15] Herbelin, A., and Westall, J. (1996) "FITEQL, A computer program for determination of chemical equilibrium constants from experimental data" Version 3.2.

Chapter 4

[4.1] Herbelin, A., and Westall, J. (1996) "FITEQL, A computer program for determination of chemical equilibrium constants from experimental data" Version 3.2.

[4.2] Dzombak, D.A., and Morel, F.M.M. (1990) *Surface Complexation Modeling*, John Wiley & Sons, New York, NY.

[4.3] Stumm, W. (1992) *Chemistry of the Solid-Water interface*. John Wiley & Sons, New York, NY.

Chapter 5

[5.1] Lowry, R. K. (1996) "Electronic Processes and Environment" in Electronic Materials Chemistry. Edited by H. Bernhard Pogge, MARCEL DEKKER, INC., New York.

[5.2] Corlett, G. L. (1998) "Can CMP Waste Treatment Ever be Environmentally Friendly", *Advancing Applications in Contamination Control*, pp. 19-25, Dec.

[5.3] Branning, J., Chiofalo, V., and O'Sullivan, J. (1999) "Treatment and Recycling of Wastewater Generated by Copper Metallization and Copper CMP", Presented at *WATERTECH'99*.

[5.4] Junnier, R. W., Dentel, S. K., Ramana, A., and Thuresson, D. (1999) "It Takes Metal, Oxide, and a Lot of Water", *Industrial Wastewater*, pp. 25-30, January/February.

[5.5] Reker, M., Lenart, M., and Harnsberger, S. (1999) "Treatment and Recycling of Copper CMP Slurry Waste Streams to Achieve Environmental Compliance for Copper and Suspended Solids", *Semiconductor Fabtech*, 8th Edition, pp. 141- 150.

[5.6] Mendicino, L., and Brown, P. T. (1998) "The Environment, Health and Safety Side of Copper Metallization", *Semiconductor International*, pp.105-110, June.

[5.7] Jenkins, J.V., Myers, C. W., Lesiak, S, and Viscomi, R. (2004). "The many options for managing ***CMP*** wastewater." *Solid State Technology*, Jul, Vol. 47 Issue 7, p61-134.

[5.8] Krulik, G.A., Kramasz, K., and Golden, J.H. (2000) "Copper CMP Wastewater chemistry and Treatment" from http://www.microbar.com

[5.9] Maag, B. "The Environmental Impact of Copper CMP", M.S. Thesis, MIT, 2000.

[5.10] METCALF and EDDY, Inc. (1991) Wastewater *Engineering: Treatment, Disposal, and Reuse*, 3rd edition, McGraw-Hill.

[5.11] EPA 1982 "Fate of Priority Pollutants in Publicly Owned Treatment Works" EPA #440/1-82/303, Sep.

[5.12] EPA 1983. "Guidance Manual for POTW Pretreatment Program Development" Oct.

[5.13] EPA 1988. "Copper: Water Quality Standards Criteria Summaries: Compilation of State and Federal Criteria" EPA# 440588027

[5.14] EPA 1999-1 "National Recommended Water Quality Criteria – correction" EPA-822-Z-99-001, Apr. 1999

[5.15] EPA 1999-2. "Introduction to the national Pretreatment Program" EPA-833-B-` 98-002, Feb. 1999

[5.16] EPA WEB: http://epa.gov/

Chapter 6:

[6.1] Shaw, D.J. (1966) "Introduction to Colloid and Surface Chemistry." Butterworth, London.

[6.2] O'Melia, C.R., (1989) *Colloids Surf*. 39: 255-271

[6.3] Verwey, E.J.W., and Overbeek, J.Th.G. (1948) "Theory of Stability of Lyophobic Colloids." Elsevier, Amsterdam.

[6.4] Israelachvili, J. (1992) *Intermolecular and Surface Forces*, second edition, Academic press, San Diego.

[6.5] METCALF and EDDY, Inc. (1991) Wastewater *Engineering: Treatment, Disposal, and Reuse*, 3rd edition, McGraw-Hill.

[6.6] Pouet, M. -F., and Crasmick, A. (1994) "Electrocoagulation and Flotation: application in crossflow Micorfiltrtion" *Filtration and Separation*, May, P269.

[6.7] Belongia, B.M., Haworth, P.D., Baygents, J.C., and Raghavan, S. (1999) "Treatment of Alumina and Silica Chemical Mechanical Polishing Waste by Electrodecantation and Electrocoagulation" *J of Electrochemical Society*, 146 (11), 4124-4130.

[6.8] Matteson, M.J., Dobson, R.L., Glenn, R. W., Kukunoor, N. S., and Waits III, W. H., and Clayfield, E. J. (1995) "Electrocoagulation and Separation of Aqueous Suspensions of Ultrafine Paricles" *Colloids and Surfaces*, V.104, pp.101-109.

[6.9] Vik, E.A., Carlson, D.A., Eikum, A.S., and Gjessing, E. T. (1984) " Electrocoagulation of Potable Water" *Water Res*. Vol 18, No.11, pp. 1355-1360.

[6.10] Pouet, M.-F., and Grasmick, A. (1995) "Urban Wastewater Treatment by Electrocoagulation and Flotation" *Wat. Sci. Tech*. Vol. 31, No.3-4, pp. 275-283.

[6.11] Do, J.S., and Chen, M.L. (1994)"Decolourization of Dye-containing Solutions by Electrocoagulation". *J of Applied Electrochemistry*, V. 24, pp. 785-790.

[6.12] Nukheli, M., and Korovin, N. V. (1993) "Removal of Corrosion Products from Water by Electrocoagulation" *Thermal Engineering*, Vol. 40, No. 11.

[6.13] Kin, K. –T., Tang, H. –S, Chan, S. –F, Raghavan, S., and Martinez. S. (2006) "Treatment of Chemical—Mechanical Planarization Wastes by Electrocoagulation/Electro-Fenton Method." *IEEE Transactions on Semiconductor Manufacturing*, May, Vol. 19, Issue 2, p208-215.

[6.14] Tamilmani, S., Huang, W. H., Raghavan, S., and Farrell, J. (2004) "Electrochemical Treatment of Simulated Copper **CMP** Wastewater Using Boron Doped Diamond Thin Film Electrodes A Feasibility Study." *IEEE Transactions on Semiconductor Manufacturing*, Aug. Vol. 17 Issue 3, p448-454.

[6.15] Evans, J. W., Ding, R., Doyle, F. M., Jiriçny, V. S. (2005) "Copper electrodeposition onto extended surface area electrodes and the treatment of copper-containing **waste** streams." *Journal of Metallurgy*, Dec2005, Vol. 34 Issue 6, p363-368.

[6.16] Stumm, W. (1992) *Chemistry of the Solid-Water interface*. John Wiley & Sons, New York, NY.

[6.17] Ralph K.Iler (1979) "The chemistry of Silica, Solubility, polymerization, colloid and Surface Properties, and Biochemistry" John Wiley & Sons, New York, p312-439.

[6.18] James, R.O. and Healy, T.W. (1972) "Adsorption of hydrolzable metal ions at the oxide water interface, II. Charge reversal of SiO_2 and TiO_2 colloids by absorbed Co(II), La(III) and Th(IV) as model systems." *J. colloid, Interface Sci*., 40: 53-64.

Chapter 8

[8.1] James, R.O. and Healy, T.W. (1972) "Adsorption of hydrolzable metal ions at the oxide water interface, II. Charge reversal of SiO_2 and TiO_2 colloids by absorbed Co(II), La(III) and Th(IV) as model systems." *J. colloid, Interface Sci*., 40: 53-64.